Optimal Siting and Sizing of Solar Photovoltaic Distributed Generation to Minimize Loss, Present Value of Future Asset Upgrades and Peak Demand Costs on a Real Distribution Feeder

by

Meghana Mukerji

A thesis
presented to the University of Waterloo
in fulfillment of the
thesis requirement for the degree of
Master of Applied Science
in
Electrical and Computer Engineering

Waterloo, Ontario, Canada, 2011

Author's Declaration

I hereby declare that I am the sole author of this thesis. This is a true copy of the thesis, including any required final revisions, as accepted by my examiners.

I understand that my thesis may be made electronically available to the public.

Abstract

The increasing penetration of distributed generation (DG) in power distribution systems presents technical and economic benefits as well as integration challenges to utility engineers. Governments are beginning to acknowledge DG as an economically viable alternative to deferring investment at generation, transmission and distribution levels, meeting demand growth and improving distribution network performance and security. DG technology is rapidly maturing in Ontario due to government economic incentives promoting connection, specifically, the Ontario's Feed-In-Tariff (FIT) Program.

Optimal sizing and siting of DG is well researched, traditionally studying the technical impact on distribution system such as real power loss reduction and voltage profile improvement. Equally common objectives studied are the economics of DG installation which are useful for the developer when deciding when and where to install. Although DG represents a "non-wires" solution to network asset reinforcement, the direct economic benefit to the host utility from promoting DG uptake is not fully understood by utility planners and asset managers. Some DG based asset reinforcement deferral work has been performed in the UK and Italy but is mainly at the transmission level and is not part of an overall strategy that could be applied by a utility.

This research presents a comprehensive three stage technique: optimal siting, optimal sizing and financial evaluation of cost savings over a defined planning period to quantify the economic benefit to a Local Distribution Company (LDC) of solar photovoltaic (PV) DG connections on an actual distribution feeder. Optimal sites for PV DG are determined by applying the power loss sensitivity factor method to the test feeder. The objective functions used to determine cost savings consist of loss minimization, asset investment deferral, and peak demand reduction to identify an optimal DG penetration limit. Furthermore, a utility planner can identify an optimal DG penetration limit, encourage uptake at preferred locations that would benefit the LDC, and use the positive impact of DG at existing locations as part of an asset management strategy to prioritize and schedule future asset reinforcement upgrades.

Acknowledgements

I would like to express my deepest gratitude to my supervisors and mentors, Dr. Salama and Dr. El-Saadany for their guidance and encouragement through this journey of growth and discovery. Their patience and support has enabled me to achieve my highest potential in both academic and professional work – this has been an opportunity of a lifetime for which I am truly thankful.

My sincere thanks also to staff and management at Utilities Kingston; in particular, my manager, Jim Miller, for his support in obtaining the tools necessary for conducting my research and for facilitating my schedule so that I could meet my commitments. I gratefully acknowledge the many helpful conversations I had with my colleagues at Utilities Kingston, namely, Chris Xu, Dan Micallef, Sherry Gibson, Steve Sottile, Malcolm King, Randy Murphy and Joel Melburn who were generous with their time and knowledge. The quality of this work is directly attributable to their help and I am proud to be a member of this team. My gratitude also goes out to all my friends and family for their understanding of my schedule for the last year. Thank you also to my readers for your time in reviewing this work – I hope you find it relevant and interesting.

My final dedication goes to my fiancé, Corey Gauthier, whose unwavering belief in my abilities saw me through to the end of my studies. Your help and support has made this possible and I am honoured to share this achievement with you.

Table of Contents

Author's Declaration ii
Abstract iii
Acknowledgements iv
List of Figures vii
List of Tables x
Chapter 1 – Introduction 1
1.1 – Background 1
1.2 – Thesis Scope and Objectives 3
1.3 – Thesis Outline 4
Chapter 2 – Theory 7
2.1 – The Case for Renewable Generation 7
2.2 – Optimal Siting and Sizing of Distributed Generation 9
2.2.1 – Load Flow Equations 9
2.2.2 – Optimal DG Allocation 11
2.3 – Background Information for Feeder Model Development 14
2.3.1 – Description of Kingston Hydro's Distribution System 14
2.3.2 – Overview of Study Feeder 15
2.3.3 – Load Data and Load Profile 16
2.4 – Solar PV Technology in Ontario 21
2.4.1 – Solar PV Technology Overview 21
2.4.2 – Solar PV Inverters 23
2.5 – Utility Project Planning Horizon 24
Chapter 3 – Feeder & Generator Model Development in CYMDIST using Monthly Load and Generation Profiles 25
3.1 – CYMDIST Modelling Environment and Load Flow Simulation Settings 25
3.2 – Detailed Feeder Model 25
3.1.1 – Conductor and Cable 27
3.1.2 – Overhead Line Conductor Configuration 29
3.2 – Generator Model 30
3.3 – Load Model 31
3.3.1 – Load Allocation 32

3.3.2 – Annual Load and Generation Profile 34
Chapter 4 – State of the Discipline 35
4.1 – Previous Work on Optimal DG Allocation 35
4.2 – Previous Work on Optimal DG Siting using Sensitivity Factors 50
4.3 – Previous Work on DG and Asset Reinforcement Investment Deferral 52
4.4 – Summary of Literature Review and Justification for this Work 59
Chapter 5 – Problem Formulation and Execution: Power Loss Sensitivity Method for Optimal Siting, Genetic Algorithm for Optimal Sizing, Objective Functions and NPV Analysis 64
5.1– Introduction 64
5.2 – Optimal Siting using the Loss Sensitivity Factor (LSF) Method 65
5.3 – Optimal DG Sizing using the Continuous Domain Genetic Algorithm 68
5.3.1 – Basic Concepts of the Genetic Algorithm 69
5.3.2 – Application of the Continuous Domain GA to Optimal Sizing of PV DG 72
5.3.3 – Objective Functions for Optimal Sizing of PV DG 74
5.4 – Net Present Value (NPV) Analysis 79
Chapter 6 – Results and Discussion 81
6.1 – Summary of Method and Application 81
6.2 – Simulation Results 81
6.2.1 – Objective 1 – Minimization of Real Power Loss 82
6.2.2 – Objective 2 – Minimization of Present Value of Future Asset Reinforcement (Maximization of Asset Deferral) 85
6.2.3 – Objective 3 – Minimization of Transmission Peak Demand Charges 86
6.2.4 – Financial Evaluation of each Objective Function using a NPV Analysis 88
6.3 – Discussion 89
Chapter 7 – Conclusions and Recommendations for Future Work 91
7.1 – Conclusions 91
7.2 – Recommendations for Future Work 92
References 95

List of Figures

Figure 1 - Traditional Power Delivery Topology 1

Figure 2 – 2007 Ontario Supply Mix [4] 8

Figure 3 - Ontario's Target Supply Mix for 2025 [4] 8

Figure 4 - One Line Diagram of a Two-Bus Distribution System [13] 12

Figure 5 – Kingston Hydro Distribution Territory 15

Figure 6 – Test Feeder (Feeder X) in CYMDIST 16

Figure 7 – Feeder X Annual Load Profile 2010 17

Figure 8 – Feeder X Monthly Load Profile for Winter Peak Month January 2010 18

Figure 9 – Feeder X Monthly Load Profile for Summer Peak Month June 2010 19

Figure 10 – Feeder X Monthly Load Profile for Shoulder Month October 2010 20

Figure 11 – Thin Film Solar Cell Layers [17] 22

Figure 12 – Production of Thin Film Solar Panels [17] 22

Figure 13 – Light Striking the Light Guided Solar Optic Lens (LSO) is Concentrated to the Optic's Centre Located on a high-efficiency PV Cell. The Sun Simba is Morgan Solar's Product [34] 23

Figure 14 – Typical Inverter Structure 24

Figure 15 – Feeder X with Electronically Coupled PV DG at Optimal Locations with Corresponding Node Numbers (in boxes) 26

Figure 16 – Bare Aluminum Stranded Conductor for Overhead Lines 28

Figure 17 – Jacketed Copper Cable used in Underground Distribution 28

Figure 18 – Crossarm and Bracket Pole Configuration Examples on Feeder X (obtained using Google Streetview) 29

Figure 19 – Conductor Spacing for Bracket Configuration 29

Figure 20 – PV DG Model Parameters 31

Figure 21 – Load Modelling Approximations 32

Figure 22 – Load Modelling Approximations [46] 33
Figure 23 – Solar PV Solar Monthly Production Variation Factor 34
Figure 24 – Hereford Ranch Algorithm Applied to Optimal DG Sizing [6] 37
Figure 25 – Load Duration Curves for IEEE 37 Bus Reliability Test System [23] 39
Figure 26 – An Unbalanced Distribution System with Branch Currents and Harmonic Currents [13] 41
Figure 27 – Flowchart of the MO Evolutionary Algorithm used in [28] 46
Figure 28 – Singh & Verma's Results: Impact Indices Comparison for DG Penetration on IEEE 16 and 37 Bus Systems 48
Figure 29 – PV Curve for Voltage Stability Analysis [13] 51
Figure 30 – Deferral Time due to Current Decrease and Increase [39] 54
Figure 31 – Flowchart of the Successive Elimination Method [40] 58
Figure 32 – Multistage Planning in Wang et al [40] 58
Figure 33 – Three Stage Techno-Economic Technique for Optimal Siting, Sizing and Financial Evaluation of PV DG for Minimization of: Real Power Loss, Present Value of Future Asset Reinforcement and Transmission Peak Demand Cost 64
Figure 34 – 25 Candidate Nodes (red) and 7 Feasible Nodes (green) Ranked by Power Loss Sensitivity 66
Figure 35 – Flowchart of the Genetic Algorithm [36] 70
Figure 36 – Roulette Wheel Selection [43] 71
Figure 37 – One Point Crossover Scheme [43] 72
Figure 38 – Mutation in a Binary Encoded Chromosome [43] 72
Figure 39 – Objective 1: Power Loss Minimization & Percent Reduction due to DG 83
Figure 40 – Objective 1: Total Optimal DG Output (for All 7 Optimal Locations) by Month 84
Figure 41 – Base Case Voltage Profile for Feeder X using January 2010 Peak Loading 84
Figure 42 – Objective 2: Minimization of Present Value of Future Asset Reinforcement & Percent Reduction due to DG 85
Figure 43 – Objective 2: Total Optimal DG Output (for All 7 Optimal Locations) by Month 86

Figure 44 – 2010 Peak Demand Variation at Transmission Station Upstream of Feeder X..... 87

Figure 45 – Objective 3: Minimization of Peak Demand Charges Paid to Transmitter by LDC & Percent Reduction due to DG 87

Figure 46 – Objective 3: Cost Savings and Optimal DG Penetration by Month 88

List of Tables

Table 1 - Ontario Power Authority FIT Program Price Schedule (Aug. 2010) 2

Table 2 – Load Type and Exponent Value [12] 51

Table 3 - Candidate and Feasible Nodes Sorted by Power Loss Sensitivity Index Values 67

Table 4 - Experimental Verification Results of Power Loss Sensitivity Method 68

Table 5 - Varying GA Parameters to Determine Optimal Parameters (* indicates the maximum number before CYMDIST memory became overloaded) 73

Table 6 - Present Value Replacement Costs for Distribution Equipment 78

Table 7 - Voltage Profile Improvement Values for Objective 1 83

Table 8 - Savings over 5 Year Planning Horizon Incurred by each Objective 89

Chapter 1 – Introduction

1.1 – Background

Traditional power systems met load growth demands through installation of centralized large generation plants, transmission lines and towers and transformer stations as well as distribution infrastructure. Figure 1 shows the traditional power delivery structure, from centralized generation to long haul transmission distribution. Distributed Generation (DG) is a small source of electric power generation ranging in size from less than a kW to tens of MW that is not part of the central power system and is located close to the load, i.e., in the green distribution area in the figure.

In 2009, Ontario utilities were mandated to connect renewable generation to the grid under the Feed-In-Tariff (FIT) program under the Green Energy and Economy Act of 2009. The FIT program was introduced to help phase out large coal-fired electricity generation plants and increase the amount of renewable sourced DG in Ontario's power supply mix. The FIT program provides government funded financial incentives to generator applicants who use renewable energy sources, specifically, by offering long-term (20 years) fixed-price rates of return on real power produced through renewable generation sources [1]. Solar photovoltaic (PV) systems are offered the highest generation rates at 80.2 ¢/kWh as shown in Table 1 and therefore are the most common type of generation applications since program inception. Note that there is no escalation for solar PV rates for the duration of the contract.

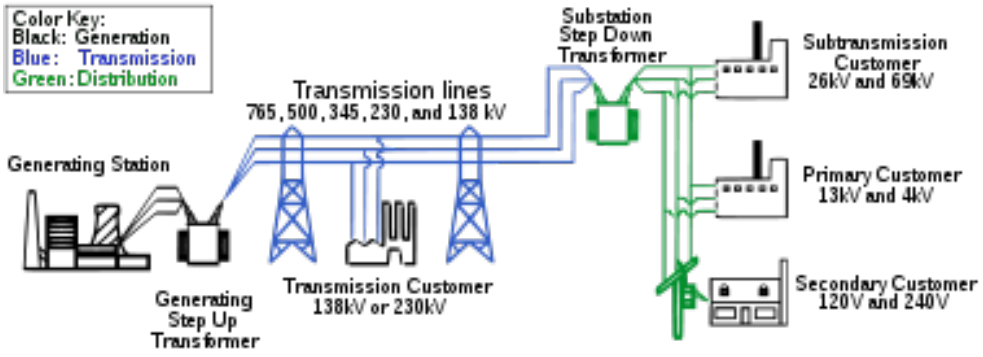

Figure 1 - Traditional Power Delivery Topology

Feed-In Tariff Prices for Renewable Energy Projects in Ontario August 13, 2010			
Renewable Fuel	**Size tranches**	**Contract Price ¢/kWh**	**Escalation Percentage[5]**
Biomass[1,2]			
	≤ 10 MW	13.8	20%
	> 10 MW	13.0	20%
Biogas[1,2]			
On-Farm	≤ 100 kW	19.5	20%
On-Farm	> 100 kW ≤ 250 kW	18.5	20%
Biogas	≤ 500 kW	16.0	20%
Biogas	>500 kW ≤ 10 MW	14.7	20%
Biogas	> 10 MW	10.4	20%
Waterpower[1,2,3]			
	≤ 10 MW	13.1	20%
	> 10 MW ≤ 50 MW	12.2	20%
Landfill gas[1,2]			
	≤ 10MW	11.1	20%
	> 10 MW	10.3	20%
Solar PV			
Rooftop	≤10 kW	80.2	0%
Rooftop	> 10 ≤ 250 kW	71.3	0%
Rooftop	> 250 ≤ 500 kW	63.5	0%
Rooftop	> 500 kW	53.9	0%
Ground Mounted	≤ 10 kW	64.2	0%
Ground Mounted[2, 4]	> 10 kW ≤ 10 MW	44.3	0%
Wind[2]			
Onshore	Any size	13.5	20%
Offshore	Any size	19.0	20%

Table 1 - Ontario Power Authority FIT Program Price Schedule (Aug. 2010)

As of April 1, 2011, the FIT program has received applications totalling approximately 180MW of micro-FIT (under 10kW) connections, and 5500MW of FIT (over 10kW) of PV connections. With a significant increase in PV installations over a relatively short period of time, the majority of mid-size local distribution companies (LDCs) are unsure of the technical impact of DG connections on power distribution systems and the investment required to make a traditional power distribution system "green energy ready". The FIT program requires the LDC to conduct a Distribution Availability Test (DAT) to evaluate the "readiness" of the distribution system to accept generation (the transmission level counterpart is the Transmission Availability Test performed by transmission utilities). The DAT is specific to the LDC's system characteristics and the amount of generation being connected.

While larger utilities have commissioned engineering studies to investigate operational and protection issues due to bidirectional power flows introduced by DG, to date, mid-size and smaller utilities generally use high-level criteria for the DAT, e.g. DG connected capacity shall not exceed 20% of the nearest distribution transformer (pole mounted or pad mounted) to prevent reverse power flow [2]. In addition to meeting regulatory requirements in connecting DG, LDCs recognize that an increase in DG can defer investment in assets such as distribution transformers and lines; therefore, utility planners are interested in quantifying the technical and economic effects of increasing DG penetration on the distribution system as part of an asset management strategy. Although decision on DG placement and sizing are not made by LDCs, studying the optimal siting and sizing of DG aids the utility planner in estimating the network impacts of DG and can provide the basis for policies or financial incentives encouraging DG uptake in preferred locations.

1.2 – Thesis Scope and Objectives

This thesis takes the LDC's view on studying the technical benefit and translating that into economic savings due to PV DG uptake on an actual distribution feeder in the Kingston Hydro distribution system by optimal siting and sizing PV DG. The objectives for this thesis are as follows:

a) Select and collect monthly loading data from a real distribution feeder in the Kingston Hydro System, referred to in this study as Feeder X, for a typical one year period.
b) Collect PV generation data from an actual PV installation for a typical one year period and identify a monthly solar generation variation derating multiplier.
c) Gain experience with, and interface, industry standard software tools CYMDIST and MATLAB. Create a feeder model using CYMDIST, implement the optimization algorithm in MATLAB as the back-end programming engine and interface the two applications using CYME's Component Object Model (COM) module.

d) Identify optimal sites for PV DG location on a distribution feeder based on real power loss sensitivity.

e) Employ an optimization algorithm to determine the optimal penetration limit of solar PV DG using the following objective functions independently:

    a. Minimization of real power loss resulting in reduced annual distribution loss.

    b. Minimization present value of future asset investment costs (by maximizing asset deferral) due to DG offset of asset loading.

    c. Minimization of monthly demand peaks resulting in reduced transmission charges for the LDC.

f) Evaluate results from feeder data relative to the entire Kingston Hydro distribution system data over a planning period of five years. Five years is a common capital project planning cycle in the utility industry and is used at Kingston Hydro. Monthly solar output and feeder load variations are incorporated as are annual load growth and load factor variations.

1.3 – Thesis Outline

This thesis is divided into seven chapters as follows:

Chapter 1 – Introduction

This chapter introduces the thesis topic and structure.

Chapter 2 – Theory

This chapter describes general issues related to DG optimal siting and sizing emphasizing solar PV DG uptake on utility distribution systems. The nature of the optimal siting and sizing problem, the optimization techniques, and technical and economic objectives used in research literature are also discussed.

Chapter 3 – Feeder & Generator Model Development in CYMDIST using Monthly Load and Generation Profiles

This chapter describes the actual medium voltage distribution feeder from the Kingston Hydro distribution system. The feeder structure (voltage, conductor type, number of overhead and underground line sections) is presented. Based on the physical layout of the feeder, the method for identifying candidate and feasible nodes for PV units is discussed. The load flow study, technical constraints, load type, load model and load growth rates are reviewed. A typical annual load profile of the feeder is presented and "discretized" to give monthly feeder peak loading conditions. A monthly generation factor for solar generation, obtained from an actual 9.88 kW PV microFIT installation on Kingston Hydro's system, is also described and applied to the simulations. To apply these annual and monthly values across a multi-year planning period, specifically five years in this study, annual load growth variation must be taken into account, and a typical value based on historical data is selected.

Chapter 4 – State of the Discipline

This chapter presents a literature review of other work done on optimal siting and sizing of DG. In academia, optimal siting and sizing of DG is well researched and this section presents the evolution of techniques and objective functions in studying the optimal allocation of DG on distribution networks. The chapter concludes with a justification of the work performed in this thesis.

Chapter 5 – Problem Formulation and Execution: Power Loss Sensitivity Method for Optimal Siting, Genetic Algorithm for Optimal Sizing, Objective Functions and NPV Analysis

Chapter 4 presents the three stage technique developed to assess the economic benefit of optimal siting and sizing of DG to the LDC. First, power loss sensitivity analysis is applied to the feeder model to identify candidate and feasible nodes thereby ranking the most optimal DG locations. A continuous domain Genetic Algorithm (GA) is then applied to identify optimal PV DG size. The main GA operators such as selection method and mutation rate are explained in the context of optimal sizing of DG. Finally,

the individual objective functions adapted to the optimal siting and sizing problem which are used to drive the GA to an optimal sizing solution are presented.

Chapter 6 – Results and Discussion

Chapter 6 presents simulation results obtained by applying the genetic algorithm to Feeder X and comparing the results of the three individual objective functions. Since the asset reinforcement deferral objective is an instantaneous capture of the savings due to reduced loading from DG, while both the minimum loss and minimum transmission system delivery peak demand objectives are monthly cash flows, the results are treated with a Net Present Value analysis over a defined, i.e. five years, planning horizon, brought back to a present value savings and compared. Moreover, because load and generation conditions are dynamic, a monthly resolution for the financial analysis is chosen, so that it coincides with metering, billing and financial reporting intervals which all occur monthly [3]. The chapter concludes with a discussion of the results obtained in this work.

Chapter 7 – Conclusions and Recommendations for Future Work

This chapter presents conclusions as well as recommendations for future work.

Chapter 2 – Theory

2.1 – The Case for Renewable Generation

The utility industry is required to meet increasing power demands while effectively managing capital investments and operating costs, and, at the same time, maintaining or improving existing power quality and reliability. Ontario's electricity infrastructure is aging and may soon require large scale upgrades if load growth continues to increase. Encouraging electricity conservation and promoting uptake of renewable generation, especially distributed generation (DG) are the two key approaches to reducing dependence on, and future investments in, centralized power plants, long haul transmission systems and distribution system capacity upgrades. To improve the uptake of DG, it is necessary to fully understand the technical impact of DG on the existing power delivery infrastructure to build a viable business case in favour of increasing DG in Ontario's power supply mix.

Figure 2 shows the 2007 supply mix as predominantly nuclear, hydroelectric and coal. Coal fired generation produces large amounts of CO_2 emissions and is the least desirable generation source and the province's goal is to phase out coal plants by achieving increased renewable generation and conservation targets. In June 2006, the Ontario Ministry of Energy released its Target Supply Mix Directive (shown in Figure 3) as part of the Integrated Power System Plan to be implemented by 2025. Both renewable energy and conservation reduce the peak power demand requirement, which can then be met by cleaner sources such as natural gas and nuclear generation resulting in fewer emissions. While renewable energy uptake is facilitated by the FIT program, conservation is currently being implemented by government subsidized energy retrofit (appliance upgrade) programs targeted at residential and commercial customers. Moreover, as of January 1, 2010, the Distribution System Code was amended by the OEB to mandate LDCs to set and meet annual conservation targets as a condition of license – a requirement which has raised the importance of conservation in utility planning and operations.

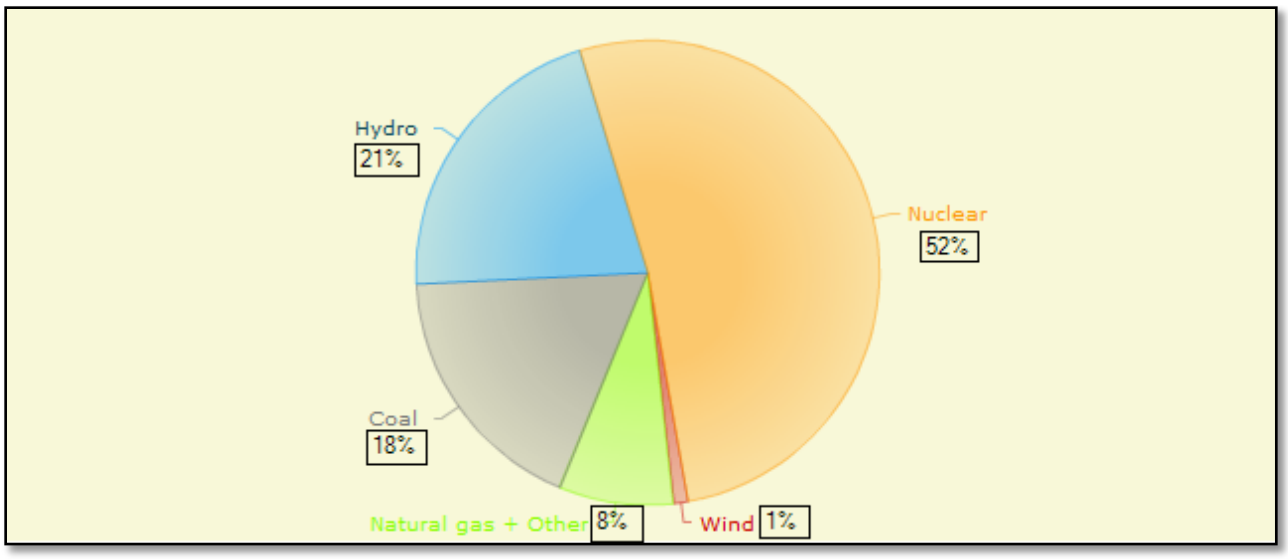

Figure 2 – 2007 Ontario Supply Mix [4]

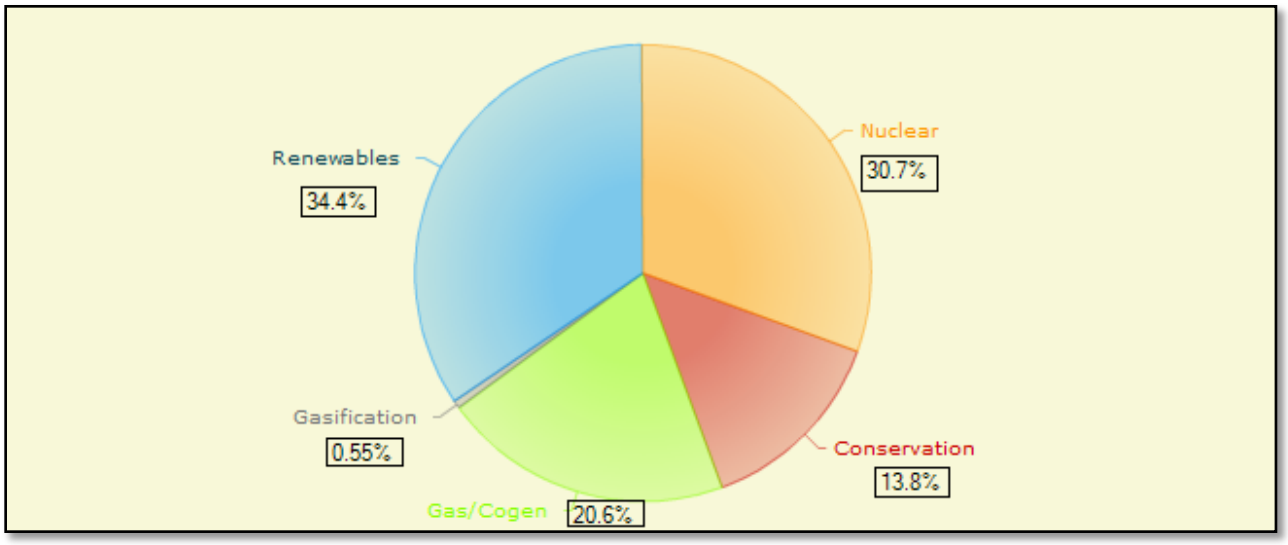

Figure 3 - Ontario's Target Supply Mix for 2025 [4]

Small DG installations, including solar PV, are becoming increasingly attractive to utilities and consumers because these units produce energy close to the load, and are more efficient (less losses), easier to site and have less environmental impact. DGs are primarily installed on the distribution and subtransmission networks. Their main technical and economic benefits include [5]:

- Reduced line losses
- Voltage profile improvement
- The potential for improved reliability and security
- Reduced GHG emissions from central power plants
- Reduced or deferred investment in generation, transmission and distribution infrastructure upgrades due to relieved T&D congestion
- Lower operating costs due to peak shaving

Several optimization studies have been performed to quantify these benefits and identify DG penetration threshold limits by optimally locating and sizing DG to improve a particular objective, or a combination of objectives, and these will be discussed next.

2.2 – Optimal Siting and Sizing of Distributed Generation

2.2.1 – Load Flow Equations

DG siting and sizing is analogous to the optimal capacitor allocation and sizing problem. The exact solution of the combined siting and sizing problem can be obtained by applying load flow simulations to the complete enumeration of all feasible combinations of sites and sizes of DG in the network. The load flow equations are obtained from basic Kirchoff's Laws [6]:

$$P_i - PD_i = \sum_j |V_i||V_j|Y_{i,j} \cos(\theta_{i,j} + \delta_j - \delta_i) \quad (2.1)$$

$$Q_i - QD_i = \sum_j |V_i||V_j|Y_{i,j} \sin(\theta_{i,j} + \delta_j - \delta_i) \quad (2.2)$$

where V is bus voltage, δ is the angle associated with V, $Y_{i,j}$ is the element of the bus admittance matrix, θ is the angle associated with $Y_{i,j}$, P and Q are the active and reactive power generation values, and $PD$and QD are the active and reactive power consumption (demand) values, respectively. The solutions to these

equations are constrained by active and reactive power generation limits and voltage variation limits as follows:

$$P_i^{Min} \leq P_i \leq P_i^{Max} \tag{2.3}$$

$$Q_i^{Min} \leq Q_i \leq Q_i^{Max} \tag{2.4}$$

$$V_i^{Min} \leq V_i \leq V_i^{Max} \tag{2.5}$$

where P_i^{Min} and P_i^{Max} are the lower and upper limits of active power generation, Q_i^{Min} and Q_i^{Max} are the lower and upper limits of reactive power generation and V_i^{Min} and V_i^{Max} are the operating voltage limits at each bus.

Traditional methods such as Newton Raphson and Fast Decoupled Power Flow are effective for "well conditioned" power systems but tend to encounter convergence problems with distribution systems because distribution systems are radial or weakly meshed, have a low X/R ratio, feature a mix of low and high impedance elements (e.g. switches, voltage regulators etc) and have unbalanced loads. A more suitable algorithm for distribution systems such as the ladder technique (backward forward sweep) or power summation must be used. CYMDIST performs load flow analysis using the power summation method, i.e., an iterative voltage drop analysis method designed for radial or weakly meshed systems [7] which computes the power flows at every section within a specified number of iterations. Convergence is achieved when the solutions, i.e. calculated voltages, fall within the specified tolerance value. This study uses unbalanced voltage drop which assumes that the load is not distributed equally among all phases, at a tolerance of 0.01% V and 40 iterations. The voltage thresholds are set to Kingston Hydro's normal operating voltage range, i.e. voltage must not exceed 105% nominal and not dip below 95% nominal and are a power flow constraint [8].

2.2.2 – Optimal DG Allocation

Since the optimal DG allocation and sizing problem suffers from "combinatorial explosion," the application of heuristic algorithms and artificial intelligence in solving optimal DG allocation is justified. This is because although analytical methods are more accurate compared with heuristic methods for smooth objective functions, the solutions for a non-smooth, i.e. discrete, problem such as optimal DG allocation are likely to be trapped in local optima. In contrast, heuristic methods are based on a systematic random exploration of the solution space increasing the chances of finding the global optimum.

The tasks of optimal siting and optimal sizing are decoupled and solved separately such as in [9] where the locations are assumed fixed and the DGs are then optimally sized for the improvement of a specific objective. Inappropriate selection of location and size of DG can lead to greater system losses than the base case losses without DG, therefore, it is of interest to the distribution planner what the optimal threshold of DG penetration is for a given system, a series of objectives and at a given load condition. Research literature shows that several heuristic optimization algorithms applied to the optimal DG siting and sizing problem including genetic algorithm, tabu search, differential evolution, particle swarm optimization, simulated annealing, harmony search, artificial bee colony algorithm as well as hybrid algorithms. Artificial intelligence techniques such as fuzzy logic [10], [11], have also been applied.

From 2004 onwards power loss sensitivity and voltage sensitivity factors have been applied to optimal DG siting as in [12] and [13]. These siting methods are discussed in detail in Section 4.2 "Previous Work on Optimal DG Siting using Sensitivity Factors". The power loss sensitivity factor is derived from the "exact loss formula", P_L, which is widely used in the capacitor allocation problem and gives the real power loss in a system [25]:

$$P_L = \sum_{i=1}^{N} \sum_{j=1}^{N} \left[\propto_{ij} \left(P_i P_j + Q_i Q_j \right) + \beta_{ij} \left(Q_i P_j - P_i Q_j \right) \right] \tag{2.6}$$

where

$$\alpha_{ij} = \frac{r_{ij}}{V_i V_j}\cos(\delta_i - \delta_j) \quad (2.7)$$

$$\beta_{ij} = \frac{r_{ij}}{V_i V_j}\sin(\delta_i - \delta_j) \quad (2.8)$$

The exact loss formula is then linearized to give the sensitivity of power loss at a specific node after each load flow simulation. The nodes are then ranked in descending order of loss sensitivity to identify the most optimal location for DG to minimize power loss. The sensitivity factor, α_i, is thus the partial derivative of the exact loss formula with respect to the injected power, given by [13] as:

$$\propto_i = \frac{\partial P_L}{\partial P_i} = 2\sum_{i=1}^{N}(\propto_{ij} P_j - \beta_{ij} Q_j) \quad (2.9)$$

Voltage stability is an alternate method of ranking nodes to identify optimal sites for DG. For example, in [13], the following simple voltage stability index is derived based on a two bus distribution feeder model:

$$SI(r) = 2V_1^2V_2^2 - V_2^4 - 2V_2^2(PR + QX) - |Z|^2(P^2 + Q^2) \quad (2.10)$$

where V_1 and V_2 are the voltages at the sending and receiving ends of a line (shown in a typical two-bus distribution system in Figure 4) P and Q are the real and reactive power loads on the receiving end of a line, R is the line resistance, X is the line reactance and Z is the line impedance.

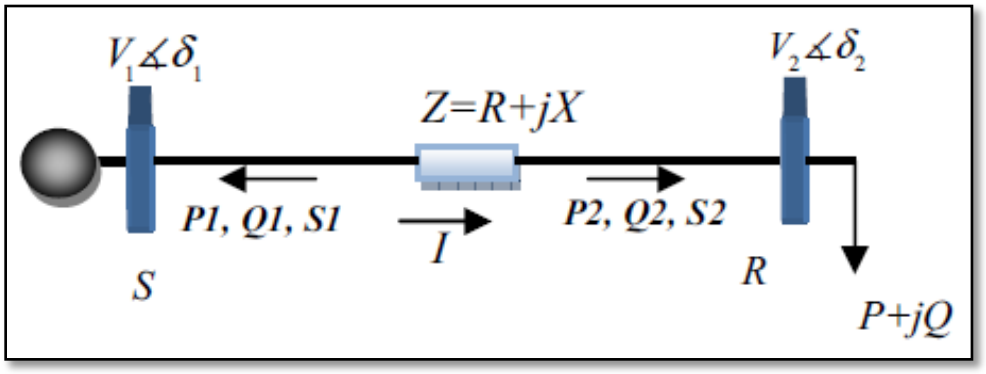

Figure 4 - One Line Diagram of a Two-Bus Distribution System [13]

Research literature shows that the application of transmission level techniques to distribution systems is becoming more common with the introduction of bi-directional power flows due to DG. For example, voltage stability indices are typically used in transmission systems to improve power transfer capacity and plan for voltage collapse contingencies. The node at which the stability index is at a minimum is the most sensitive to voltage collapse. In the distribution system, a node with a low stability could benefit the most by placement of the DG at that location. Both power loss sensitivity and voltage stability indices are calculated based on the peak load demand condition when losses are at their maximum.

Optimal DG sizing is a well investigated problem where the DG is typically modelled as optimal active power injection. The most common objective found in academic literature is real power loss minimization. Power loss is inherent to the power delivery system and consists of power dissipation in electrical system components such as transmission and distribution lines, transformers and measurement devices due to internal resistance. Real power loss is defined as $P_{loss} = I^2R$, or in terms of voltages and angles as a variation of $P_{loss} = \frac{V^2}{R}$ [6]:

$$Loss = \frac{1}{2}\sum_i \sum_j G_{i,j} \left(V_i^2 + V_j^2 - 2 \times V_i \times V_j \times \cos\left(\delta_j - \delta_i\right)\right) \quad (2.11)$$

where $G_{i,j}$ is the conductance of line i to j, V_i and V_j are line voltage and δ_i and δ_j are the angles at line i to j ends, respectively. Other objectives include reliability improvement by quantifying and reducing the cost of interruption (avoided by having DG operational in islanded mode), power quality improvement by total harmonic distortion (THD) reduction, DG installation, operation and maintenance (O&M) cost reduction, minimizing peak demand to defer asset reinforcement investment, and GHG emission reduction. This work is unique in that it uses optimal DG sizing as part of a comprehensive three stage approach quantifying the technical impact of PV DG as financial savings for the LDC on a real

distribution feeder. Moreover, optimal sizing of DG due to equipment loading relief to determine asset lifetime extension and deferral of reinforcement costs is relatively recent, and in combination with the other technical objectives of real power loss minimization and peak demand minimization, results in a novel and definitive tool that utility engineers can use to determine the economic savings due to PV DG on the distribution system.

As of June, 2011 Kingston Hydro has received 70 microFIT applications and 6 FIT applications totalling 1789 kW of solar PV generation connection applications. This thesis quantifies the technical benefits of increased uptake of solar PV DG installations on a typical urban distribution feeder from a distribution utility's view and translates them into economic savings over a five year planning horizon. The cumulative impact of several small solar PV generation is expected to result in reduced power losses, reduced peak loading and transmission costs, as well as an increase in present value of existing assets (due to reduced equipment loading and extended lifetime).

2.3 – Background Information for Feeder Model Development

2.3.1 – Description of Kingston Hydro's Distribution System

Kingston Hydro's service territory supplies approximately 26, 000 customers bounded by the Cataraqui Creek on the West, the Great Cataraqui River on the East, Lake Ontario on the South and Highway 401 to the North. Kingston Hydro also serves the Canadian Forces Base (CFB) Kingston on east of the Cataraqui River, accessible by a bridge highway. The primary distribution voltage for Kingston Hydro is 4.16kV, also referred to as "5kV". The distribution system is fed by 17 distribution stations located throughout the City which are themselves fed by subtransmission voltage (44kV) feeders originating from two transmission stations. The distribution system is one of the earliest installed systems in Canada, with the original city built in the 1850s and is the main reason for a comparatively low operating voltage, i.e. 4.16kV was a common distribution voltage at the time. Figure 5 shows the Kingston Hydro distribution territory. This map, as well as operating voltages and layout of the

subtransmission, primary and secondary systems can be readily found on the Kingston Hydro website [15].

Figure 5 – Kingston Hydro Distribution Territory

2.3.2 – Overview of Study Feeder

The study feeder, Feeder X, is a primary voltage (4.16kV) distribution feeder located in downtown Kingston and supplies power to residential and commercial customers. Approximately 85% of the feeder consists of overhead conductors and poles including the three phase main trunk, single phase branch subfeeders, and overhead secondary/service feeds. The remaining 15% is made up of underground primary cable sections and all associated switches, terminations and protective devices, i.e. fuses. Figure 6 shows the model built to scale in CYMDIST using an imported GIS file as a background map and 'reads' right to left from source to load. The feeder is supplied by a 3 MVA ONAN (4 MVA ONAF) transformer located in the bottom right hand corner of the figure. The transformer is part of a six

transformer line-up in the oldest substation in Kingston Hydro's system. The test feeder is one of the most heavily loaded feeders on the distribution system, making it an ideal test bed for studies that quantify technical and economic impact of connecting DG.

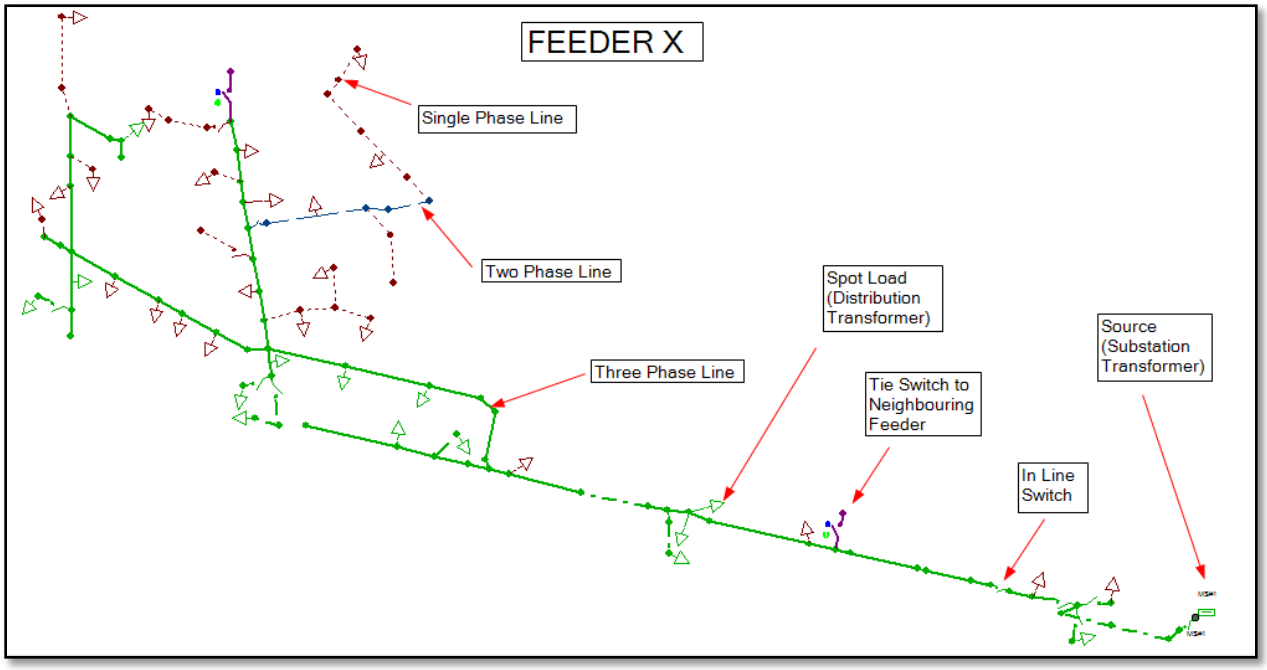

Figure 6 – Test Feeder (Feeder X) in CYMDIST

2.3.3 – Load Data and Load Profile

Kingston Hydro is currently a winter peaking system, although in some parts of the system summer loads are comparable to winter loads as air conditioning demands increase to keep up with increasingly hot summers. Annual and monthly load profiles were captured by the SCADA system for the test feeder during 2010 for the peak loading months of January and June, as well as a shoulder (moderate load) month of October. Shoulder months such as April, May, September and October are characterized by moderate outside temperatures resulting in low heating or air conditioning demand. The current values are totalled at the feeder head end by measurement grade metering CTs located at the substation then transmitted back to the SCADA network at 15 minute intervals.

Figure 7 shows Feeder X's annual load profile in 2010 by phase. The summer load is significantly less than winter load. This is characteristic of feeders located in downtown Kingston where load patterns vary with the presence of students attending Queens University. Figures 8 to 10 show the feeder monthly load variation during the peak months of January, June and October. The feeder phase currents are relatively well balanced compared to other feeders in the system. Distribution systems are inherently unbalanced due to their radial nature and the fact that most loads at the distribution level are unbalanced (fed by single phase lines and their corresponding secondary systems); therefore, current imbalance levels of up to 20% are normal.

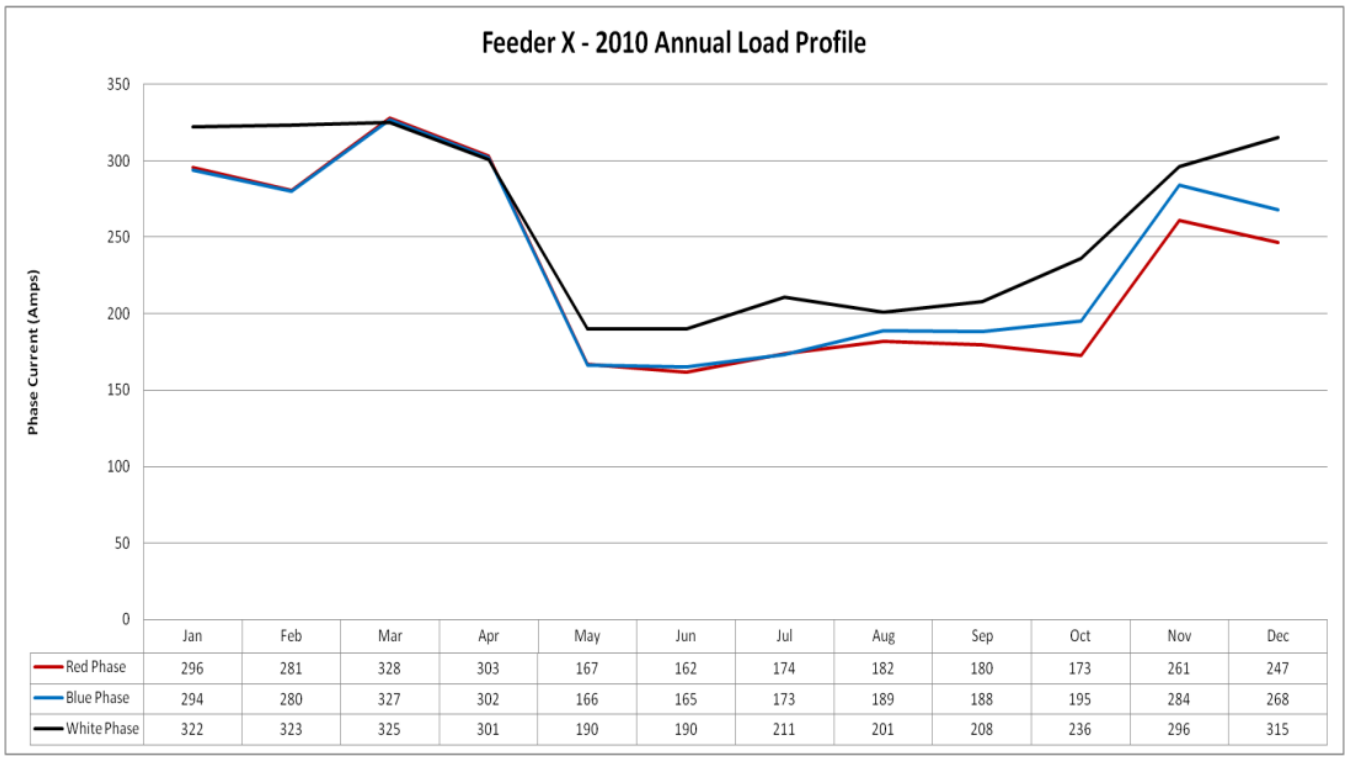

	Jan	Feb	Mar	Apr	May	Jun	Jul	Aug	Sep	Oct	Nov	Dec
Red Phase	296	281	328	303	167	162	174	182	180	173	261	247
Blue Phase	294	280	327	302	166	165	173	189	188	195	284	268
White Phase	322	323	325	301	190	190	211	201	208	236	296	315

Figure 7 – Feeder X Annual Load Profile 2010

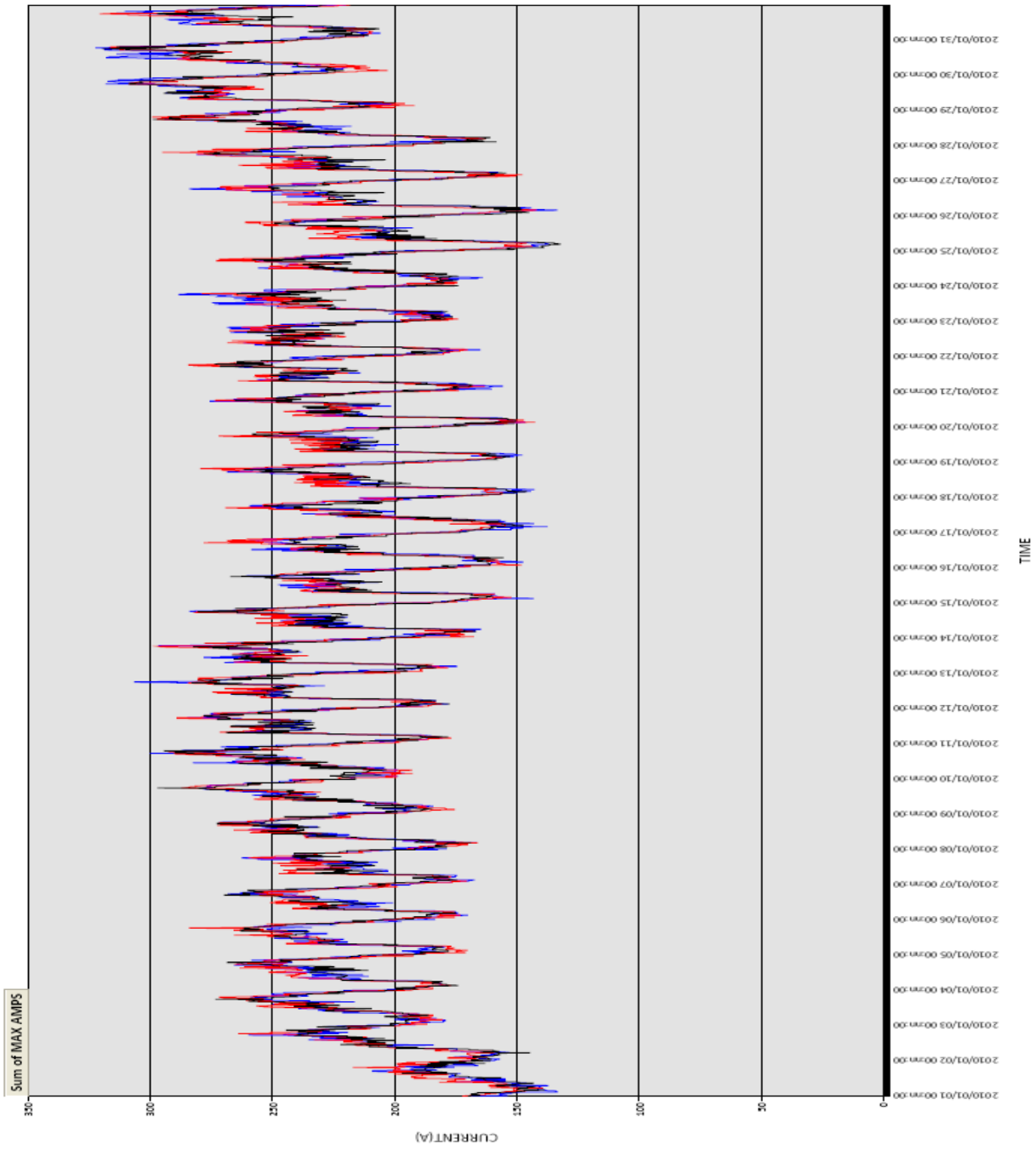

Figure 8 – Feeder X Monthly Load Profile for Winter Peak Month January 2010

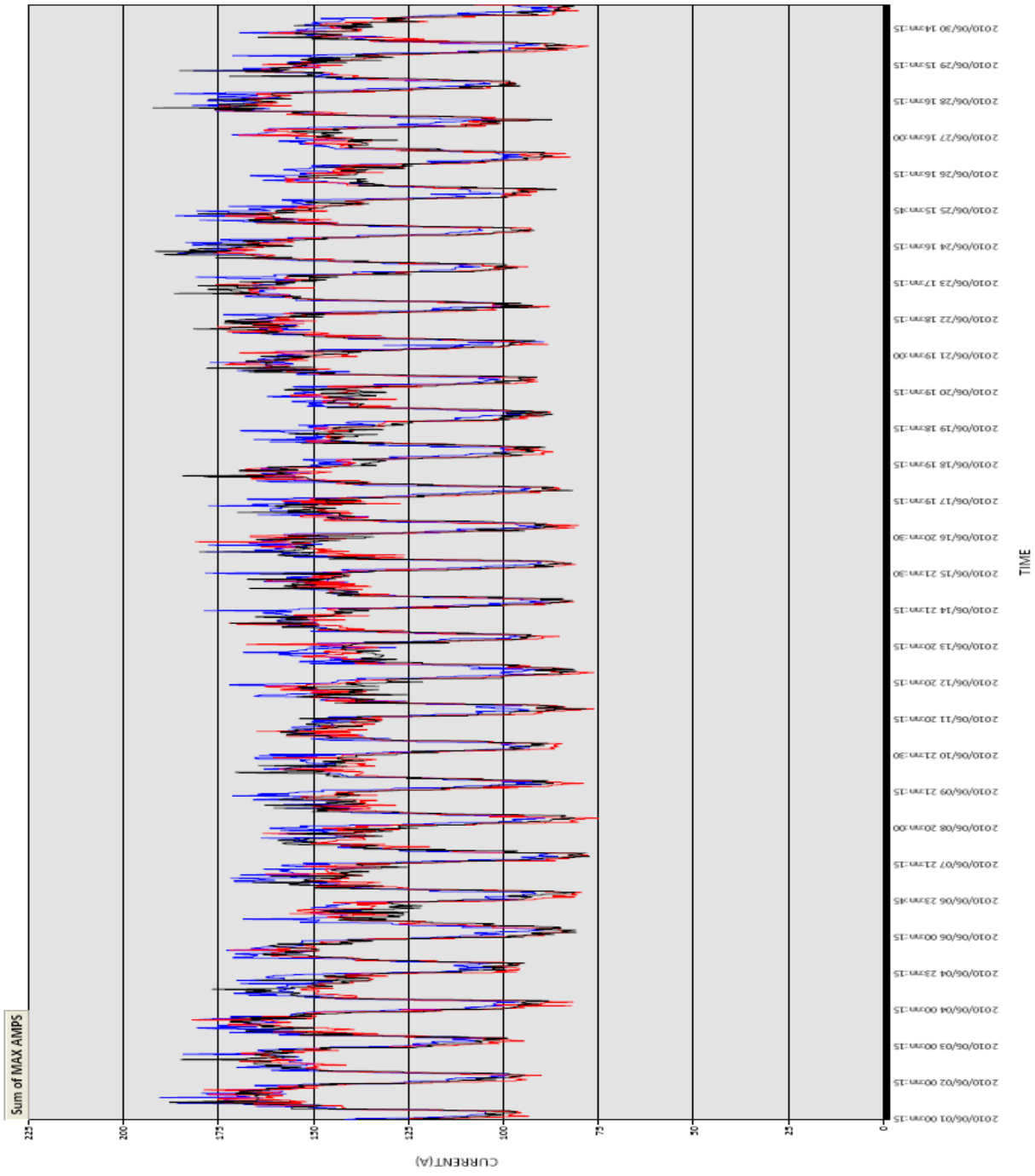

Figure 9 – Feeder X Monthly Load Profile for Summer Peak Month June 2010

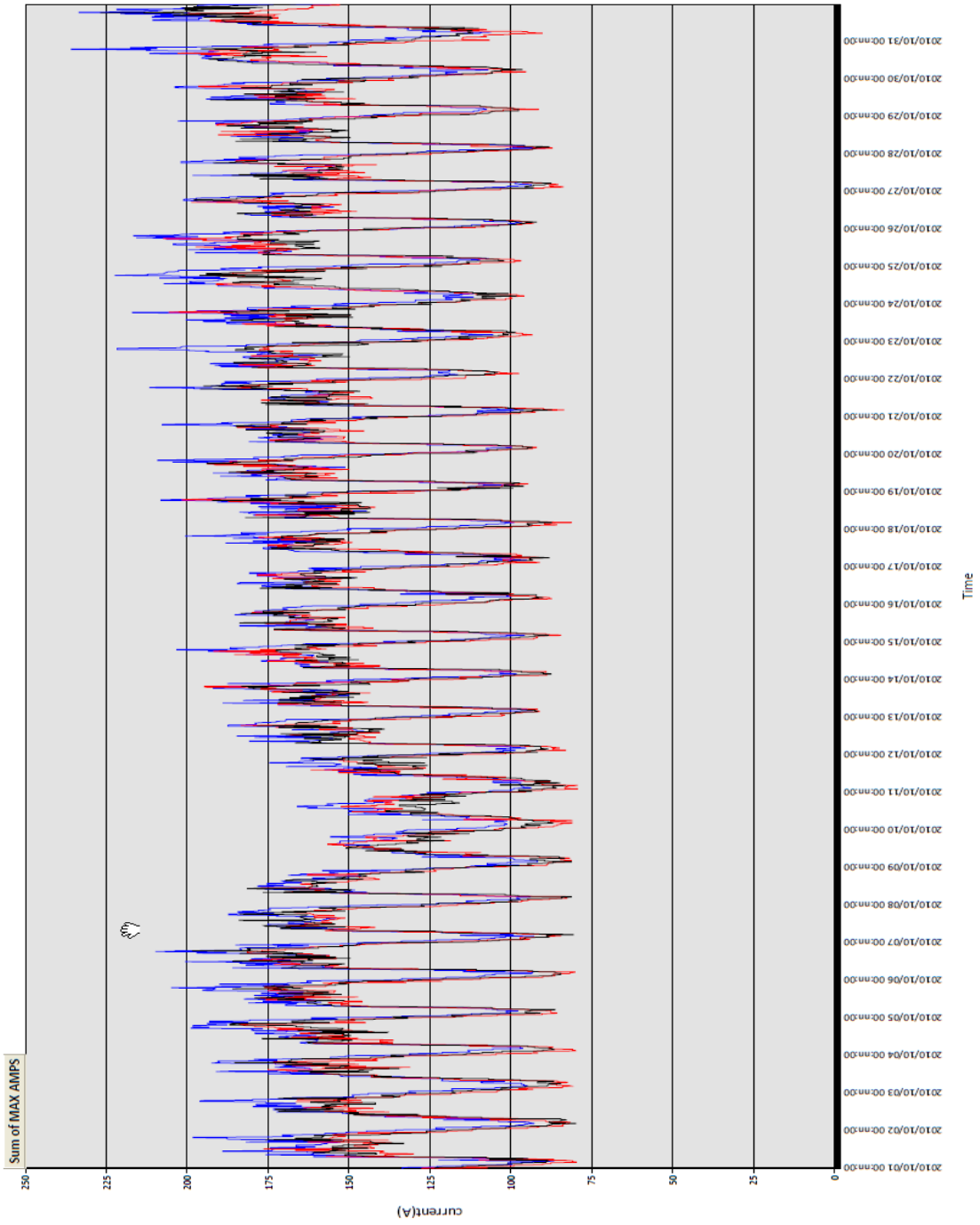

Figure 10 – Feeder X Monthly Load Profile for Shoulder Month October 2010

2.4 – Solar PV Technology in Ontario

2.4.1 – Solar PV Technology Overview

Solar photovoltaic panels, or PV panels, have been commercially available since the 1980s and use semiconductors to convert solar energy into electric energy. Modern PV panels reach up to 15% conversion efficiency and although PV panels generate significantly less electricity in the winter, they can still generate a considerable amount on a sunny January day [16]. To increase energy conversion, PV panels may be ground mounted or roof mounted and may also be attached to motorized tracking units which track the sun across the sky during the day. Large arrays of solar panels are combined to make solar farms, and produce large scale electricity output such as the world's largest solar farm (as of September 2010) in Sarnia, Ontario. The Sarnia plant consists of 80MW of installed generation capacity covering an area of 873, 000 square metres and was installed by First Solar and commissioned by the owner, Enbridge.

In an effort to make PV technology more affordable and accessible to the public, simpler and cheaper methods have been developed. For example, thin film solar panels can now be produced by depositing layers of semiconductors on aluminum foil similar to the process of printing a newspaper [17]. Refer to Figures 11 and 12 for a cross section of a thin film solar PV cell and a thin film solar PV in production, respectively. Another example of improvements to PV technology includes light-guided solar optic lens concentrators based on refractive lens technology known as "concentrated solar" or CPV [18]. Figure 13 shows the various methods used to concentrate light on PV cells to increase generation.

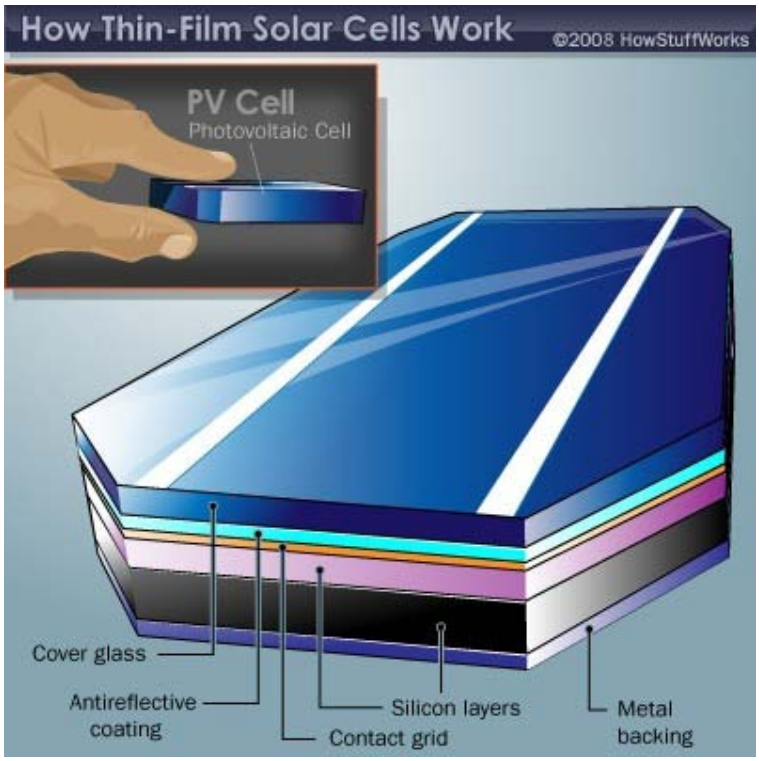

Figure 11 – Thin Film Solar Cell Layers [17]

Figure 12 – Production of Thin Film Solar Panels [17]

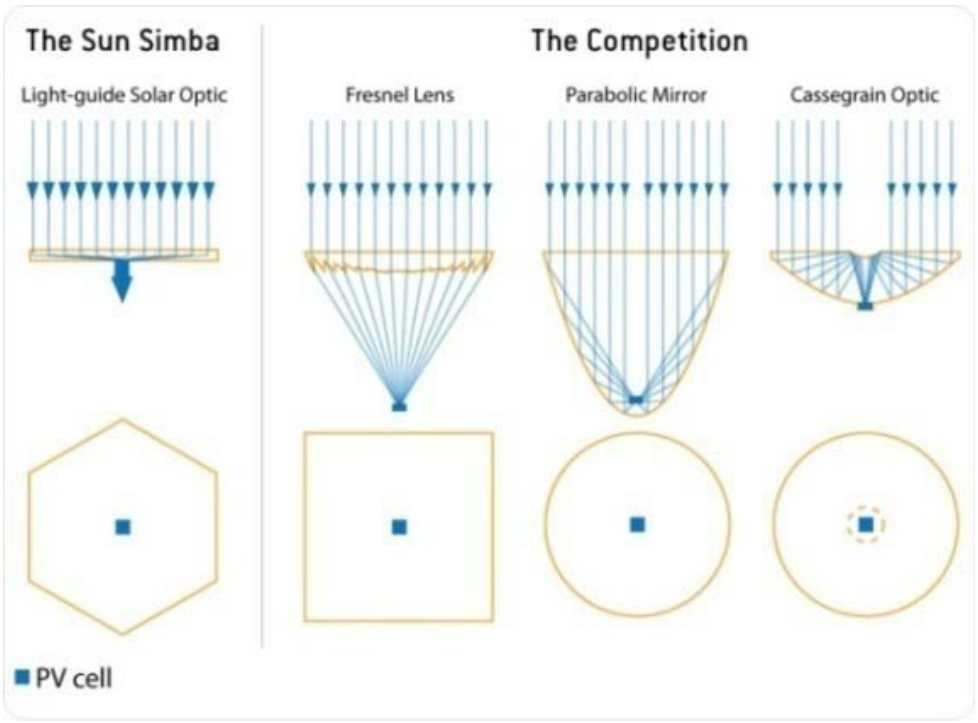

Figure 13 – Light Striking the Light Guided Solar Optic Lens (LSO) is Concentrated to the Optic's Centre Located on a high-efficiency PV Cell. The Sun Simba is Morgan Solar's Product [34]

2.4.2 – Solar PV Inverters

Kingston Hydro tracks the number, owner information, and technical specifications of micro/FIT solar PV installations on a Generator Connections spreadsheet. Applications are evaluated against a micro/FIT installation checklist administered by an electrical technologist. As of June 2011, 30 microFIT applications had been received for 2011, averaging five microFIT applications a month. In 2010, 24 microFIT applications and one FIT application were received, indicating an increased uptake of generation in 2011.

Due to modern inverter technology, inverters operate at unity to 0.95 lagging power factor and inverter efficiencies of over 95%. Typical solar PV inverter manufacturers encountered by Kingston Hydro include Enphase, Solaris, Sunnyboy, Aurora and Solar Edge and meet the C22.7-107.1-01, UL

1741 and IEEE 1547 standards. Figure 14 shows a typical inverter structure in a functional block diagram format [19].

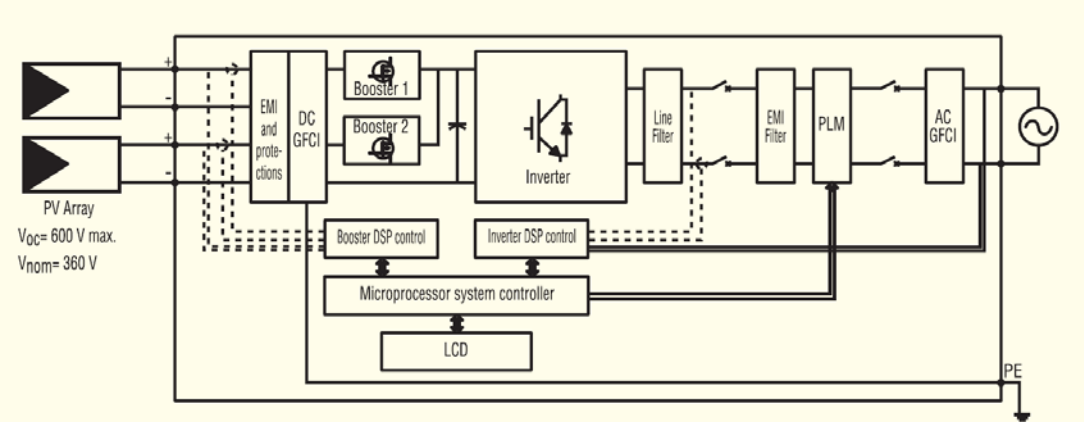

Figure 14 – Typical Inverter Structure

2.5 – Utility Project Planning Horizon

This thesis develops a comprehensive method designed to quantify dollar savings from DG installation, specifically PV DG, due to loss minimization, asset investment deferral and transmission system supply peak demand reduction over a planning horizon of five years. Five years was chosen since this is the utility standard in capital project planning. Every five years, Utilities Kingston (Kingston Hydro's Services Provider) and the City of Kingston develop a joint infrastructure upgrade reconstruction plan and present to the City Council for approval. A ten year internal planning horizon has also been developed for long term electric utility projects to forecast financial needs, however, in the past, this plan has not been part of a formal decision making process and is used only as a reference with the understanding that the further out the proposed project is in the planning horizon, the less accurate the scope and cost.

Chapter 3 – Feeder & Generator Model Development in CYMDIST using Monthly Load and Generation Profiles

3.1 – CYMDIST Modelling Environment and Load Flow Simulation Settings

The software used to model the test feeder is a utility-grade load flow simulation tool developed specifically for distribution systems, CYMDIST, and is operated by Montreal-based CYME International Inc. (now owned by Cooper Power Systems). CYMDIST is widely used in distribution utilities in the U.S, Ontario and Quebec. The base package includes load flow and short circuit simulation tools; however, specialized analyses require additional software modules. One such module was required for this work, specifically, the Component Object Model (COM) module. The COM module allows external applications (in this case MATLAB) to access simulation results and feeder model attributes stored in CYMDIST's back end database. In MATLAB, the "ActiveXServer" utility was used to establish the software "pipe" to CYMDIST. Interfacing the two applications greatly increased the speed of simulation since it enabled automatic update of the PV DG's optimal output after each load flow simulation.

For the load flow simulation, this study used an unbalanced voltage drop algorithm with a convergence tolerance limit set at 0.01% voltage drop and number of iterations at 40 – default values used by CYMDIST. These convergence criteria are relaxed (increased) by the user if the load flow simulation has difficulty in converging, however the simulations run in this work converged successfully with these values. In addition, the voltage constraints are set at 105% and 95% and the capacity constraint is 100% of the conductor current carrying capacity.

3.2 – Detailed Feeder Model

To increase the validity and accuracy of the results, a detailed model of the test feeder was developed using CYMDIST. The model is drawn to scale using an imported GIS map in the background. Figure 15 shows Feeder X with the PV DG at the proposed sites. The three phase feeder trunk is energized at 2.4kV

line-to-ground or 4.16kV line-to-line and is shown in green in Figure 15. Single phase lines are shown as maroon and dashed. The only two phase section is shown as a blue dashed line.

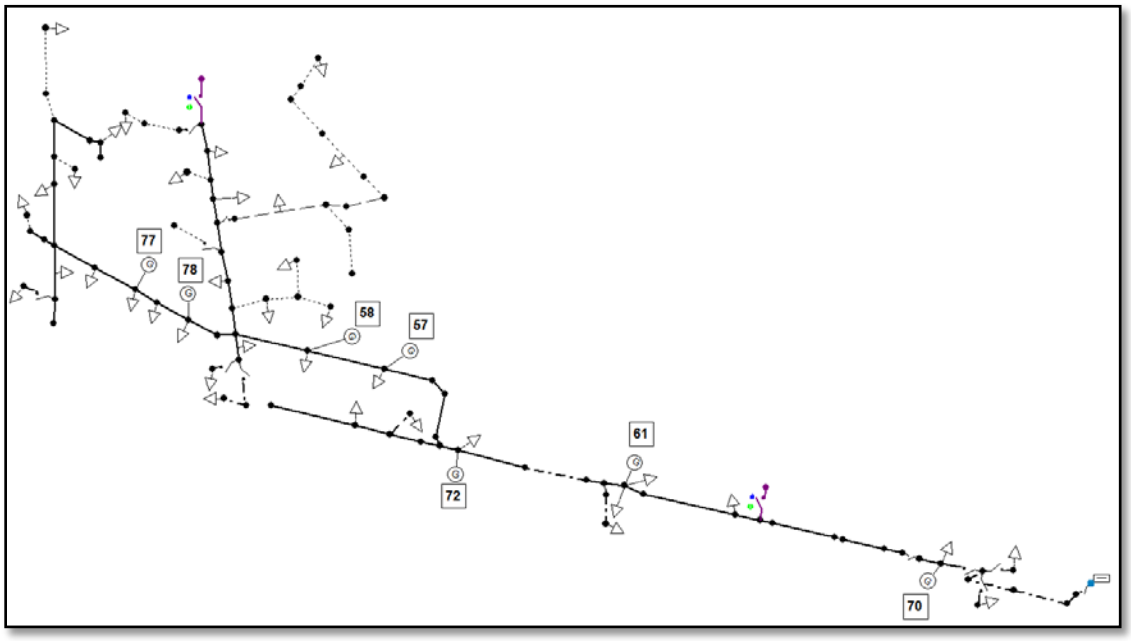

Figure 15 – Feeder X with Electronically Coupled PV DG at Optimal Locations with Corresponding Node Numbers (in boxes)

Feeder X is supplied by a substation transformer rated 3 MVA (ONAN), or 4MVA (ONAF), situated in the utility's oldest substation. This substation transformer steps the 44kV delta connected subtransmission system down to a grounded wye 4.16kV primary distribution voltage. Additional features include 37 spot loads (distribution transformers), 92 nodes (or buses), 71 overhead line sections, 7 candidate PV DG units installed at the top 7 optimal locations, 14 underground cable sections, 15 switches (13 of which are normally closed in line switches and the remaining 2 are tie switches to neighbouring primary feeders indicated in purple in Figure 15). The load mix for this feeder is approximately 65% residential and 35% commercial. A modest load growth rate of 1.06% was estimated from 2009-2010 load data and applied. Load growth in downtown Kingston is quite static since there is no land available for development, and businesses simply set up and leave from existing buildings and

services. Increasingly, conservation and demand management schemes are being targeted at commercial customers and implemented and the program success has also contributed to a low load growth rate in the downtown commercial core.

This study performs optimal sizing of PV DG at 7 fixed locations determined from the optimal siting step. First, all 92 nodes were ranked in descending order of power loss sensitivity by applying the power loss sensitivity factor in the optimal siting step. The top ranked 25 nodes were identified as candidate locations (25 were chosen because this is roughly the top quartile). A subset of the optimal candidate sites list was then selected by identifying those optimal nodes at which distribution transformers (spot loads) were already present, and became the feasible nodes list. The presence of distribution transformers indicates existing service infrastructure where PV DG connections were most likely to occur. This is especially valid on an urban feeder, such as Feeder X, since existing load customers are more likely to install PV DG than prospective proponents who would require land to develop a business or residence. Conversely, if a utility were to find that generation was exceeding local load requirements, the feasible sites are among the first that would be considered for reinforcing equipment such as increasing the rating of the distribution transformer to handle reverse power flow, or increasing the service conductor size.

3.1.1 – Conductor and Cable

To build the feeder model in CYMDIST, a library of overhead conductors and underground cables as well as pole configurations was built. For Feeder X, the main conductor type for three phase overhead lines is 336 KCM aluminum stranded conductors (ASC) with a nominal rating of 480 amps. 336 KCM Al is a bare overhead conductor consisting of 19 strands of aluminum area of 170.5 mm^2 or 336, 000 circular mils. Single phase overhead conductors are either 1/0 aluminum or #2 Copper (in the older sections) with nominal capacities of 230 amps and 310 amps respectively. Figure 16 shows a cross section of aluminum stranded conductor.

Figure 16 – Bare Aluminum Stranded Conductor for Overhead Lines

The underground three phase cable is a 500 MCM vintage paper insulated lead cable (PILC) type with a nominal capacity of 553 amps and the underground single phase feeds are 4/0 copper jacketed cable with nominal capacity of 311 amps (as in Figure 17). The underground cables are formed with a concentric neutral rated 1/3 the capacity of the phase conductors.

Figure 17 – Jacketed Copper Cable used in Underground Distribution

Similarly, a separate neutral sized approximately 1/3 the capacity of the phase conductors is carried on the overhead pole line and located approximate 0.5 m below the phase conductors on the poles. The neutral conductors are sized 1/3 because the primary system is multi-grounded, which means that because of the numerous ground connections at poles, distribution transformers, and customer service feeds, and to a lesser extent, line losses, the maximum return current on the neutral conductor is estimated to be approximately 1/3 the phase conductor current carrying capacity. This is an example of the many rules of thumb used in the distribution system as a result of years of successful operating experience.

3.1.2 – Overhead Line Conductor Configuration

Feeder X's overhead line was initially built in the 1950s using the cross-arm configuration. Modern overhead distribution lines feature a metal stand-off bracket (known as "chicken wing") style that is less visually distracting. Since Feeder X's overhead line was rebuilt in the last decade using modern construction standards, the configuration style is defined in CYMDIST as shown in Figure 18 using typical values obtained from standard installation drawings [20].

Figure 18 – Crossarm and Bracket Pole Configuration Examples on Feeder X (obtained using Google Streetview)

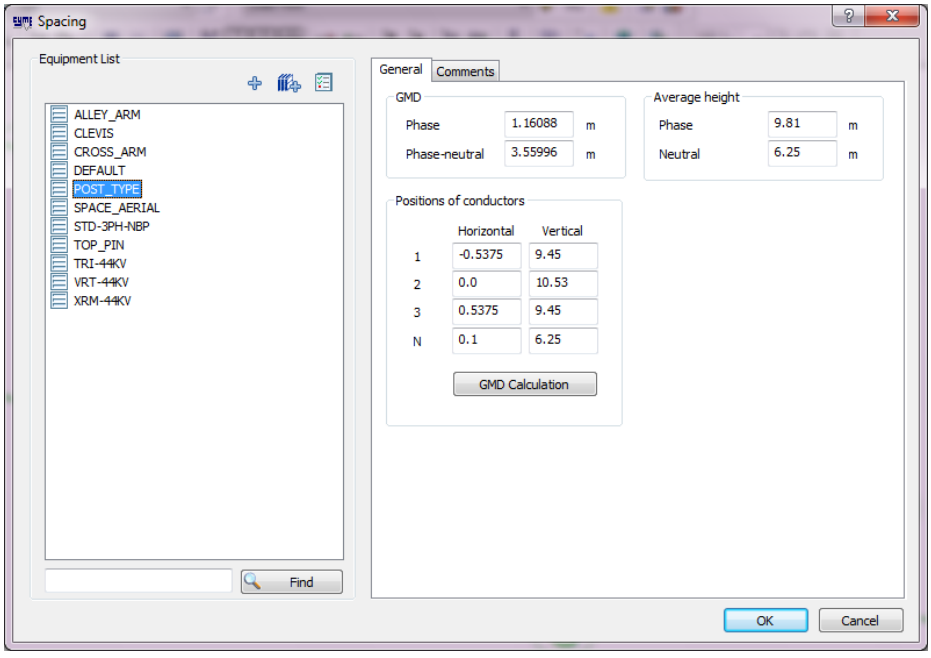

Figure 19 – Conductor Spacing for Bracket Configuration

3.2 – Generator Model

CYMDIST features built-in software models for synchronous, induction and electronically coupled generators. This study used the built-in electronically coupled generator model available in CYMDIST as a simple active power injected source specified at rated primary voltage (2.4kV or 4.16kV) operating at 95% power factor (PF) and fault contribution of 100%. Figure 20 shows a CYMDIST screenshot of the user specified parameters to set up an electronically coupled DG. The rated power is set to a very large value, in this case 3000 kVA, so that the optimal DG size does not exceed the rated power during simulation. The rated voltage is set to line voltage and the active generation field is set at a default value of 5.0kW which varies during the optimization process. The power factor is set conservatively at 95% - most inverters operate at unity power factor, or slightly below. In CYMDIST, the power factor can be defined as positive or negative. A positive power factor indicates that the generator generates both active and reactive power. A negative power factor implies that the generator generates active power and consumes reactive power. The fault contribution is assumed to be 100%, and is only applicable to fault studies, so is therefore outside the scope of this work. In reality, Kingston Hydro, and other LDCs requires the generator inverter to disconnect or "cut out" after a fault within 9 cycles. The ANSI motor group setting is specified when running ANSI standard short circuit studies, therefore, is not applicable to this work which makes use of load flow simulations and Automatic is set as the default. Finally, the Converter field is for informational purpose only.

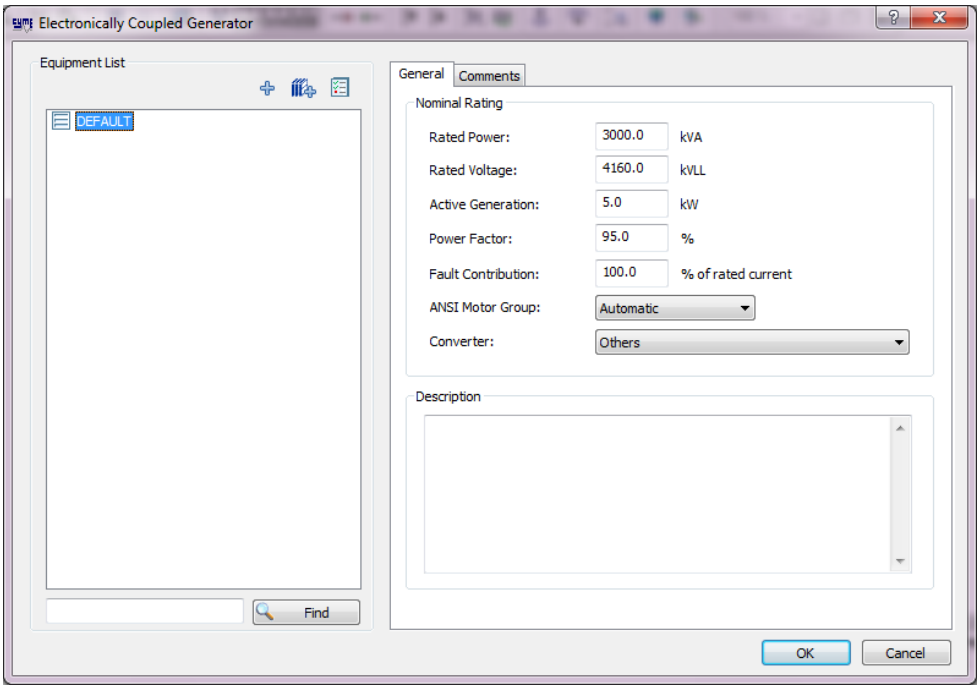

Figure 20 – PV DG Model Parameters

3.3 – Load Model

Distribution system loads are characterized by voltage sensitivity, and most distribution load flow programs offer the following standard models:

- Constant Power – The real and reactive power stays constant as the voltage changes. As voltage decreases, this load draws more current, which increases the voltage drop. A constant power model is typically used to model induction motors.
- Constant Current – The current stays constant as the voltage changes, and the power increases with voltage. As voltage decreases, the current draw stays the same, so the voltage drop does not change.
- Constant Impedance – The impedance is constant as the voltage changes, and the power increases as the square of the voltage. As voltage decreases, the current draw drops off linearly; so the voltage drop decreases. The constant impedance model is good for incandescent lights and other resistive loads.

A typical load mix is 40 to 60% constant power and 40 to 60% constant impedance (see Figure 21 for recommendations found in the classic ABB Westinghouse T&D Reference Book compiled by H.L. Willis). Modelling all loads as constant current is a good approximation for many circuits while modelling all loads as constant power is conservative for voltage drop analysis [20]. In this study, since Feeder X's load is modelled as a composite PZ load, i.e. 40% constant power and 60% constant impedance, because of the winter peaking characteristics of Kingston Hydro's system and the fact that Feeder X supplies residential and commercial load. Note, CYMDIST also allows the user to select the exponential load model (both exponential and second degree polynomial load model representations can be found in literature) as follows:

$$P = P_0 \left(\frac{V}{V_{base}}\right)^{nP} \tag{3.1}$$

$$Q = Q_0 \left(\frac{V}{V_{base}}\right)^{nQ} \tag{3.2}$$

Where P_0 is the nominal active power and Q_0 is the nominal reactive power. Also, nP or nQ = 0.0 means constant-power load, nP or nQ = 1.0 means constant-current load and nP or nQ = 2.0 means constant-impedance load.

Load Modeling Approximations Recommended by Willis (1997a)

Feeder Type	Percent Constant Power	Percent Constant Impedance
Residential and commercial, summer peaking	67	33
Residential and commercial, winter peaking	40	60
Urban	50	50
Industrial	100	0
Developing countries	25	75

Source: Willis, H. L., "Characteristics of Distribution Loads," in *Electrical Transmission and Distribution Reference Book*. Raleigh, NC, ABB Power T&D Company, 1997.

Figure 21 – Load Modelling Approximations

3.3.1 – Load Allocation

CYMDIST provides four load allocation options: connected kVA, consumption in kWh, Rural Electric Association method (REA) and actual kVA (see Figure 22). The connected kVA method assigns the metered load demand defined at the substation among the spot loads in proportion to the distribution

transformer capacity. Similarly, the connected kWh divides the metered demand among the loads in proportion to a load's energy consumption. The REA method apportions the metered demand among the loads according to the kWh and the number of consumers each load type represents. Finally, the actual kVA divides the metered demand among the loads in proportion to the kVA defined for each load. This is useful if the peak load on each section is specified in the load database. The load can be re-allocated to correspond with demand metered at some time other than peak demand. With all of the above methods, the original load kVA is replaced by the new allocated value within the study. This work uses the connected kVA load allocation technique which distributes the substation load demand (entered by the user in amps for each phase) along the feeder according to the connected kVA of the distribution transformers. In CYMDIST, the alternative to performing load allocation is to explicitly assign meters to protection devices at various locations on the feeder and define the demand measured by each meter.

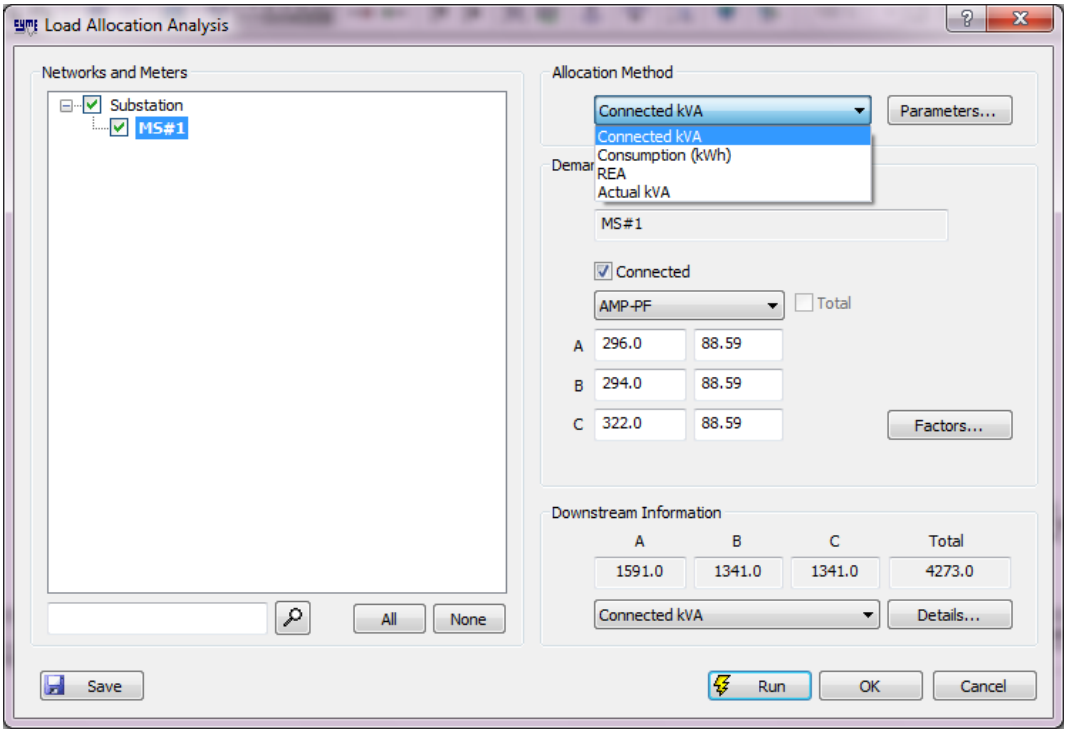

Figure 22 – Load Modelling Approximations [46]

3.3.2 – Annual Load and Generation Profile

Figure 7 in Chapter 2 showed the monthly peak loading variation for Feeder X. The monthly peaks were entered into the CYMDIST feeder model substation demand prior to running load flow simulations for each month in the five year horizon (for a total of 60 months) and for Objectives 1 and 3 (loss minimization and peak demand minimization). Superimposed on the monthly maximum load variation is the monthly variation in solar generation due to weather patterns in Kingston, Ontario. Meter data recorded (from April 2010 to March 2011) from an actual 9.88 kW solar PV microFIT installation was obtained from the metering department, and used to develop a high level solar generation variation "factor" as shown in Figure 23. This solar variation factor is applied to each objective during load flow simulations to account for variations in solar strength due to season. Figure 23 also shows that July is the most productive month for solar PV installations, while December to February are poor PV energy producing months due to overcast weather, snow cover, and weak sunlight. Note, this factor was obtained from eleven months of data. Future work could be performed to refine the solar generation variation to include data from additional years as it becomes available as well as the type of PV technology, location and angle of installation.

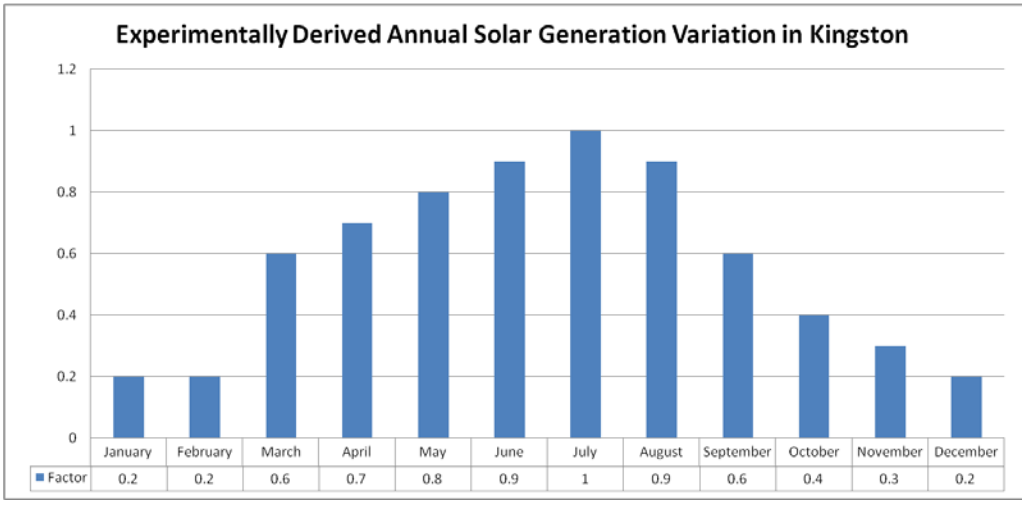

Figure 23 – Solar PV Solar Monthly Production Variation Factor

Chapter 4 – State of the Discipline

4.1 – Previous Work on Optimal DG Allocation

Optimal DG siting and sizing is a well researched topic with work dating back to the early 2000's. The research literature has traditionally emphasized the technical benefits of connecting DG to the distribution system as in [5], [9], [14], [21] and [22] – [24] using a variety of optimization techniques such as the heuristic algorithms (evolutionary programming and genetic algorithm, tabu search, harmony search, simulated annealing, particle swarm optimization), artificial intelligence such as expert systems and fuzzy logic and analytical techniques such as optimal power flow and exhaustive load flow. The most popular technical objectives are active power loss reduction, voltage profile, reliability, and power quality (e.g. THD) improvement. Recent studies, from 2008 onward, have also developed multi-objective approaches to optimizing DG location and size.

In 2003, Borges and Falcão in [21] presented a method to quantify the technical impact of DG on losses, voltage profile and reliability indices of SAIFI and SAIDI, but did not optimize the DG values and explicitly state that their proposed method should be used as part of an automatic optimization method or as a tool to simply evaluate different DG installation alternatives. The authors used a power summation load flow method to quantify real power loss for specific DG size and location alternatives. The effect of DG on the feeder voltage profile is discussed, but not shown: improper DG allocation can cause under or over-voltages, but can benefit the feeder by providing direct voltage support instead of formal reactive power compensation i.e., capacitor banks. To be precise, the authors also recommended modelling multiple DG sources with the operation of voltage regulators and warned that, while DG can improve the voltage profile at the installation site, undesired voltages could result at other parts of the feeder [21]. To capture the effect of DG on reliability indices SAIDI and SAIFI, the authors assumed that islanding was permitted, that there are sufficient switches to isolate the fault from the healthy feeder and that switches

and DG breakers can be operated within half an hour. The DG is modelled as a "backfeed with a transfer restriction equal to the DG unit capacity" [21].

As aforementioned, the process of DG allocation is similar to capacitor allocation, except DG impacts both active and reactive power flows while capacitor banks only impact reactive power flows [15]. To decouple the siting and sizing subproblems, Gandomkar *et al* in 2005 fixed the DG candidate locations, number of available DG units, and total DG capacity then optimized binary encoded DG sizes to minimize real power loss on a standard IEEE 34 bus test feeder [6]. The study also assumed balanced, constant current load. They use a variant of the Genetic Algorithm, known as the Hereford Ranch Algorithm, to minimize the loss objective function given by:

$$f = \sum_{i=1}^{n} P_i \tag{4.1}$$

where P_i is the nodal injected power at bus i and n is the total number of buses. The Hereford Ranch (HR) algorithm employs a parent selection in a scheme that the authors claimed to outperform the traditional roulette wheel or tournament selection scheme for candidates to be promoted to future generations of the algorithm. Figure 24 shows the flowchart of the HR algorithm.

Ziari *et al* in [23] use an approximate time-varying multi-load level model (over a year) with a hybrid optimization technique combining a discrete form of PSO and GA operators to simultaneously reduce the sum of system loss, peak power and improve reliability at a minimum DG installation cost formulated by:

$$OF = C_{INSTAL} + \sum_{t=1}^{T} \frac{C_{O\&M} + C_{INTERRUPTION} + C_{LOSS}}{(1+r)^t} \tag{4.2}$$

where OF is the objective function which is the NPV (net present value) of the total cost, C_{INSTAL} is the total installation cost for DGs, $C_{O\&M}$ is the total operation and maintenance cost for DGs, $C_{INTERRUPTION}$ is the interruption cost, C_{LOSS} is the loss cost, r is the discount rate and T is the number of years in the study timeframe [23].

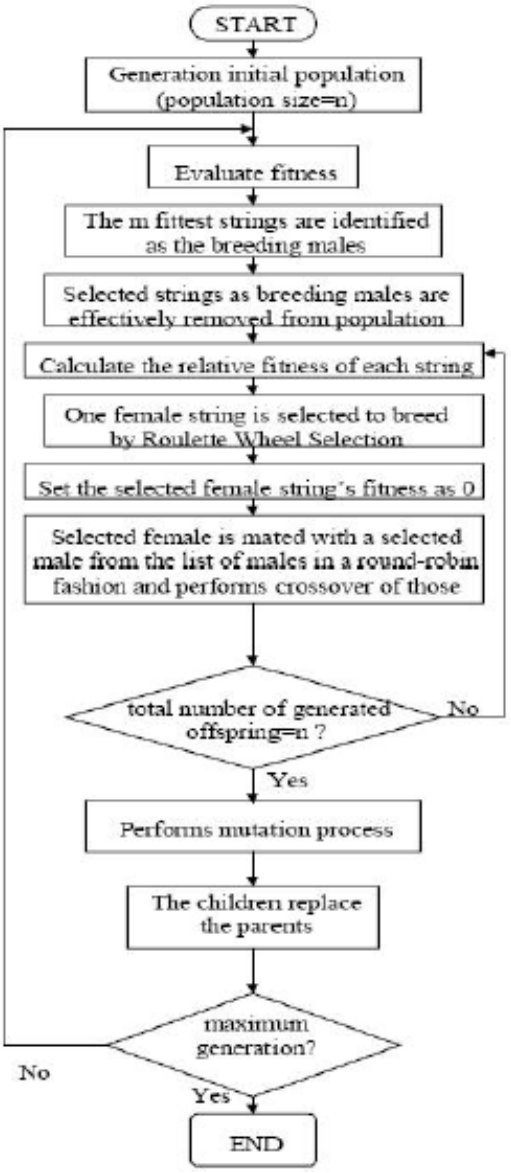

Figure 24 – Hereford Ranch Algorithm Applied to Optimal DG Sizing [6]

The DG cost is formulated as:

$$C_{DG} = C_{INSTAL} + \left(\sum_{t=1}^{T} \frac{1}{(1+r)^t}\right) C_{O\&M} \tag{4.3}$$

$$C_{INSTAL} = \sum_{j=1}^{NDG} C_{1_j} \cdot P_j \tag{4.4}$$

$$C_{O\&M} = \sum_{t=1}^{LL} \sum_{j=1}^{NDG} C_{2_j} \cdot P_j \cdot T_t \quad (4.5)$$

where NDG is the number of DGs, P_j is the rating of DG j, LL is the number of load levels, T_t is the duration of the corresponding load level, C_{1_j} is the installation cost per kW for DG j, and C_{2_j} is the operation and maintenance cost per kW for DG j. The installation cost is assumed to be proportional to the DG rating and the O&M cost is assumed proportional to the DG energy (kWh) output. The interruption cost is calculated by multiplying the number of customers, the average interruption duration per customer and the cost per unit time of an interruption as given by:

$$C_{INTERRUPTION} = \sum_{t=1}^{LL} NC \times SAIDI \times CI \times \frac{T_t}{8760} \quad (4.6)$$

$$C_{INTERRUPTION} = \sum_{t=1}^{LL} W_{SAIDI} \times SAIDI \times \frac{T_t}{8760} \quad (4.7)$$

where NC is the number of customers, CI is the cost of interruption per hour for a customer and W_{SAIDI} is the SAIDI weight factor specific to the LDC (defined as the product of number of customers multiplied by cost per unit time of interruption). The loss cost and total transmission line loss relations are:

$$C_{LOSS} = k_L \cdot TLoss + C_{PL} \quad (4.8)$$

$$TLoss = \sum_{t=1}^{LL} T_t \cdot TLoss_t \quad (4.9)$$

$$TLoss_t = \sum_{l=1}^{NL} Loss_{t,l} \quad (4.10)$$

$$Loss_{t,l} = R_{Line,t} I_{Line\ t,l}^2 \quad (4.11)$$

where k_L is the cost per kWh of losses, $TLoss$ is the total annual loss in kWh, LL is the number of load levels, T_t is the duration of load level t, $TLoss_t$ is the total loss value for load level t, NL is the number of transmission lines, $Loss_{t,l}$ is the loss in line l for load level t, $R_{Line,l}$ is the line resistance in line l, $I_{Line\ t,l}$ is the current of line l for load level t, and C_{PL} is the peak power loss cost. The peak power loss occurs at the peak load level. Reduction of the peak power demand allows reduced investment in high rated

equipment. Ziari *et al* refer to this incremental investment as "peak power loss cost" and is assumed to be proportional to the peak power loss defined as:

$$C_{PL} = k_{PL} \cdot TLoss_{LL} \tag{4.12}$$

where k_{PL} is the saving per MW reduction in peak power loss. The test system's actual and approximated load duration curves are shown in Figure 25. The load is at its peak for 2% of the year, at its lowest for 3% of the year, at an average load for 40% of the year, at 120% of the average load for 30% of the year and finally at 80% average load for 25% of the year. Different energy costs are associated with different load levels.

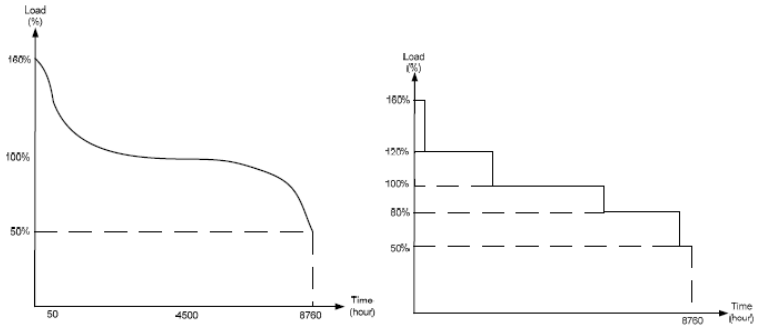

Figure 25 – Load Duration Curves for IEEE 37 Bus Reliability Test System [23]

Parizad *et al* in [13] used the Harmony Search heuristic algorithm to optimally site and size DG to reduce losses, improve voltage profile, improve system security and reduce THD. They assumed the number of DG given is fixed (in this case 2), but the locations and size are optimized according to the following fitness (or objective) function:

$$F = a_1 \cdot J_P + a_2 \cdot J_V + a_3 \cdot J_{Losses} + a_4 \cdot J_{THD} \tag{4.13}$$

The coefficients a_1 to a_4 are optimized by trial and error. The objective functions are given by:

$$J_V = \sum_i w_i \left| V_i - V_{ref,i} \right|^2 \tag{4.14}$$

$$J_P = \sum_j w_j \left(\frac{S_j}{S_{j,max}}\right)^2 \quad (4.15)$$

where V_i is the voltage amplitude for bus i, S_j is the apparent power for line j, $V_{ref,i}$ is the nominal voltage, $S_{j,max}$ is the nominal apparent power of the j_{th} line and w_i, w_j are weighting factors.

$$J_{Losses} = \sum_{j=1}^{nb} \alpha_j \cdot Max(0, (P_j^{DG} - P_j^{Base})) \quad (4.16)$$

where P_j^{DG} is the loss in the j^{th} branch after DG installation, P_j^{Base} is the loss in the j^{th} branch before DG installation (base case) and nb is the number of branches. The power loss is expressed as a function of the bus current injection and the full expression can be found in [13].

$$J_{THD} = \sum_{j=1}^{nb} \alpha_j \cdot Max(0, (THD_j - THD_{max})) \quad (4.17)$$

where THD_j is the total harmonic distortion in the i^{th} bus with DG and THD_{max} is the total acceptable harmonic distortion in the i^{th} bus. The standard definition of THD (voltage harmonic distortion) is used. The study used the ladder technique, i.e. forward/backward sweep load flow method, which is well suited for a distribution feeder, but unable to be used directly for harmonic analysis since the harmonic currents absorbed by shunt capacitors are unknown [13]. Therefore, the loads were modelled as composite linear and non-linear loads consisting of harmonic current sources and impedances – the equivalent harmonic current injections are calculated at each load flow iteration. Figure 26 shows the branch current and harmonic currents used in [13]. The harmonic current associated with that load is calculated as the quotient of the harmonic voltage and the harmonic impedance:

$$Ih_i^{(h),k} = \frac{V_i^{(h),k}}{Z_i^{(h)}} \quad (4.18)$$

The system components, i.e. transformers, lines, cables, capacitors and inductors, are modelled using practical approximations whose reactance values are frequency dependent.

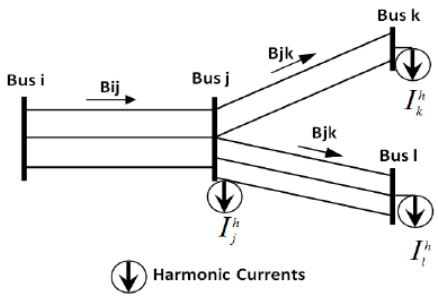

Figure 26 – An Unbalanced Distribution System with Branch Currents and Harmonic Currents [13]

The authors applied the HS algorithm to an IEEE 12 bus test system with unbalanced three phase loads, single phase loads and motor loads. By reducing the losses and improving voltage profile and THD, the maximum loading, power transfer capacity and voltage stability margin were consequently improved [13].

In 2011, Hung *et al* in [14] used an improved analytical (IA) method to optimally size all DG types (synchronous machines, inverter-connected DG and induction generators) to find the optimal operating DG power factor based on real and reactive power loss minimization. The authors compare the IA's performance to the exhaustive load flow (ELF) method that enumerates all optimal size and location combinations. The IA method approximated the DG sizing first with the IA formulas then enumerated the optimal DG locations according to the actual minimum losses obtained by the DG size obtained by a load flow run. The authors also compared results from the IA and ELF methods to the loss sensitivity factor (LSF) method. Their results show that the IA achieved a loss reduction of 61.62% which was slightly worse than the ELF at 64.83%. The LSF yielded the worst performing loss reduction at 59.72%. Results were consistent for three IEEE test systems (16, 33 and 69 bus).

The IA relations were developed according to the active/reactive power quadrant in which the DG operated in the author's previous work. However, [14] presented a summary of the formulas as given below.

- Type 1 DG ($0<PF_{DG}<1$) is capable of injecting real and reactive power. The optimal size of DG is given by:
    - $P_{DGi} = \frac{\propto_{ii}(P_{Di}+aQ_{Di})-X_i-aY_i}{a^2\propto_{ii}+\propto_{ii}}$ (4.19)
    - $Q_{DGi} = aP_{DGi}$ (4.20)

    where
    - $a = (sign)\tan(\cos^{-1}PF_{DG})$ and sign = +1 (DG injecting reactive power) (4.21)
    - $X_i = \sum_{\substack{j=1 \\ j\neq i}}^{n}(\propto_{ij} P_j - \beta_{ij} Q_j)$ (4.22)
    - $Y_i = \sum_{\substack{j=1 \\ j\neq i}}^{n}(\propto_{ij} Q_j + \beta_{ij} P_j)$ (4.23)

The loss coefficients $\propto$ and β are obtained from the base case load flow, and while strictly speaking, they should be updated at every load flow step, the authors state that the changes in the loss coefficients are small and have a negligible effect on the optimal DG size result.

- Type 2 DG ($0<PF_{DG}<1$) is capable of injecting real but consumes reactive power (sign = -1). Other than the sign change, the optimal size of DG is given by the same formulas as Type 1.
- Type 3 DG (PF_{DG} = 1) is capable of injecting real power only (sign=0), e.g. inverter-connected DG such as PV, microturbines and fuel cells. The optimal DG size at bus i is given by
    - $P_{DGi} = P_{Di} - \frac{1}{\alpha_{ii}}\sum_{\substack{j=1 \\ j\neq i}}^{N}(\propto_{ij} P_j - \beta_{ij} Q_j).$ (4.24)
- Type 4 DG (PF_{DG} = 0) is capable of injecting reactive power only (sign = ∞), e.g. synchronous compensator. The optimal DG size at bus i is given by:
    - $Q_{DGi} = Q_{Di} - \frac{1}{\alpha_{ii}}\sum_{\substack{j=1 \\ j\neq i}}^{N}(\propto_{ij} Q_j + \beta_{ij} P_j)$ (4.25)

It should be noted that although utilities, manufacturers and the research community agree that reactive power support is a useful by-product of DG installation, a typical distribution utility's

communications infrastructure is not yet equipped for the two-way communications between small DG and the utility's planning and operations centre, which would be required to manage reactive power control. Therefore, the current practice is to maintain DG at unity power factor. The authors also recognized the relevance of the results, and, while the software they developed can handle all four DG types at various load levels, the studies were run with Type 3 and Type 1 DG only.

Celli and Pilo's approach to optimal DG allocation in [22] was based on a fixed total DG penetration limit on the feeder based on user-specified economic and technical constraints, a fixed number of DG units of randomly generated sizes of DG units to meet the overall penetration limit. The GA was then used to optimize the location given the randomized sizes of the DG. The objective functions investigated were the cost of network upgrading, energy losses in kWh, and network reliability in terms of energy not served. The authors also add the reduction of CO_2 emission as an environmental constraint with different emission costs and values depending on the type of DG used, i.e. wind turbine, CHP and gas turbine.

- Assuming a fixed network topology, the cost of network upgrading objective function is given as:

$$C_U = \sum_{j=1}^{N_{branc\ hes}} C_{0j} = \sum_{j=1}^{N_{branc\ hes}} \left(B_{0j} + M_{0j} - R_{0j}\right) \quad (4.26)$$

where $N_{branc\ hes}$ is the number of network branches, C_{0j} is the present cost of the j^{th} branch, and B_{0j}, M_{0j} and R_{0j} are building, management and residual cash costs transferred to the cash value of the beginning of the planning period.

- The planning period of N years is divided into m total sub-periods (the customer's load demand varies piecewise linearly from one sub-period to the next) and the losses are calculated for each k^{th} sub-period. The energy loss is formulated as follows:

$$E_L = \sum_{j=1}^{N_{branc\ hes}} \sum_{k=1}^{m} E_{Ljk} = 8760 \cdot \sum_{j=1}^{N_{branc\ hes}} 3 \cdot r_j \cdot L_j \cdot \left[\sum_{k=1}^{m} N_k \cdot \left(I_{fjk}^2 + I_{0jk}^2 + I_{fjk} \cdot I_{0jk}\right)\right]$$

(4.27)

where r_j is the resistance per km, L_j is the branch length in km, 8760 is the number of hours in a year, I_{0jk} and I_{fjk} are the branch currents at the beginning and end of the sub-period, N_k is the subperiod duration in years, and y is the generic year of the subperiod. The reader is referred to [28] for the complete derivation.

- Assuming intentional islanding is allowed, the network reliability measured by energy not supplied (E_{NS}) is given by:

$$E_{NS} = \sum_{j=1}^{N_{branches}} \lambda_j \cdot L_j \cdot \sum_{k=1}^{m} \left(\sum_{i=1}^{N_{loc,j}} P_{0ik} \cdot t_{loc} + \sum_{i=1}^{N_{rep,j}} P_{0ik} \cdot t_{rep} \right) \quad (4.28)$$

where r_j is the fault rate of the j^{th} branch (number of faults per year and per 100 km of feeder length), $N_{loc,j}$ and $N_{rep,j}$ are the number of nodes isolated due to a fault in the j^{th} branch during the fault location and repair stages, P_{0ik} is the node power (kW) at the beginning of the k^{th} subperiod and t_{loc} and t_{rep} are the durations of the fault location and repair stages. Automatic Sectionalizing Switching Devices (ASSDs) are used in the test system (a real distribution system in Italy) to improve reliability and to meet the maximum allowable customer minute loss and frequency of interruptions set by the system regulator.

- Finally, the environmental impact of DG is quantified by the overall CO_2 emission given by:

$$\Psi^{CO_2} = (E_C + E_L - E_{DG}) \cdot \Psi_T + \sum_{j=1}^{N_{DG}} \left[(8760 \cdot N \cdot P_{DGj}) \cdot \Psi_{DG_j} \right] \quad (4.29)$$

where Ψ_T is the CO_2 emission assigned to the grid, Ψ_{DG_j} is the CO_2 emission associated with the j^{th} generator, E_C and E_L are the total customer energy demand and total energy loss on the feeder respectively. The total energy produced by the N_{DG} allocated DGs in the network is formulated as:

$$E_{DG} = 8760 \cdot N \cdot \sum_{j=1}^{N_{DG}} P_{DG_j} \quad (4.30)$$

The purpose of the study is to demonstrate the validity and the robustness of the multiobjective approach on DG allocation. Note that this study does not use renewable DG which would bias the environmental emission constraint to renewable DG only in a mixed DG scenario. Moreover, it is not explicitly stated why the environmental emission constraint is not one of the objective functions rather than a constraint.

From 2006 onwards, multiobjective (MO) optimization in the context of optimal DG allocation has been investigated as an integrated tool for distribution planners. In 2008, Celli and Pilo extended the GA approach and used a MO method to optimally site and size DGs using a Non-dominated Sorting Genetic Algorithm (NSGA) on a real distribution system [22]. The classical multiobjective optimization approach involves converting the MO problem to a single-objective optimization problem by emphasizing one goal at a time. The multiple objectives give rise to solution sets of optimal solutions, known as Pareto-optimal solutions, rather than a single solution. MO evolutionary algorithms, on the other hand, can find multiple Pareto-optimal solutions in one simulation run due to their ability to maintain a diverse set of solutions during the optimization process. NSGA-II is found to be one of the most efficient and is thus adopted for use in [22]. The process is summarized in a flowchart presented in Figure 27. The routine starts by randomly generating an initial parent population, G_0, of N individuals and evaluating the objectives for each of them. The population is sorted based on the non-domination. Next, binary tournament selection, crossover and mutation operators are applied to create the first offspring population, O_1, of size N. After this initial phase, the optimization procedure continues in a slightly different manner to introduce elitism. First, a combined population of parents and offspring is formed:

$$C_{gen} = G_{gen-1} \cup O_{gen} \tag{4.31}$$

of size $2N$ which the authors claim ensures elitism. Then, the combined population C_{gen} is sorted according to non-domination. The new population of parents, G_{gen}, is formed by choosing primarily the best non-dominated front, P_1, of the combined population, and then by adding the subsequent fronts in ascending order (P_2, P_3, etc.) until no more sets can be accommodated. Finally, to choose exactly N

population members, the solutions of the last front are sorted using a crowded comparison operator (which denotes how close a population member is close to its neighbour – the preferred solutions are those from a less crowded region) in descending order and the best solutions needed to fill all population slots are chosen. The new population G_{gen} of size N is now used for selection, crossover, and mutation to create a new population 0_{gen+1} of size N.

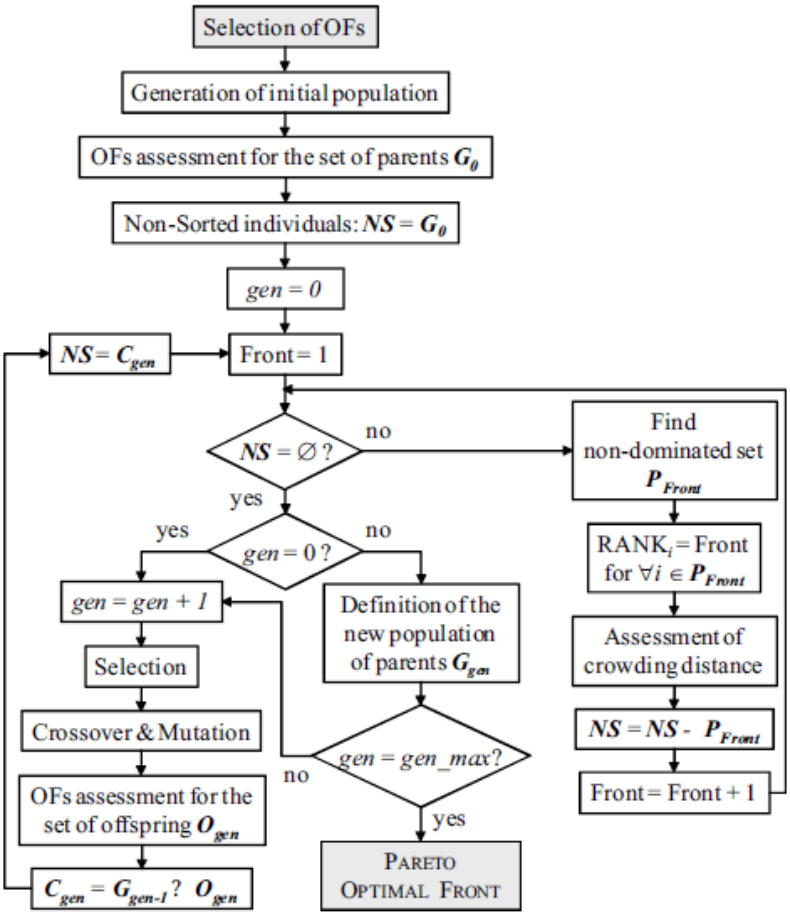

Figure 27 – Flowchart of the MO Evolutionary Algorithm used in [28]

Additional work in multi-objective DG allocation has been carried out by Singh and Verma in 2009 [25] and Hejazi *et al* in 2010 [26]. While Celli and Pilo assumed one load curve as an average for a year within the planning period to avoid excessive computation times, Singh and Verma performed an

exhaustive analysis to show the effect of load models on multi-objective optimization using a single DG allocated at each node successively. The load models used in the study were constant, industrial, commercial, residential and mixed. The authors then developed system objectives for real and reactive power indices, voltage profile index and MVA capacity index minimization, then combined it using weightings specified by the user, and optimized a DG size-location pair using a GA. Figure 28 shows the comparative index results for the IEEE 16 bus system in the top table and the IEEE 37 bus system in the lower table. When these results are graphed (the reader is referred to the original paper), the variation in patterns for each DG value, IMO result and individual indices for each load class suggests that the optimal location and size of DG changes depending on the load model. ILP and ILQ represent real and reactive power indices, respectively, while IC and IVD are the MVA capacity and voltage profile deviation indices. The formulation for each index is given below:

$$ILP = \frac{P_{LDG}}{P_L} \tag{4.32}$$

$$ILQ = \frac{Q_{LDG}}{Q_L} \tag{4.33}$$

$$IVD = \max_{i=2\rightarrow n}\left(\frac{\bar{V}_1 - |\bar{V}_i|}{|\bar{V}_1|}\right) \tag{4.34}$$

$$IC = \max_{i=1\rightarrow m}\left(\frac{|\bar{S}_{i,j}|}{|C\bar{S}_{i,j}|}\right) \tag{4.35}$$

where P_{LDG} and Q_{LDG} are the total real and reactive power losses of the distribution system after DG is installed and P_L and Q_L are the base case (no DG) total real and reactive power losses. $\bar{V}_1$ is the nominal voltage, taken to be 1.03 p.u. in this study. $\bar{S}_{i,j}$ is the MVA flow in the line connecting *i* and *j* and $C\bar{S}_{i,j}$ is the MVA capacity of the line connecting *i* and *j*.

The individual indices are then combined to create a multiobjective performance index, IMO, with corresponding weightings as follows:

$$IMO = \sigma_1 \cdot ILP + \sigma_2 \cdot ILQ + \sigma_3 \cdot IC + \sigma_4 \cdot IVD \quad (4.36)$$

where $\sigma_1 = 0.4$, $\sigma_2 = 0.2$, $\sigma_3 = 0.25$ and $\sigma_4 = 0.15$. The authors state that these weights are selected based on the relevance of each impact index to the utility planner, and should be tailored to the required analysis and the network characteristics. In this case, the active power loss index (ILP) received a significant weight (0.40). The current capacity index (IC) received the second major weighting (0.25) since it gives important information about the level of currents through the network. The reactive power loss index (ILQ) is designated a weight of 0.20 and the voltage profile index (IVD) received a weight of 0.15 due its potential impact on power quality [25]. Since the goal is to minimize each index, the minimum IMO is also desirable.

Impact Index	Const load	Ind. load	Res. load	Com. load	Mixed load
ILP	0.3540	0.4012	0.3832	0.3801	0.4099
ILQ	0.3286	0.3517	0.3557	0.3767	0.3643
IC	0.6622	0.7012	0.7043	0.7093	0.7117
IVD	0.0108	0.0104	0.0107	0.0110	0.0102
Min IMO	0.3745	0.4077	0.4021	0.4064	0.4163
Optimal size-loc pair	0.63-7	0.61-8	0.59-8	0.58-8	0.62-8

Impact Index	Const. load	Ind. load	Res. load	Com. load	Mixed load
ILP	0.7104	0.8819	0.8822	0.8846	0.8839
ILQ	0.7048	0.8958	0.8941	0.8957	0.8977
IC	0.8739	0.8795	0.8812	0.8825	0.8821
IVD	0.0689	0.0739	0.0738	0.0732	0.0737
Min IMO	0.6539	0.7629	0.7631	0.7645	0.7647
Optimal size-loc pair	0.62-14	0.63-25	0.63-25	0.63-25	0.63-25

Figure 28 – Singh & Verma's Results: Impact Indices Comparison for DG Penetration on IEEE 16 and 37 Bus Systems

Hejazi *et al* in [26] use a Differential Evolution Algorithm (DEA) to conduct a techno-economic study to for optimal DG allocation. The authors optimize a multiobjective function combining the cost of network upgrading, cost of purchased energy, energy loss cost, total voltage deviation and total capacity

release (which is really a technical constraint ensuring that MVA flow and currents through the substation and network are within their capacity limits, respectively). The DEA is another population based heuristic but is found to be faster and more accurate than the traditional GA when applied to certain problems and is gaining popularity. Hejazi *et al* use the IEEE 37 bus system, which is an actual feeder located in California and features DG based on CHP technology, i.e. micro-turbines, mini gas turbines, and reciprocating engines. Using a multi-step approach, optimal DG siting and sizing is performed as follows:

1. Optimize DG location for technical objectives only, based on a predetermined number of DG available and user-specified DG penetration limit (in this work 64%). Multiple optimal DG locations are possible.
2. Apply the Feed-In-Tariff price uniformly to all installation locations to reduce amount allocated to each DG from Step 1. This also optimal location of DG due to improvements in Total Voltage Deviation (TVD) and Total Capacity Release (TCR) indices.
3. "Customize" each location by applying different prices for each installation point due to location-specific installation requirements. The study finds that the total cost increases but the TVD decreases showing the regulatory impact on the network characteristics. A non-unity optimal power factor value for each DG is also obtained as the TVD is improved.
4. The final step in the study involves applying the voltage stability index to identify the effect on optimal DG location while keeping all other parameters constant. This study found that the optimal locations changed and that the TVD and the overall objective function were adversely affected when considering the stability index in isolation. It is not clear which index the authors chose as the stability index, since two are described in [26]: the Fast Voltage Stability Index (FVSI) and the Line Stability Index (LQP).

4.2 – Previous Work on Optimal DG Siting using Sensitivity Factors

Chapter 2 presented the formulations for power loss sensitivity and voltage stability indices. Ideally, DG units should be allocated at locations where they provide a higher reduction of losses [27]. The degree of loss reduction in response to injected active power can be measured and ranked by power loss sensitivity. In 2004, Rahman *et al* in [27] applied real and reactive power loss sensitivity factors (LSF) to optimal DG allocation, as derived from a voltage stability index formulation, the details of which are available in earlier work from 1997. Using an IEEE 69 bus test system, the authors ranked the buses in descending order of real power loss sensitivity. The top-ranked values represented optimal DG locations after which optimal sizing was then performed using evolutionary programming. In 2009, Dasan *et al* in [12] extended Rahman's work in three ways:

1. By applying both the voltage stability and power loss indices to reduce the solution space and rank optimal DG locations. Buses that are common i.e., sensitive, to both sets of indices are selected to be allocated with DG.
2. Multiple scenarios run with different types of DG such as inverter-connected supplying real power only (DG1), synchronous machine type DGs supplying both real and reactive power (DG2), e.g., wind turbines and induction machine type DGs supplying real power but consuming reactive power, e.g., fixed speed wind turbines (DG3). One scenario also considers two combinations of the DGs, i.e. DG1-DG2 and DG1-DG3.
3. Static load models are used to represent customer classes, specifically, constant, industrial, residential and commercial using the following relations:

$$P = P_0 \left(\frac{V}{V_0}\right)^{np} \tag{4.37}$$

$$Q = Q_0 \left(\frac{V}{V_0}\right)^{nq} \tag{4.38}$$

where np and nq are load exponents vary with the type of load as shown in Table 2 and are obtained from a reference given in [12].

Load Type	***np***	***nq***
Constant	0	0
Industrial	0.18	6.00
Residential	0.92	4.04
Commercial	1.51	3.40

Table 2 – Load Type and Exponent Value [12]

In 2010, Hejazi *et al* applied a voltage stability index to examine the effect of voltage stability on optimal placement of DG – a method more suitable when applied to long rural feeders with induction or synchronous machine based DGs attached. As mentioned in Chapter 2, voltage stability indices have been traditionally used in transmission system contingency planning where stability improvement increases power transfer capacity and power system loading, preventing voltage collapse. Figure 29 shows the PV curve used to study voltage stability in power systems, commonly referred to as the "nose curve".

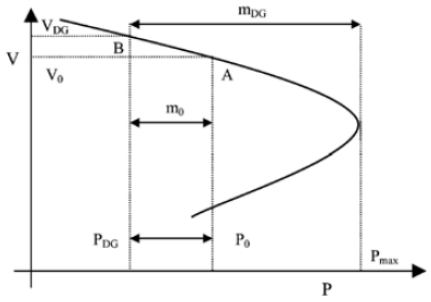

Figure 29 – PV Curve for Voltage Stability Analysis [13]

Also in 2010, Parizad *et al* [13] applied the LSF approach to optimal DG placement, creating a priority list then optimally sized the DG using the exact power loss formula. This "base case" approach is

compared to an alternate scenario where voltage stability indices are used for optimal DG placement. The authors also presented two formulations for voltage stability (shown below) which are derived from a 2 bus model: Fast Voltage Stability Index (FVSI) and Line Stability Factor (LQP).

$$FVSI_{ij} = \frac{4Z^2 Q_j}{V_i^2 X} \leq 1 \tag{4.39}$$

$$LQP_{ij} = 4\left(\frac{X}{V_i^2}\right)\left(-\frac{X}{V_i^2}P_i^2 + Q_j\right) \tag{4.40}$$

where Z is the magnitude of the line impedance. The values of $FVSI_{ij}$ and LQP_{ij} must be less than 1 for the system to be stable. When compared, the authors found that the "FVSI reflects the system stability well in terms of reactive load but not as well in terms of active load;" therefore, LQP was used [13]. After the optimal DG placement is found using the LQP relation, the optimal sizing was performed using the exact power loss formula and increasing the DG size from 0 to 5 MW. The test systems are a 30 bus meshed and a 33 bus radial system. As expected, the voltage profile and losses were improved, therefore the contribution from [13] was the review and application of voltage stability indices in optimal DG allocation (siting). Finally, Hung *et al* in 2011 also used the LSF as an alternative to the Improved Analytical method of optimal siting of DG [14].

4.3 – Previous Work on DG and Asset Reinforcement Investment Deferral

While it is widely recognized that DG can defer system investment and expansion for a utility, it is only recently that methods of quantification of the economic impact have been developed (2006 onwards). Much of this work has been performed in the UK (Li et al in [28] and Wang & Ochoa in [29]), Italy (Piccolo & Siano in [30]) and Canada (Gil & Joos in [31] and [32]). There are two broad approaches in the literature: loading-based analysis of investment deferral based on a time horizon, and planning-based which relies on traditional distribution planning techniques.

Gil and Joos' work in [31] is an example of the first approach, and discusses the benefits realized by customers, the LDC and the System Operator by asset deferral and DG installation. From the LDC's point of view, the benefit of asset upgrade deferral is based on the time value of money where money is worth more to the owner left in the bank i.e. withheld from investment than spent upgrading the system, as defined in [31] by:

$$B_i = \sum_f C_f \left(1 - \frac{1}{e^{\rho \tau f_i}}\right) \tag{4.41}$$

where B_i is the benefit to the utility given by connecting DG at bus i, C_f is the cost of the needed upgrade on feeder f without DG, ρ is the monthly or annual interest rate, τf_i is the time (monthly or annually) by which the investment on feeder f is deferred by the operation of DG located at bus i during peak load hours. The quantification of the benefit is specific to the distribution utility, the time horizon used (cost structure), type of feeder and region served [31]. Note that if the utility can claim savings due to DG, it must also be allowed to assume control of the DG when required to maintain its service quality and respond to liability issues after interruptions [31]. Gil and Joos refer to their earlier work as well as research literature that quantifies the dollar value of installed DG from \$265/kVA to \$1200/kVA depending on DG location, type and load growth. The LDC also benefits by reducing electricity purchase cost from the transmission system, and loss reduction. In Gil and Joos' earlier work, the incorporation of DG is related to the change in feeder currents and the resulting effect on the deferral time horizon [32]. The full derivation of the relations are available in [32] however, Figure 30 is a visual representation of the concept of asset deferral and time value of money. τ_k is defined as the time it takes the current in feeder k, I_k, to reach the value it had before the DG was installed at the load growth rate. τ_k varies for each feeder, and in most cases, ΔI_k is negative due to DG reducing feeder currents by supplying load at the point of connection.

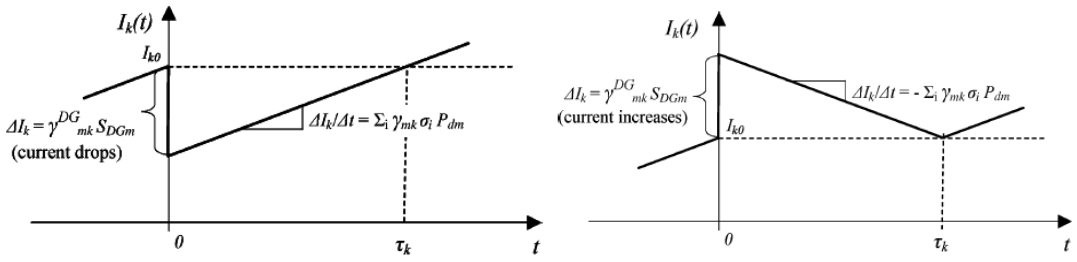

Figure 30 – Deferral Time due to Current Decrease and Increase [39]

If the installed DG is large enough, current in immediate upstream nodes or feeders may reverse to the point where the reverse current reaches the feeder limit. This occurs when the DG power output equals the bus load plus the total feeder's capacity. The utility may then choose to upgrade network capacity to accommodate the current flows introduced by the DG at peak generation times, or limit the DG output [32].

In 2010, Li *et al* present an investment deferral evaluation method similar to Gil & Joos, but relate the economic benefit to the present value of assets on a feeder that may be increased or decreased depending on DG installation at different locations, penetration and concentration levels [28]. The mathematical formulations are as follows:

$$\Delta PV = \sum_{l=1}^{M}(PV_l - PV_{lNew}) = \sum_{l=1}^{M}\left(\frac{Asset_l}{(1+d)^{n_l}} - \frac{Asset_l}{(1+d)^{n_{lNew}}}\right) \quad (4.42)$$

where l is the asset number such as a circuit or a conductor, PV_l is the Present Value of future investment without DG (base case), PV_{lNew} is the Present Value of the future investment with DG installation, ΔPV is the change in present value which could be "regarded as either investment deferral or acceleration depending on the direction of change", M is the total number of assets in the network, d is the discount rate, $Asset_l$ is the modern equivalent assets cost, i.e. the cost to replace them today, or the book value, n_l is the time to reinforce a network asset if no DG is installed (base case) and n_{lNew} is the time to reinforce

a network asset if DG is installed (test case) [28]. The value of n_l can be determined from the current loading level and the load growth rate as follows:

$$C_l = D_l \times (1 + r)^{n_l} \tag{4.43}$$

$$n_l = \frac{\log C_l - \log D_l}{\log (1+r)} \tag{4.44}$$

where network component (asset) l has a capacity of C_l and supports a power flow of D_l and r is the load growth rate which drives the time the network asset takes to grow from D_l to C_l. The underlying assumption is that reinforcement will occur when the circuit is fully loaded; however, these formulas can be modified to any capacity based upgrade schedule, e.g. upgrade asset at 80% loading. Another assumption is that operational and maintenance costs are not incorporated and that the load growth rate is fixed over the planning horizon. The present value of future reinforcements is given by:

$$PV_l = \frac{Asset_l}{(1+d)^{n_l}} \tag{4.40}$$

To account for the test case of additional DG, especially for multiple DG added to the network, the power flow changes from D_l to D_{lNew}. Therefore, the new time to reinforce the network is formulated as:

$$n_{l,New} = \frac{\log C_l - \log D_{l,New}}{\log (1+r)} \tag{4.41}$$

The two time horizon values, n_l and n_{lNew}, are then entered into the ΔPV relation. Li *et al* applied this load based economic quantification on a real 33kV subtransmission network in the UK and compare the results of present value (PV) of future reinforcement between the base case of no DG with three DG allocation scenarios (DG in this study is micro-CHP rated at 1.2kW and can provide both heat and electricity). The objective of this work was not to optimally allocate DG to determine the minimum PV but rather to study the effect of the PV quantification method to the different DG allocation approaches, specifically, DG installed at load buses proportional to loading level, DG installed evenly at load buses, and DG installed at load buses proportional to nodal charges, calculated by a Long Run Incremental

Charging (LRIC) method [28]. It was found that the greatest reduction in the present value investment was for DG installed at load buses proportional to the loading level.

The second broad class of techniques found in the literature is based on the successive elimination approach from multistage planning to assess the deferral of demand-led investment, as demonstrated in the work done by Wang and Ochoa in [29]. The motivation for the successive elimination approach is the UK's Engineering Recommendation (ER) P2/6 which specifies the security of supply standards and provides a mechanism "by which DG contributes to system security by acknowledging a fraction of the nominal capacity of the generator during a first circuit outage (N-1) condition" [29]. Successive elimination, shown in Figure 31, is used to initially overbuild the network considering the loading at the end of the planning horizon, including all expansion options such as new lines and transformers. Then the least cost-effective option, in terms of capacity margin, is removed until the further removal of any remaining candidates causes violation of system constraints, i.e. voltage and thermal limits. The resulting reinforcements from the successive elimination step are fed into the multistage planning method which then schedules the implementation of reinforcements within a planning horizon. Refer to Figure 32 for a flowchart depicting the main steps in multistage planning. Given the reinforcement from successive elimination, and the schedule of reinforcement work from multistage planning, the investment deferral is then quantified by calculating the present value (PV) of each asset upgrade in the base case (no DG) and test case (with DG) and subtracting the test case PV from the base case PV.

1. Calculation of the cost-effectiveness (CE) of each expansion option:

   a. $$CE_a = \frac{\sum_{k \neq a} |P_{k\ new} - P_{k\ original}|}{Cost_a} \quad (4.45)$$

   where CE_a is the cost-effectiveness measurement of option a in MW/$, $P_{k\ original}$ is the MW flow on branch k after eliminating expansion option a and $Cost_a$ is the expansion cost of option a. If constraints are violated, CE_a is set to a large number.

b. If all CEs are set to large numbers, then the final expansion plan is reached. Otherwise, eliminate expansion option with lowest CE and go to step (a).

2. Multistage Planning Analysis:
    a. Starting at the final year of the planning horizon, assume the connection of DG unit(s) along the whole planning horizon and calculate the contribution using its capacity factor.
    b. Use the cost-effectiveness technique in Step 1 to identify those candidates not necessary in the current year. Repeat until the remaining options are essential to prevent any system violations for both normal and N–1 security requirements.
    c. Consider the demand forecast for the previous year unless the current year is the base year, in which case this subroutine ends.
3. Investment Deferral – Steps 1 and 2 give the reinforcements required as well as the schedule. To obtain the total investment incurred by each planning scenario, the present value (PV) of each upgraded asset is calculated as follows:
    a. $PV = \sum_{t=1}^{h} \sum_{i=1}^{n} \frac{C_{i,t}}{(1+\rho)^t}$ (4.46)

    where h is the number of years in the planning horizon, n is the number of reinforcements required for year t, C_i is the cost of asset i required for year t and ρ is the discount rate.
    b. The "before and after DG" investment deferral is given by subtracting the PV of the total investment required by a given DG planning scenario (test case) from that of the original planning scenario (base case):

    $$Inv.Deferral = \sum_{t=1}^{h} \sum_{i=1}^{n} \frac{C_{i,t,\ NoDG}}{(1+\rho)^t} - \sum_{t=1}^{h} \sum_{i=1}^{n} \frac{C_{i,t,DG}}{(1+\rho)^t} \quad (4.47)$$

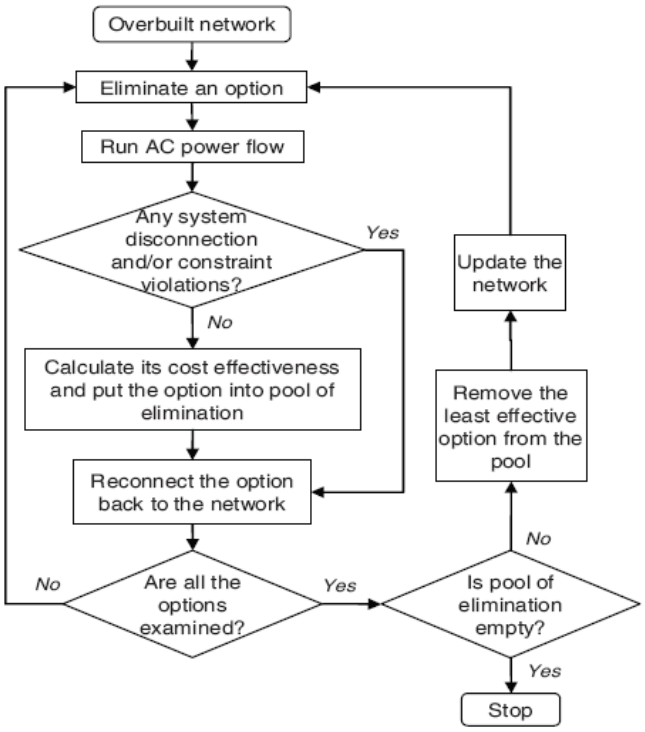

Figure 31 – Flowchart of the Successive Elimination Method [40]

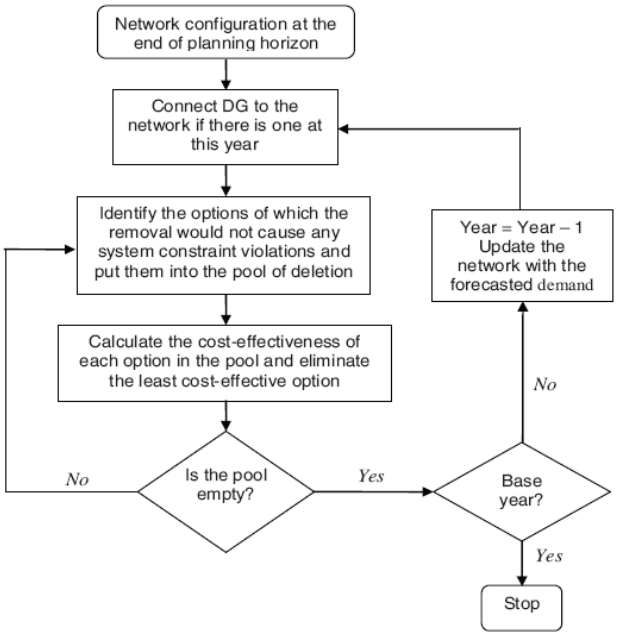

Figure 32 – Multistage Planning in Wang et al [40]

In 2009, Piccolo and Siano in [30] built on earlier work by Wang *et al* published in 2008 by differentiating between groups of feeders in a distribution network, each with their own upgrade schedules. A feeder group's upgrade schedule is determined by the first feeder requiring upgrade. A disadvantage to the planning-based method, also acknowledged by the authors in [29], state that successive elimination and other "automated planned" approaches have not achieved widespread use by utilities due to concerns over the representation of circuit configurations, switching and N-1 contingency scenarios, not to mention the effort required to encode each scenario and update as circuit reconfigurations are required.

4.4 – Summary of Literature Review and Justification for this Work

Borges and Falcão's contribution in [21] was to quantify the effect of DG on system reliability improvements, but did not use this to specifically allocate DG optimally. Gandomkar in [9] fixed the DG candidate locations, number of available DG units, and total DG capacity before optimally allocating binary encoded DG units of a predefined size (rather than real-valued DG output) to minimize real power loss only. Ziari *et al* in [23] combined two optimization methods, a discrete form of PSO and GA operators, to perform optimal DG allocation using technical objectives but assigned costs to the objectives. Thus, Ziari's work was one of the few available in research literature that attempts to translate technical goals into economic savings. The objective functions were minimization of DG installation costs, DG operational and maintenance costs, avoided cost to the utility of interruption (assuming islanding is permitted, which it rarely is, and when it is, only with large dispatchable DG equipped with high-speed communication infrastructure to a control centre to supervise line re-synchronization or) and reduced loss costs incurred by the utility. In reality, DG installation and O&M costs are usually borne by the developer, not the LDC and therefore are not considered in this thesis.

Parizad in [24] used the Harmony Search Algorithm as a novel approach; however, the optimal penetration limit for DG is set by the user before running the optimal allocation routine. In contrast, the

method in this thesis allows the optimal DG sizes to swing for each objective function. Hung *et al* combined the loss sensitivity concept with optimal siting and sizing, but only studies the real and reactive loss reduction objectives. However, the authors did execute a rigorous comparison of the IA method with the benchmark ELF method lending credibility to their work. Celli and Pilo in [22] used an energy-savings goal based on emission reduction, which are typically highly specific to the region and power supply mix, and can be difficult to quantify accurately. Also, there was no emphasis on the resulting financial savings for utility. Singh & Verma in [25] also focussed on the technical impact of optimal DG allocation due to load models and showed that the optimal allocation of DG (size-location pair) varied by load model. Hejazi *et al* in [26] used a multiobjective DEA to optimally allocate DG size, location and power factor. A thorough techno-economic procedure was developed; however, savings were calculated based on system-level loss reduction based on a uniform FIT rate (not DG technology specific) and location-specific installation prices. This study does not consider loading of each asset and the cost of network upgrading was simplistic (defined as the summation of the present value of upgrade costs necessary for the j^{th} branch of line for *n* nodes). Finally, a voltage stability index evaluation was performed on an inherently low voltage system (4.8kV) indicating that power loss, rather than voltage stability, should have been a greater concern.

Each of the methods presented in this literature review has its merits; however, there is still an emphasis on investigating the technical impacts of DG, and not as much work performed on quantifying the technical impact into savings (although this trend is on the rise). Thus, the purpose, and novelty, of this work lies in developing a comprehensive "off-the-shelf" three stage technique that enables LDCs to effectively answer the following question posed by utility asset managers (especially in the Ontario context with the introduction of the FIT program): **how does the connection of PV DG benefit utility planning and operations, and how do these improvements translate into financial savings for the utility?** Moreover, the proposed technique is directly applicable to other feeders and can be extended to a group of feeders, a region or a network. Assuming a feeder model is developed, the user simply has to

customize the following parameters specific to the feeder: the modern replacement value of their system's assets (distribution transformers, lines and cables, although other classes of equipment may be added), discount rate, distribution rate charge, load factor, load model and load growth rate.

The first stage in the technique presented in this work is optimal siting by applying the power loss sensitivity factor (LSF). The topmost nodes are ranked to create a candidate nodes list, and within this list, a sub-list of feasible nodes is created based on the presence of distribution equipment (indicating infrastructure is available to connect the DG units). Both voltage sensitivity and power loss sensitivity indices were implemented in MATLAB; however, given that real power loss was an objective and that only active power generation is allowed from electronically coupled generators (in this case PV DG) power loss sensitivity only was applied. Moreover, due to the system characteristics, i.e. short feeders, power loss is of greater concern to Kingston Hydro than voltage stability. Voltage stability indexing would be more suitable to long, rural feeders with machine-based DG where low voltage and voltage fluctuations are of concern. Therefore, the method of optimal siting implemented in this work can be tailored to the LDC's system characteristics. Note that there other optimal siting methods found in literature; for instance, DG allocation based on loading level as demonstrated by Li *et al*. However, it is the opinion of this author that ranking based on power loss sensitivity represents a more general case than ranking based on a specific loading level, due to the fact that the LSF method measures the sensitivity of a node to *changes* in loading.

The second stage in the comprehensive technique finds the optimal PV DG real power output at the feasible locations by applying a continuous-domain GA to one objective at a time (for three objective functions). The GA was chosen as a benchmark algorithm against which other algorithm performance can be measured in future work. Moreover, the GA is robust, widely applied in several fields of study, and can be viewed as the "workhorse" of heuristic optimization algorithms. The objectives in this work were chosen specifically for the LDC's benefit only, not the developer. The objectives of minimization of real power loss, maximization of investment deferral, and minimization of peak transmission demand charges

were then studied individually at monthly peak loading conditions over a 5 year planning period. While loss minimization and peak demand minimization objectives are readily found in the literature, the asset reinforcement deferral objective is not as common, and has not been applied to a real distribution feeder on a per-asset (distribution transformer, line and cable) level of detail, as in this work. Recall that Li *et al* had applied the asset reinforcement deferral to an entire subtransmission network in the UK and used feeder-level replacement costs.

The third stage evaluates and compares the net present value (NPV) of the dollar savings incurred by each objective separately with the "no DG" base case. It is up to the utility planner to decide which objective is most relevant to their assignment, perform the analysis, and assess the resulting savings. The loss and peak demand objectives were evaluated at monthly intervals (these are typically evaluated monthly per the billing cycle) and hence generated a cash flow over five years. The NPV was applied to the cash flows using the built-in NPV formula available in MS Excel which is a standard accounting technique. The asset deferral objective, which is an instantaneous capture of asset loading relief is already expressed in Present Value dollars and thus can be directly compared to the savings incurred by the loss and demand minimization objectives. However, due to significant seasonal and monthly load variations, an annual average loading condition in the base year of the planning horizon is evaluated.

Finally, this three-stage techno-economic evaluation technique (of PV DG) is applied to an actual distribution feeder at a per-asset level of detail rather than at a network level which is more common, thus making this technique more complete. The costs to replace each asset were obtained from recent project estimates provided by Kingston Hydro's engineering staff. This comprehensive technique can be readily customized to either substitute (or add to) the LSF with the voltage stability index evaluation in the optimal siting stage. Moreover, reactive power loss reduction can be added as an objective for systems where reactive power support is a concern, e.g. for a system that features long rural feeders with machine based DG.

This work succeeds in creating a ready-to-use techno-economic technique for LDCs in which only those objectives that are of interest to LDCs are used. This technique, which is especially relevant in the Ontario context given the proliferation of DG due to the introduction of the FIT program in 2009, translates the technical benefits of connecting PV DG to the distribution feeder into dollar savings which can then be presented to utility management.

Chapter 5 – Problem Formulation and Execution: Power Loss Sensitivity Method for Optimal Siting, Genetic Algorithm for Optimal Sizing, Objective Functions and NPV Analysis

5.1– Introduction

Figure 33 shows the program flow for the three stage algorithm for optimal PV DG siting and sizing and financial (NPV) evaluation for each objective function. The NPV analysis is performed on the savings obtained from each objective at Year 1 (present) of a 5 year planning period. Chapter 5 concludes with a brief description of NPV analysis.

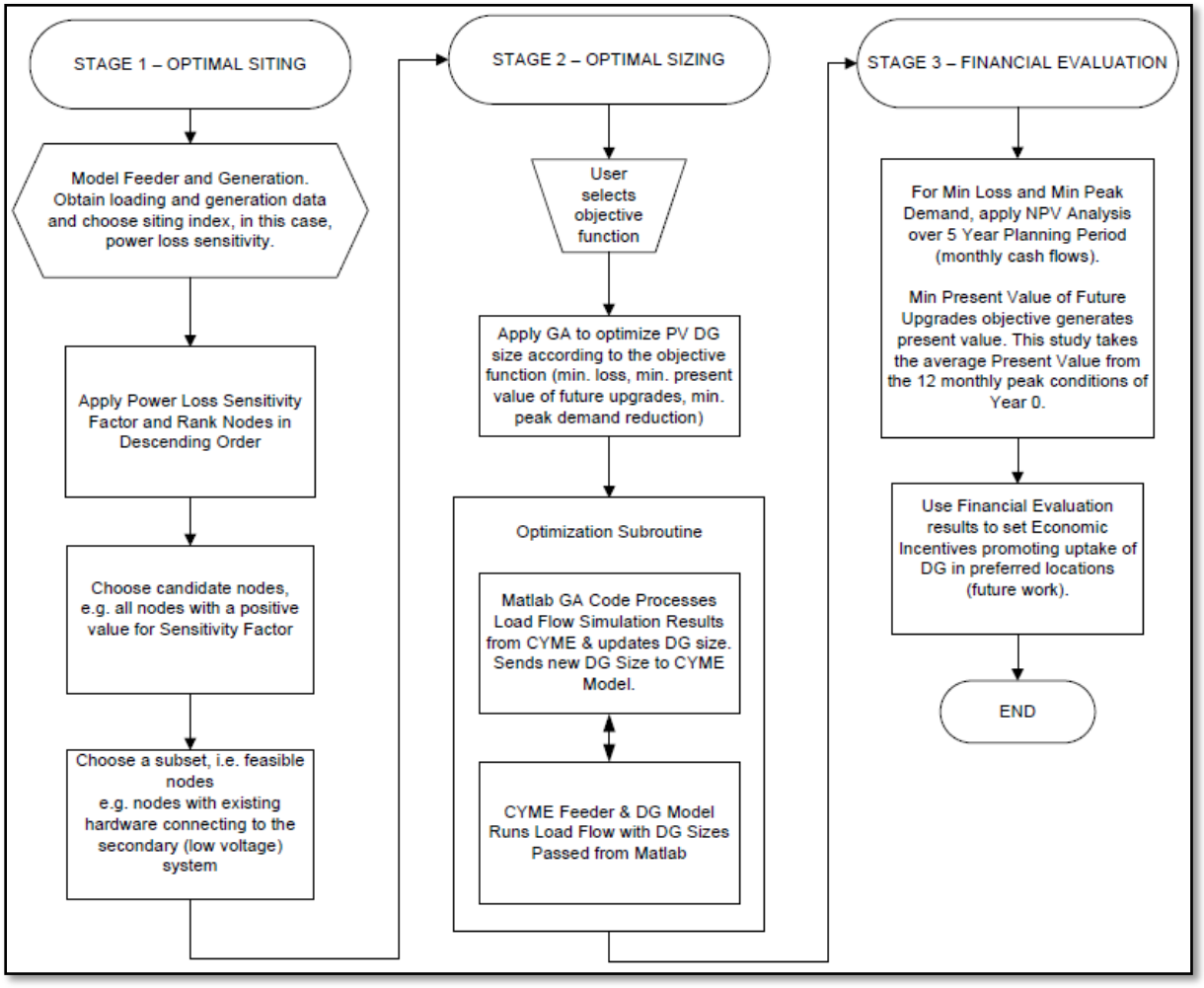

Figure 33 – Three Stage Techno-Economic Technique for Optimal Siting, Sizing and Financial Evaluation of PV DG for Minimization of: Real Power Loss, Present Value of Future Asset Reinforcement and Transmission Peak Demand Cost

5.2 – Optimal Siting using the Loss Sensitivity Factor (LSF) Method

The problem of optimal siting and sizing of inverter-connected PV DG is decoupled in this work. Optimal siting in this thesis is performed by applying the power loss sensitivity formula (refer to formula 2.9) and ranking the top 25 nodes out of 92 to identify the candidate locations of DG. 25 was chosen as loosely representing the top quartile out of the 92 nodes. The 25 candidate locations are then further reduced to 7 feasible locations by identifying which nodes, among the 25, featured distribution transformers (spot loads). Distribution transformers represent existing tie points to the low voltage distribution (secondary) system since they supply customer loads via service conductors to a customer's electric service entrance (panel). These preferred locations may then be used to develop a financial incentive program encouraging DG proponents to connect to these locations and share the utility cost savings.

The LSF optimal siting method was applied to Feeder X for one loading condition: winter peak using January 2009 values reported from Kingston Hydro's SCADA system. Specifically, the source demand was set to be 329A, 325A, 340A and 88.59% power factor at the substation transformer. Figure 34 shows the 25 candidate nodes highlighted in red ranked in descending order of power loss sensitivity, the 7 feasible nodes highlighted in green, the three most sensitive nodes and the three least sensitive nodes (note that the prefix "MS1" is excluded from the node labels). Table 3 shows the 25 candidate nodes including the 7 feasible nodes in green and their corresponding sensitivity index values.

To validate the LSF method, experimental verification was performed by injecting 10kW, 50kW and 200kW PV DG at the three most sensitive nodes (MS1-71, MS1-51, MS1-64) as well as at the three least sensitive nodes (MS1-137, MS1-157, MS1-114) generated by the analytical method. A load flow simulation was then run and the power loss measured for each phase at the sending end side of a node. These power loss values were then compared to the base case (no DG) power losses. Table 4 summarizes the experimental results and supports the theoretical approach by demonstrating that the largest difference

in power loss is indeed in the top ranked sensitive nodes as determined by the LSF method. Comparing the top three sensitive nodes, between Tables 3 and 4, it was found that in general, the most sensitive 3 nodes had larger variations in experimental power loss compared to the least sensitive 3 nodes, although there was sometimes slight variation between adjacent nodes in actual power loss sensitivity e.g., MS1-64 was found to be slightly more sensitive using the experimental approach than MS1-51.

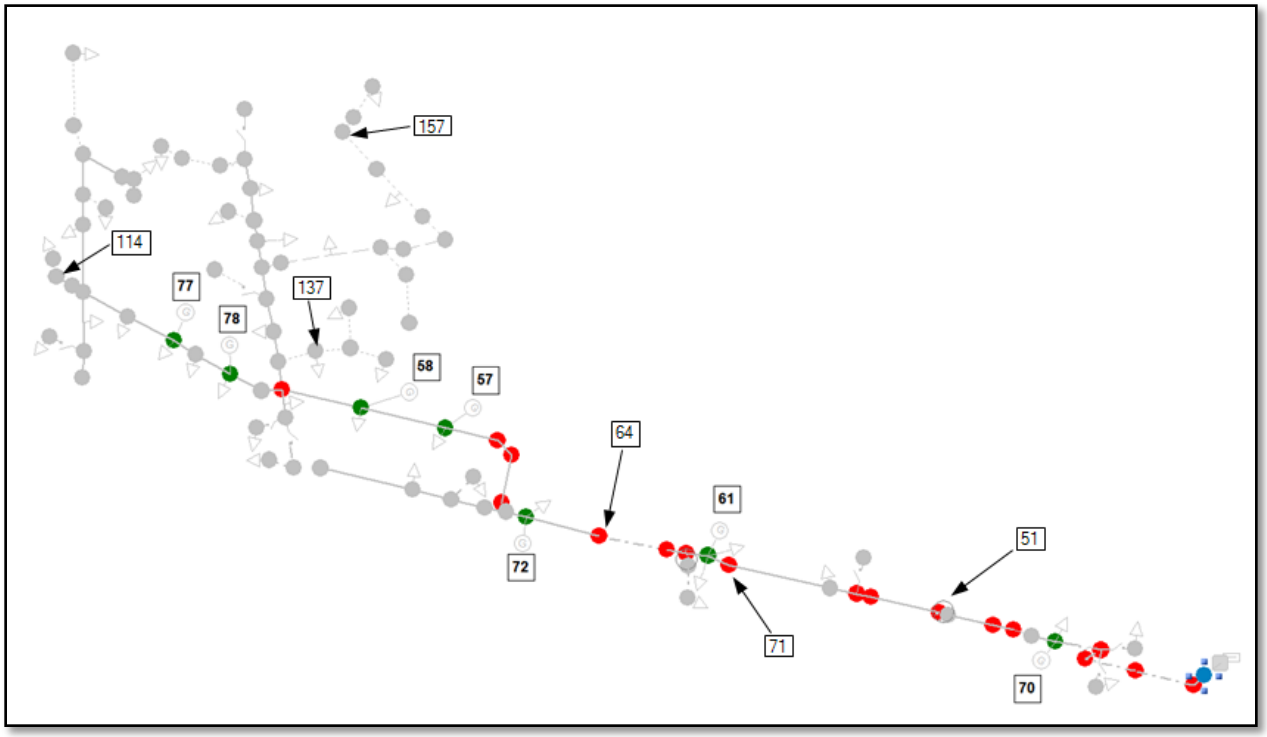

Figure 34 – 25 Candidate Nodes (red) and 7 Feasible Nodes (green) Ranked by Power Loss Sensitivity

Node	Sensitivity Factor (α)
MS1-71	0.00002214129
MS1-51	0.00001391580
MS1-64	0.00001258168
MS1-89	0.00001150247
MS1-91	0.00001045369
MS1-3	0.00001045169
MS1-9	0.00001034650
MS1-59	0.00000948307
MS1-63	0.00000932855
MS1-4	0.00000921980
MS1-48	0.00000822902
MS1-88	0.00000773213
MS1-86	0.00000684280
MS1-54	0.00000486447
MS1-60	0.00000484755
MS1-47	0.00000484363
MS1-32	0.00000483550
MS1-93	0.00000367580
MS1-65	0.00000321028
MS1-52	0.00000309017
MS1-87	0.00000282529
MS1-5	0.00000266825
MS1	0.00000265551
MS1-109	0.00000253420
MS1-105	0.00000242853

Table 3 - Candidate (red) and Feasible Nodes (green) Sorted by Power Loss Sensitivity Index Values

EXPERIMENTAL OUTPUT			
200kW PV DG Injection			
Node	Base Case (No DG) Power Loss (kW by phase)	Post DG Injected Power Loss (kW by phase)	Δ Power Loss (kW by phase)
MS1-71	1.36, 1.24, 1.74	1.20, 1.11, 1.56	0.16, 0.13, 0.18
MS1-51	0.71, 0.48, 0.84	0.62, 0.44, 0.76	0.09, 0.04, 0.08
MS1-64	0.85, 0.67, 0.79	0.76, 0.58, 0.69	0.09, 0.09, 0.1
MS1-137	0.01	0.15	-0.14
MS1-157	0.01	0.21	-0.2
MS1-114	0	0.01	-0.01
50kW PV DG Injection			
Node	Base Case (No DG) Power Loss (kW by phase)	Post DG Injected Power Loss (kW by phase)	Δ Power Loss (kW by phase)
MS1-71	1.36, 1.24, 1.74	1.33, 1.20, 1.69	0.03, 0.04, 0.05
MS1-51	0.71, 0.48, 0.84	0.69, 0.47, 0.82	0.02, 0.01, 0.02
MS1-64	0.85, 0.67, 0.79	0.83, 0.64, 0.76	0.02, 0.03, 0.03
MS1-137	0.01	0.01	0
MS1-157	0.01	0.01	0
MS1-114	0	0	0
10kW PV DG Injection			
Node	Base Case (No DG) Power Loss (kW by phase)	Post DG Injected Power Loss (kW by phase)	Δ Power Loss (kW by phase)
MS1-71	1.36, 1.24, 1.74	1.36, 1.23, 1.73	0, 0.01, 0.01
MS1-51	0.71, 0.48, 0.84	0.71, 0.48, 0.83	0, 0, 0.01
MS1-64	0.85, 0.67, 0.79	0.85, 0.66, 0.78	0, 0.01, 0.01
MS1-137	0.01	0.01	0
MS1-157	0.01	0	0
MS1-114	0	0	0

Table 4 - Experimental Verification Results of Power Loss Sensitivity Method

5.3 – Optimal DG Sizing using the Continuous Domain Genetic Algorithm

While deterministic methods are used where possible, heuristic methods are more popular when the user has little knowledge of the optimization function and its behaviour, so that a near optimal solution can be found [33]. A heuristic designates a computational method that optimizes a problem by iteratively trying to improve a candidate solution with regard to a given measure of quality. Heuristics make few or no assumptions about the problem being optimized and can search very large spaces of candidate solutions [35]. However, heuristics do not guarantee an optimal solution is ever found. Many heuristics implement some form of stochastic optimization. The user may then choose to refine the solution by switching to a deterministic method such as an exhaustive search in the vicinity of the global optimum. A popular subset of heuristic optimization algorithms include biologically-inspired algorithms such as such as evolutionary programming, evolutionary strategies, genetic algorithms, differential evolution, particle

swarm optimization, harmony search and ant colony optimization. Algorithms inspired by non-organic processes include simulated annealing and tabu search. The genetic algorithm (GA) was chosen for this research as a benchmark algorithm against which performance of other heuristics could be compared. Numerous engineering problems have been successfully investigated and optimized using genetic algorithms.

5.3.1 – Basic Concepts of the Genetic Algorithm

Genetic algorithms belong to the larger class of evolutionary algorithms (EA), which generate solutions to optimization problems using techniques inspired by natural evolution, such as inheritance, mutation, selection, and crossover (or mating) [35]. They have been widely applied in the fields of bioinformatics, engineering, science and are robust, although recent developments include variants of selection and crossover methods designed to improve performance. In the classic GA, a population of strings, called chromosomes or the genotype of the genome, represent encoded candidate solutions (called individuals, creatures, or phenotypes) to an optimization problem which evolve toward better solutions through each iteration or "generation" [35]. Traditionally, solutions are encoded in binary as strings of 0s and 1s, but other encodings are also possible, such as in this work, which uses the continuous domain genetic algorithm to represent real-number valued candidate solutions, i.e. the DG penetration limit at a node based on optimal loss minimization. Evolution usually starts from a population of randomly generated individuals and happens in generations. Note that the initial population affects the performance of the GA and a poorly selected initial population may extend the number of iterations required to reach an optimum.

The fitness of every individual in the population is evaluated at each iteration and then multiple individuals are stochastically selected from the current population based on their fitness modified, i.e. recombined and possibly randomly mutated to form a new population. The new population is then used in the next iteration of the algorithm. Commonly, the algorithm terminates when either a maximum number of generations has been produced, or a satisfactory fitness level has been reached for the population. If the

algorithm is terminated due to a maximum number of generations, a satisfactory solution may or may not have been reached. Figure 35 shows the main components genetic algorithm in a flowchart with the pseudocode presented as follows:

```
begin GA
  g:=0  { generation counter }
  Initialize population P(g)
  Evaluate population P(g)  { i.e., compute fitness values }
  while not done do
    g:=g+1
    Select P(g) from P(g-1)
    Crossover P(g)
    Mutate P(g)
    Evaluate P(g)
  end while
end GA
```

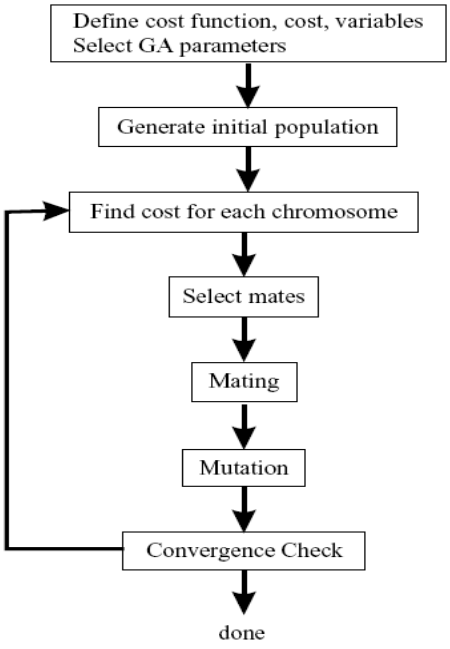

Figure 35 – Flowchart of the Genetic Algorithm [36]

Thus, the three main GA operators are:

1. **Selection** – individuals with higher fitness than others are selected for crossover (mating) so that their offspring can continue to the next generation. The simplest method to choose an individual is based on proportional fitness, also known as roulette wheel selection where the fitter an

individual is, the more likely they are to get selected. Figure 36 illustrates this concept. For each individual, its proportional fitness is calculated, so that the sum of all individual fitness equals 1.0. On a line between 0.0 and 1.0, the better individuals will take up a larger proportion of the line than less fit individuals. An individual is then chosen by generating a random number between 0.0 and 1.0 and then selecting the individual in whose region of the number line the random number falls. By repeating this each time the individual needs to be chosen, the better individuals will be chosen more often than poorer ones thus promoting survival of the fittest [36]. Other popular selection methods include tournament selection where two or more individuals are selected randomly from the population and compared for fitness (winner gets to be a parent) and rank selection which is a straightforward ranking of the fittest individuals (top two become parents).

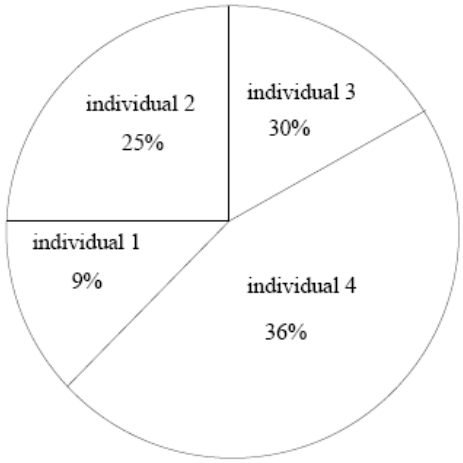

Figure 36 – Roulette Wheel Selection [43]

2. **Crossover** – the combination of two selected parents by randomly selecting one or more crossover points in each parent, exchanging the corresponding parts of each parent, creating two offspring which survive to the next generation. This work uses a one point crossover scheme, illustrated in Figure 37.

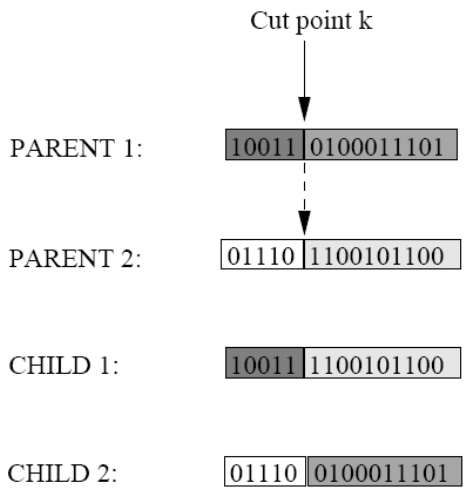

Figure 37 – One Point Crossover Scheme [43]

3. **Mutation** – the occasional (with low probability) change of part of an individual, i.e. a gene within a chromosome. Mutation introduces randomness and enables the heuristic from becoming trapped in local optima. Figure 38 shows mutation in a binary encoded chromosome.

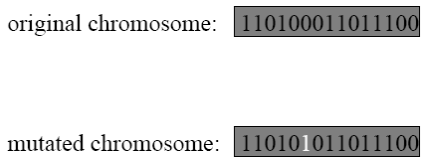

Figure 38 – Mutation in a Binary Encoded Chromosome [43]

5.3.2 – Application of the Continuous Domain GA to Optimal Sizing of PV DG

The optimal PV DG sizes in this study are real-valued and are not constrained to pre-encoded sizes as can be found in some research literature. This is so that a true representation of the ideal PV DG penetration limit on a distribution feeder, determined by optimum loss reduction, asset reinforcement deferral and peak demand reduction individually, could be set and monitored by distribution system

planners. Chromosomes were defined as a vector of feasible node length containing candidate DG sizes which represented optimum real power output. Each node's DG size represents an individual gene. The population size used in this work is 20 and the number of iterations is 20. These parameters were reached after observing that optimal solutions were reached at around the 10-12 iteration mark, well under the standard 20 iterations. The population of 20 (number of individuals) x 7 (feasible node list) is initialized using the "rand" function in MATLAB. However, it was found that since the values of the rand function are real-valued in the range of 0 to 1, a multiplier of 100 had to be applied to obtain realistic optimum PV DG outputs in the ~10-100kW range, rather than <1kW. For additional detail on the implementation of a continuous domain GA, the reader is referred to [37].

The GA parameters were tuned by varying each parameter on the power loss minimization objective function and noting the objective function value. The initial GA parameters are shown in the first row of Table 5. Subsequent entries show the effect of varying a specific parameter in red. The population size and number of iterations were both selected to be 20 since, if they were greater than approximately 30, CYMDIST's memory would become overloaded and cause the program to crash, suggesting that approximately 600 simulations can be performed in CYMDIST. However, as can be seen from the last row in Table 5, a better objective function value was achieved with a greater number of iterations. In summary, the first row in Table 5 represents the GA parameters that achieved the best compromise between obtaining the lowest objective function value while ensuring that CYMDIST did not crash.

Mutation Rate	**Elitism**	**Pop Size**	**Num Iterations**	**Base Case (kW)**	**Min Power Loss (kW)**
0.2	0.8	20	20	42.09	23.56
0.95	0.8	20	20	42.09	23.86
0.2	0.1	20	20	42.09	25.6
0.2	0.8	50	15*	42.09	24.73
0.2	0.8	20	37*	42.09	23.19

Table 5 - Varying GA Parameters to Determine Optimal Parameters (* indicates the maximum number before overloading CYMDIST's memory)

As in [37], the GA used in this work also employed elitism, where the top 80% of the individuals were considered eligible for mating. The classic roulette wheel selection (also known as rank weighting) method as well as a single point crossover method was used. The crossover point on a parent chromosome was selected based on a random operator to introduce another element of randomness in addition to the mutation parameter [37]. The chromosome represents the PV DG sizes at the 7 fixed node locations and is shown in Table 6 as a member of a sample population generated during the algorithm after a specific iteration.

		Node Number (of the 7 Feasible Nodes)						
		1	2	3	4	5	6	7
Population Member	1	96.48885	60.73892	75.46867	65.44457	56.78216	97.97484	80.00685
	2	6.359137	93.39932	79.51999	69.90767	50.00224	52.85331	77.49105
	3	71.24996	60.73892	75.46867	65.44457	56.78216	97.97484	80.00685
	4	68.43778	60.73892	75.46867	65.44457	56.78216	97.97484	80.00685
	5	91.33759	93.39932	79.51999	69.90767	50.00224	52.85331	58.83841
	6	58.59806	60.73892	75.46867	65.44457	56.78216	97.97484	80.00685
	7	91.33759	22.404	79.51999	77.88022	77.02855	52.85331	71.26945
	8	91.33759	93.39932	79.51999	69.90767	47.3486	52.85331	36.31743
	9	42.23899	93.39932	79.51999	69.90767	50.00224	52.85331	77.49105
	10	91.33759	93.39932	79.51999	54.47161	64.76176	60.98666	21.86766
	11	37.24097	45.66272	79.51999	94.51741	54.97236	52.85331	77.49105
	12	91.33759	9.111346	79.51999	69.90767	69.51405	52.85331	64.2307
	13	98.40637	39.2227	64.6313	72.10466	41.61586	45.37977	39.97826
	14	20.79431	93.39932	79.51999	69.90767	32.24718	52.85331	77.49105
	15	91.33759	93.39932	79.51999	69.90767	50.00224	38.63252	0
	16	39.09378	93.39932	33.94934	69.90767	54.65931	52.85331	77.49105
	17	96.48885	60.73892	75.46867	65.44457	56.78216	72.03316	0
	18	0	0	0	0	0	25.94168	80.00685
	19	5.495831	0	0	0	0	0	0
	20	85.84175	93.39932	79.51999	69.90767	50.00224	52.85331	77.49105

Table 6 – Example Population & Chromosome at an Iteration – Node Number represents Location and Value represents the Optimal PV DG Real Power Output

5.3.3 – Objective Functions for Optimal Sizing of PV DG

This research work actually began as a comparison of algorithm performance in optimal siting and sizing for DG, however, during the research process, the focus of the work shifted from method to results.

That is, the objective functions needed to be chosen carefully to best answer the question which LDCs have regarding the operational and economic aspects of distributed generation. Due to Kingston Hydro's generation connection experience being dominated by small PV DG connection applications within the FIT program, the question posed by utility management and asset managers was "*How does the connection of PV DG benefit utility planning and operations, and how do these improvements translate into financial savings for the utility?"* Thus, the following three objectives were formulated and simulated separately.

1. **Minimization of Real Power Loss (kW)** – in distribution systems, real power loss represents power delivery inefficiency (due to incorrectly sized conductors or unbalanced load) and lost revenue making loss reduction an obvious priority for distribution planners. The fitness function is defined as:

$$F_1 = min \sum_{i=1}^{N} P_{Loss,\ with\ DG} \tag{5.1}$$

where N is the number of nodes (92 in this study). Loss is dependent on the power flow solution which varies as load requirements and generation output change. Therefore, to avoid excessive computation, load flow simulations in CYMDIST were run for twelve monthly peak loading scenarios. The PV DG units were connected to the 7 feasible nodes, and the solar variation factor was applied to the PV DG output during the optimization process (refer to Figure 23 in Section 3.3.2). In this work, CYMDIST's load flow (voltage drop method) solution currents are used to obtain the total feeder loss in kW using the I^2R relationship. Monthly losses are calculated for a 5 year planning period based on a modest annual load growth rate (1.06% based on the actual load growth rate in Kingston Hydro) and the peak electricity distribution rate at 9.9 ¢/kWhr, resulting in a slight increase in losses every year [38]. Monthly and annual losses represent a negative monthly cash flow in the NPV analysis. To calculate the annual cost of system losses, the built-in

loss factor formula in CYMDIST is used. The loss factor is an expression of the real power loss over a given period of time (in this case annual) at a given loading condition (monthly peak load scenarios are used in this study). The loss factor is dependent on the load factor, LDF, which is the average power divided by the peak power, and is an indication of how heavily loaded distribution equipment is. For this study, the load factor is set at 80% based on an operating limit of conductors at 400 amps and given that peak demands were found to be in the range of 280 amps to 320 amps (thus the quotient of the two sets of values is approximately 80%). The loss factor formula is calculated as:

$$Loss\ Factor = 0.15 * LDF + 0.85 * LDF^2 = 0.664 \quad (5.2)$$

The annual loss cost was calculated after a load flow simulation as the product of the kW loss, number of hours in a year (8760), the loss factor (0.664) and the distribution rate (9.9 ¢/kWhr).

2. **Minimization of Present Value of Future Asset Reinforcement or Maximization of Asset Deferral ($)** – based on Li *et al*'s work in [28] and summarized in Chapter 4. The fitness function is given by:

$$F_2 = \min\left(\sum_{i=1}^{X}\left(\frac{DxTransformer_{\ i}}{(1+d)^{n_i}} - \frac{DxTransformer_{\ i}}{(1+d)^{n_{i\ New}}}\right) + \sum_{j=1}^{Y}\left(\frac{OhdLine_{\ j}}{(1+d)^{n_j}} - \frac{OhdLine_{\ j}}{(1+d)^{n_{j\ New}}}\right) + \sum_{k=1}^{Z}\left(\frac{Cable_{\ k}}{(1+d)^{n_k}} - \frac{Cable_{\ k}}{(1+d)^{n_{k\ New}}}\right)\right) \quad (5.3)$$

where X is the number of distribution transformers, Y is the number of overhead lines, Z is the number of cables, d is the discount rate, n is the time to reinforce the asset in the base case (no-DG) and n_{New} is the time to reinforce the asset in the test case (DG). The present value of future asset reinforcement is evaluated at the twelve monthly peak conditions for distribution

transformers (pole mounted and pad mounted), overhead lines and underground cables. As in the loss reduction objective, the PV DG units were connected to the 7 feasible nodes, and the solar variation factor was applied to the PV DG output during the optimization process.

Asset reinforcement in the case of conductors and cables, or asset replacement in the case of distribution transformers, is scheduled when the equipment reaches 100% loading within a five year planning period at a monthly compounding interval and at a (conservative) inflation rate of 2%. The present value increases as loading increases, causing the scheduled replacement date to move closer to Year 1 (i.e. the present) in the planning period. The resulting present value is not a cash flow, but a one-time financial interpretation of a loading condition. In this work, the present values were calculated for the 12 monthly peak loading conditions in Year 1.

Although the formulas are applied element-wise to distribution transformers, lines and cables, thus tailoring the loading and capacity for each element, in reality, the rate of load growth could vary by location from feeder to feeder and by equipment, e.g. from substation main transformer and distribution lines. The load growth rate was taken to be 1.06%; the discount rate for feeder distribution equipment, prescribed by accounting standards, is set at 4%. According to the accounting standards, the discount rate for substation equipment such as substation (power) transformers is depreciated more quickly at 3.33%. Table 6 shows the present value replacement, or modern equivalent, costs for the assets. The following interesting observation was made during the presentation of this work at a seminar at the University of Waterloo: the n_l quantity, which is based on the asset loading and capacity levels, could be adapted to represent any equipment-based metric that has a “capacity” limit and a measurable tendency for the equipment to reach that limit; for instance, transformer insulation degradation.

Distribution Transformers Present Value Replacement Cost	
kVA	**Replacement Cost ($1000's)**
37.5	5
50	5
75	5
100	10
112.5	10
150	10
167	10
225	15
300	20
337.5	20
500	20
Overhead Line Present Value Replacement Cost per Section	
Phase	**Replacement Cost ($1000's)**
1	5
2	7.5
3	10
Underground Cable Replacement Value Cost per Section	
Phase	**Replacement Cost ($1000's)**
1	10
3	20

Table 7 - Present Value Replacement Costs for Distribution Equipment

3. **Minimization of Transmission Peak Demand Charges ($)** – LDCs, as Transmission System customers, pay a network service rate $3.22, and $0.79 line connection service rate, per kW of Kingston Hydro billing demand per month to the transmission system operator (Hydro One) [38]. The minimum peak demand charge fitness function is given by:

$$F_3 = \min \sum_{i=1}^{M} [(3.22 + 0.79) * PeakSystemDemand] - [(3.22 + 0.79) * SolarVariationFactor * OptimalTotalDG] \quad (5.4)$$

where the $PeakSystemDemand$ is the peak kW demand measured at the transmission station which feeds the substation transformer supplying Feeder X. Finally, $OptimalTotalDG$ is the optimal total DG value on the feeder – a quantity optimized by the GA. The contribution of the test feeder's demand reduction to the total transmission peak demand reduction at the TS, due to the installation of PV DG, is assumed to be the ratio of the monthly peak demand of Feeder X to the monthly peak demand of the TS. For January 2010, the peak demand for feeder 104 was calculated from SCADA amp readings to be 2.19 MW and the peak demand at the TS was metered as 77.914 MW therefore the contribution can be assumed to be approximately 2.19/77.91 = 2.81%, or 3%. The monthly savings from peak demand reduction represent a monthly positive cash flow in the NPV analysis.

5.4 – Net Present Value (NPV) Analysis

Fundamental to finance is the concept of "time value of money," where the assumption is that money is worth more in your hand today then tomorrow. For example, money available now can be invested to generate interest and revenue which is a lost opportunity if one has to wait for money to have at their disposal. The NPV, or net present worth (NPW), of a time series of cash flows, both incoming (positive) and outgoing (negative), is defined as the sum of the present values (PVs) of the individual cash flows [40]. If all future cash flows are incoming and the only outflow of cash is the purchase price, the NPV is simply the PV of future cash flows minus the purchase price [40]. NPV is a valuable tool in discounted cash flow (DCF) analysis, is a standard method for using the time value of money to appraise long-term projects and is used for capital budgeting to measure the excess or shortfall of cash flows in present value terms once financing charges are met [40]. In this case, the financial benefit to LDCs of increased DG uptake at strategic locations on the distribution feeder is evaluated using NPV analysis. The NPV of a sequence of cash flows takes as input the cash flows and a discount rate or function and outputs a price; the converse process in DCF analysis – taking a sequence of cash flows and a price as input and inferring

as output a discount rate (e.g. “break even” discount rate which would yield the given price as NPV) is called the yield, and is more commonly used in finance, e.g. bond trading [45].

For this work, a planning period of five years was used to standardize the time horizon so that a NPV analysis can be performed and the financial benefit of each objective can be compared in present value terms. Moreover, as stated in Section 2.5, five years is a typical project planning range at Kingston Hydro and coincides with city wide road and utility public infrastructure planning. The inflation rate used to calculate the NPVs for fitness functions F_1 and F_3 in this study was 2%, a value deemed by accounting staff to be conservative and appropriate for this study [39].

Chapter 6 – Results and Discussion

6.1 – Summary of Method and Application

The comprehensive techno-economic method of optimal siting and sizing of PV DG and evaluation of the resulting financial benefit, presented in this work, was developed to help utility engineers and asset managers to determine the optimum penetration of PV DG on the feeder by individually measuring the economic savings incurred by the following three objective functions: minimization of loss, asset life extension and minimization of peak demand charges. The algorithm used was a real-valued genetic algorithm chosen for its proven performance in other fields (can be considered a "benchmark" algorithm) and is well suited to a combinatorial problem.

Since the provincial government of Ontario introduced the FIT program in 2009, the uptake of small scale PV DG on the distribution system has been unprecedented (large scale PV installations such as the Sarnia plant have also been installed as a result of this program). If the FIT program continues to be supported by government and the rate of generation growth continues, utility planners must be able to assess, and financially quantify, the benefits of DG as part of an asset management strategy. Planning and asset management usually involves designating a year within a defined planning horizon in which reinforcements to system equipment such as conductors, cables or transformers should occur – the timing of which can be extended by the presence of DG. Standard NPV analysis shows that deferring investment in asset upgrades results in a lower present value of total costs at Year 1 (the first year in the planning horizon which in this work is 2010).

6.2 – Simulation Results

For each objective, the total optimal PV DG output (considering all 7 nodes) ranged from 450 kW to 550 kW. At a peak demand of 2.1MW Feeder X during the winter months, 500 kW value represents approximately 25% of the feeder load. The following results are shown for the base year in the five

planning horizon, Year 1, or 2010. However, to complete the NPV evaluation, additional simulations were performed for a total of 60 monthly peak load scenarios for Objectives 1 and 3 – the loss reduction and peak demand reduction objectives, respectively. The asset investment deferral objective (Objective 2) yields its results in present value dollars, and so was directly compared to the NPV costs for Objectives 1 and 3. Objective 2, however, was simulated over 12 monthly peaks for Year 1 and then averaged, to try and account for the fact that the monthly variations were significant.

6.2.1 – Objective 1 – Minimization of Real Power Loss

The minimization of real power loss for monthly peak load scenarios in Year 1 (2010), including the solar variation factor is shown in Figure 39 for the no-DG (base) and DG (test) cases. Kingston Hydro is clearly a winter peaking utility, largely due to the students attending Queens University in the fall and winter. Figure 40 shows the total optimal DG value (the sum of all 7 nodes) by month. While the total values vary slightly, the study shows that the algorithm tends to connect more DG to compensate for the losses in the winter months.

Figure 41 shows the base case voltage profile measured at the most downstream node with DG, MS1-109. The impact of connecting PV DG on the voltage profile is not significant, which is to be expected with electronically coupled DG generating active power output at a power factor of 0.95. Voltage profile improvement would be more significant with the connection of machine-based DG especially on long feeders susceptible to a large voltage drop. Ideally, the base voltage should be 4160V; however, voltage drop along the line results in slightly lower values at the feasible nodes that are still within the acceptable operating range. Since the difference in voltage profiles is not significant from the base case and test case voltage profile, the difference between base case and test case voltage values at node MS1-109 are summarized in Table 8 as follows:

Phase	Base Case Voltage (V)	Test Case Voltage (V)
R	4003.2	4011.3
W	3990	3998.1
B	3974.6	3982.8

Table 8 - Voltage Profile Improvement Values for Objective

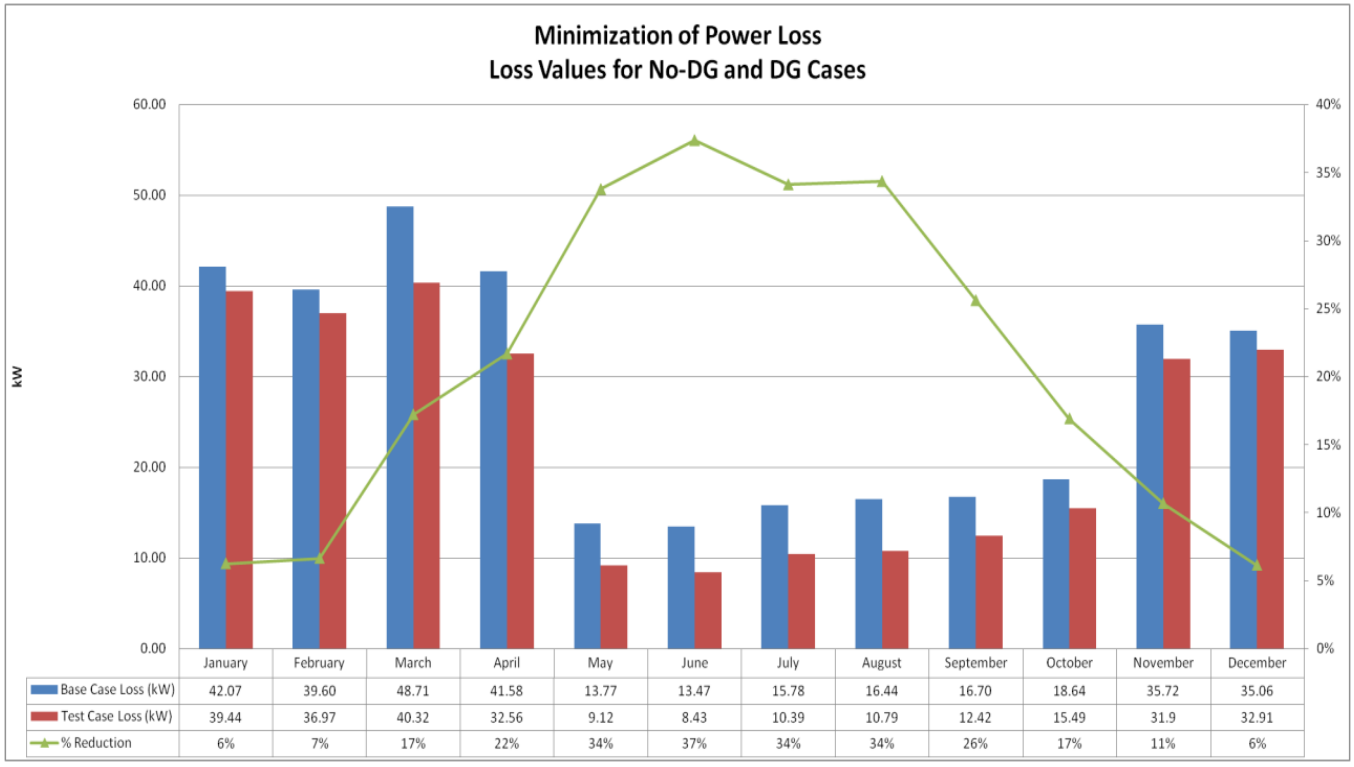

Figure 39 – Objective 1: Power Loss Minimization & Percent Reduction due to DG

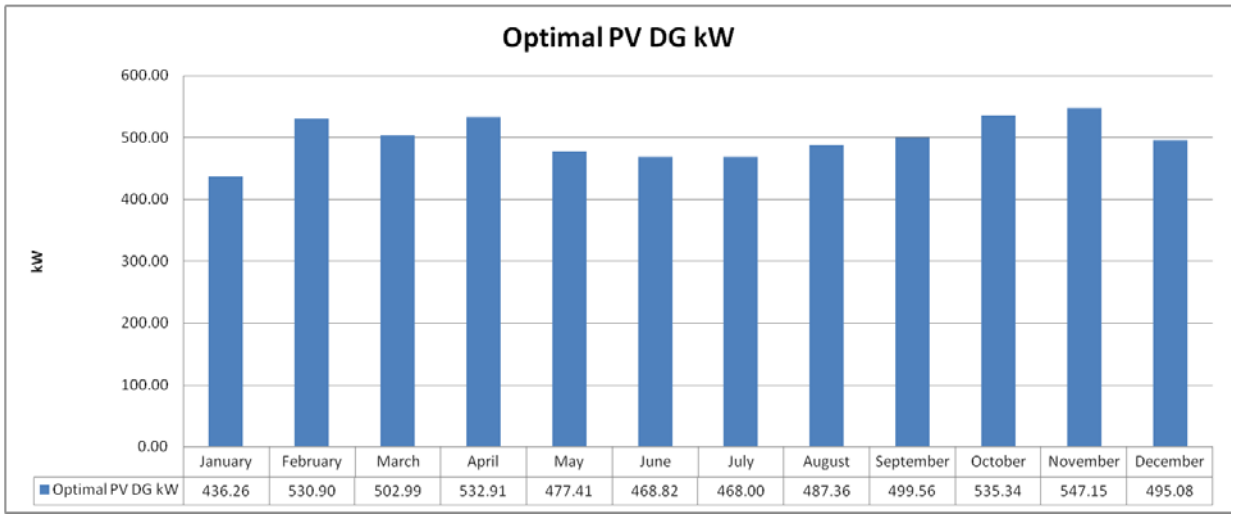

Figure 40 – Objective 1: Total Optimal DG Output (for All 7 Optimal Locations) by Month

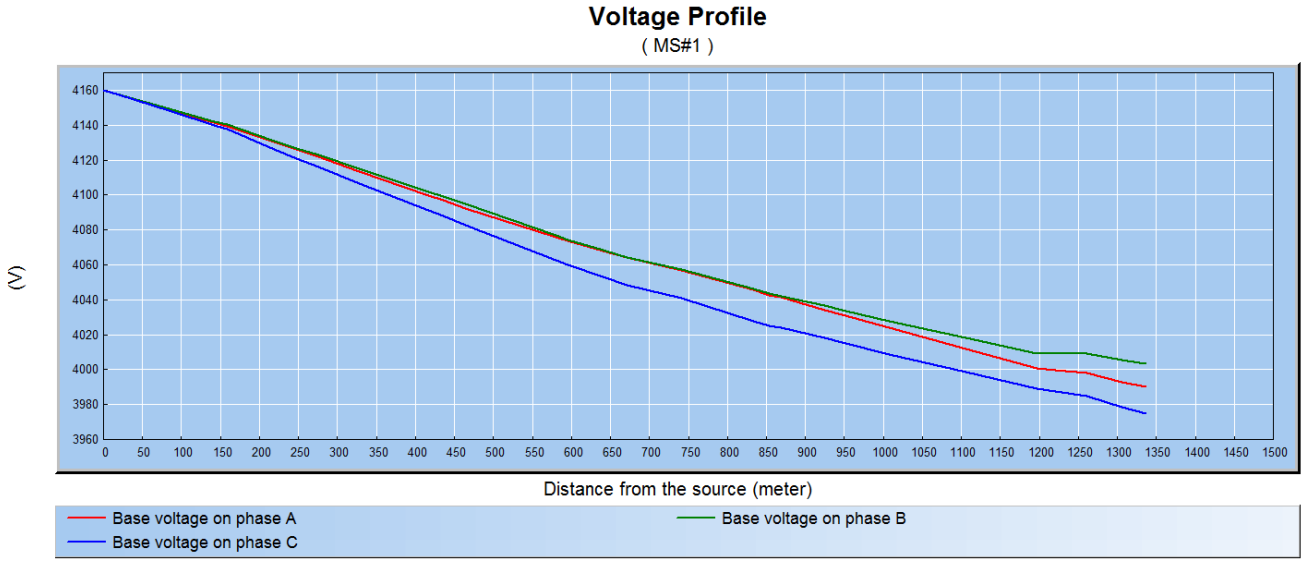

Figure 41 – Base Case Voltage Profile for Feeder X using January 2010 Peak Loading

Similarly, the difference between base case voltage and test case voltage profiles for all three objectives, relative to node MS1-109, is slight (visually indistinguishable) due to the low number of feasible locations (only 7) and the relatively low difference between the nodes for optimal DG kW.

6.2.2 – Objective 2 – Minimization of Present Value of Future Asset Reinforcement (Maximization of Asset Deferral)

The base case and test case results for the second objective, minimization of the present value of future investment in asset reinforcement, are shown in Figure 43 for each monthly peak load and scaled generation scenario and for the 7 feasible node case. The most significant reduction occurred in March 2010 (highest loading) showing that the objective is sensitive to load variations. Note that this objective does not represent a monthly cash flow, and is most useful as a real-time capture of equipment loading at the monthly peak load condition. For this study, to compare the results to the other two objectives, simulations were performed for 12 monthly peak load scenarios (using real data from 2010) and then averaged over the year to reach an annual average savings. The total optimal PV DG output is also shown in Figure 43. Compared with the optimal DG output for Objective 1, shown in Figure 40, the optimal DG output for the months of June, August and December are generally higher for Objective 2 but still within the 450 kW to 560 kW range.

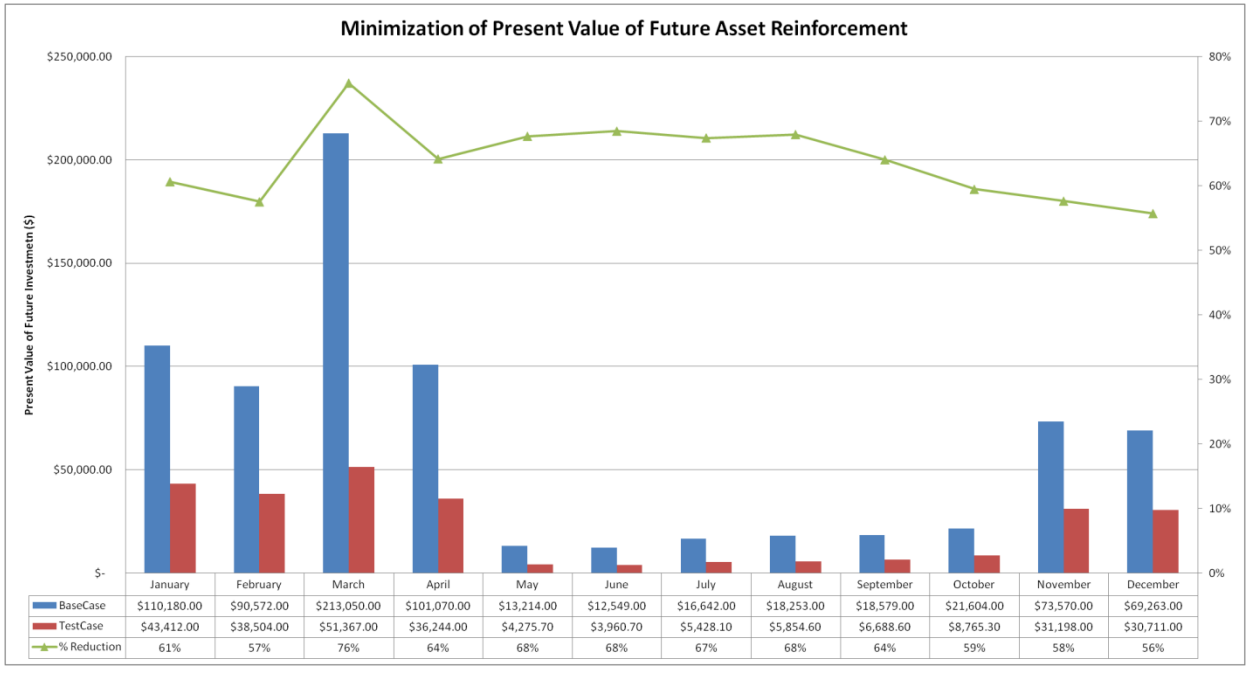

	January	February	March	April	May	June	July	August	September	October	November	December
BaseCase	$110,180.00	$90,572.00	$213,050.00	$101,070.00	$13,214.00	$12,549.00	$16,642.00	$18,253.00	$18,579.00	$21,604.00	$73,570.00	$69,263.00
TestCase	$43,412.00	$38,504.00	$51,367.00	$36,244.00	$4,275.70	$3,960.70	$5,428.10	$5,854.60	$6,688.60	$8,765.30	$31,198.00	$30,711.00
% Reduction	61%	57%	76%	64%	68%	68%	67%	68%	64%	59%	58%	56%

Figure 42 – Objective 2: Minimization of Present Value of Future Asset Reinforcement & Percent Reduction due to DG

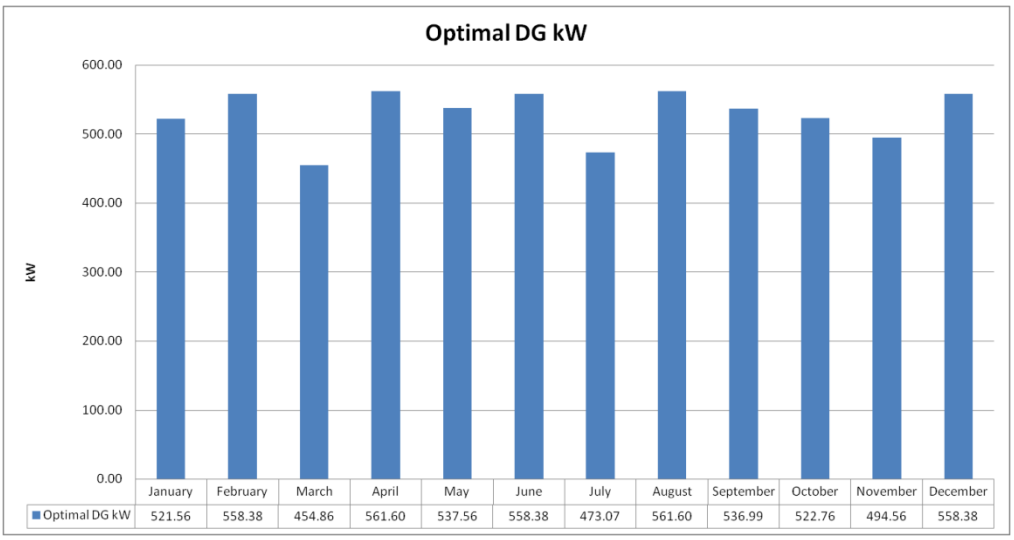

Figure 43 – Objective 2: Total Optimal DG Output (for All 7 Optimal Locations) by Month

6.2.3 – Objective 3 – Minimization of Transmission Peak Demand Charges

Figure 44 shows the variation in peak demand recorded at the transmission station supplying the distribution substation associated with Feeder X for 2010. Figure 45 shows both base case and test case peak demand charges. It was noted that, after performing the load flow, there was a slight improvement in the voltage profile from 4011.3V to 4011.4V for the red phase, 3998.1V to 3998.2V for the blue phase and 3982.8 to 3982.9V for the white phase. The amount of cost savings (base case minus test case costs) for the third objective, minimization of peak demand and resulting transmission charges to the LDC, are shown in Figure 47. As for Objectives 1 and 2, the optimal penetration of DG output, under the specified loading conditions (monthly peaks) and at the 7 nodes, is in the 500kW range. July represents the month with the highest cost savings due to the fact that July features the highest PV generation output compared with December which is characterized by high demand and lower generation values.

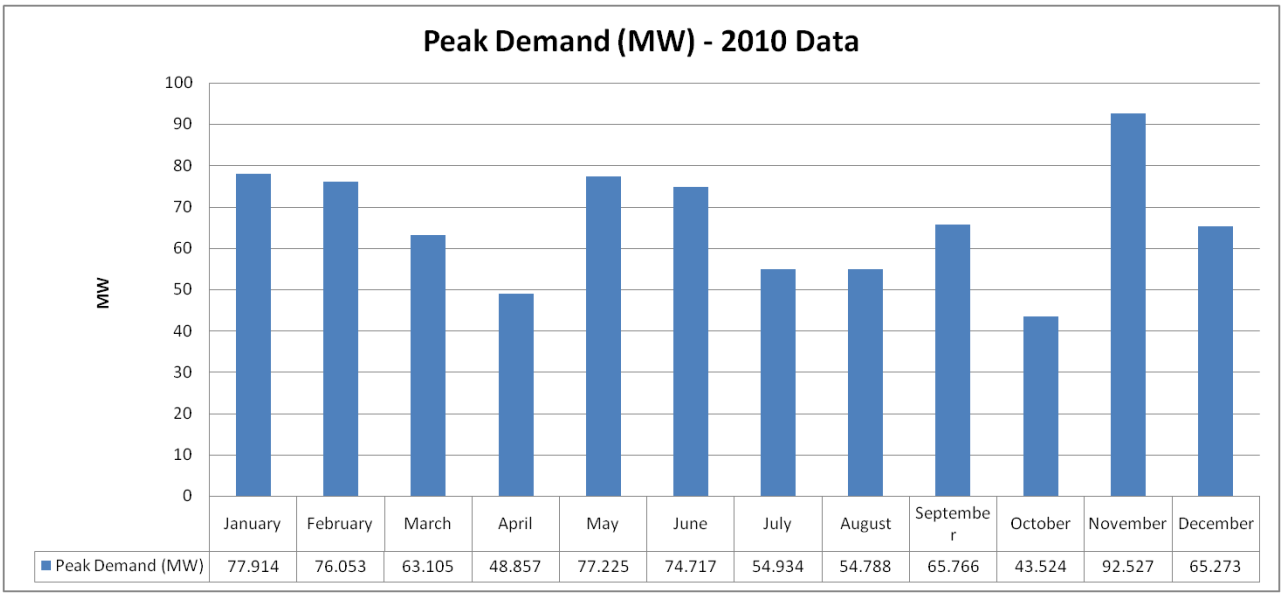

Figure 44 – 2010 Peak Demand Variation at Transmission Station Upstream of Feeder X

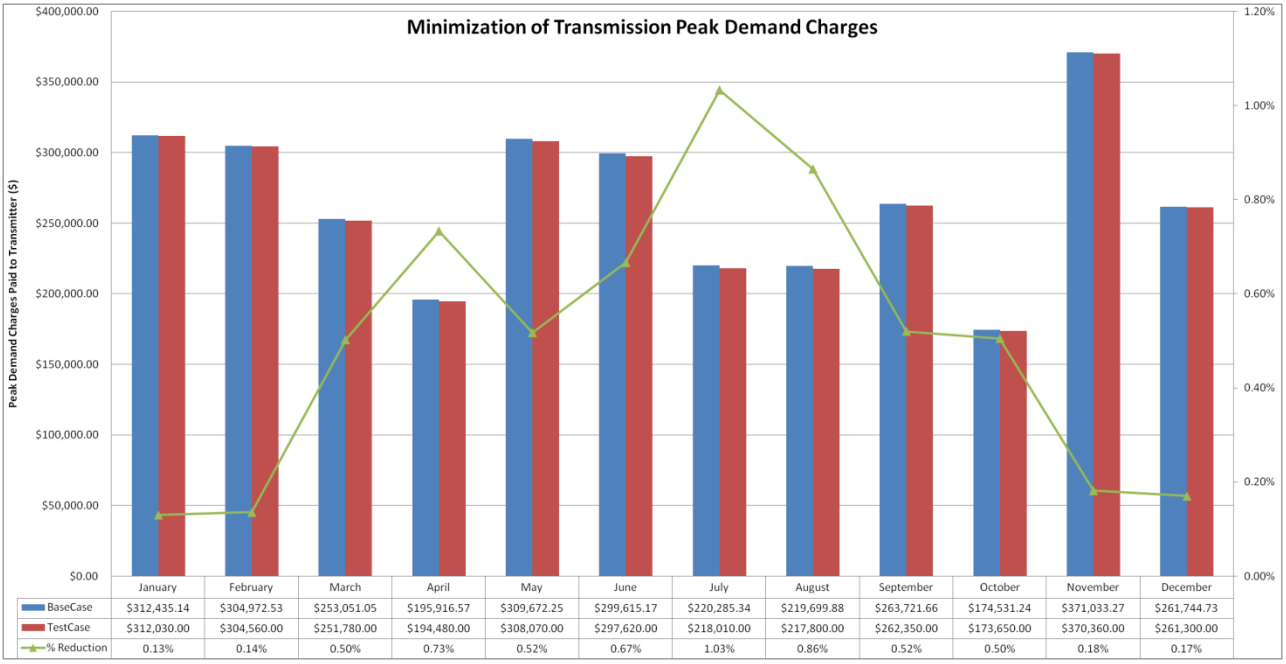

Figure 45 – Objective 3: Minimization of Peak Demand Charges Paid to Transmitter by LDC & Percent Reduction due to DG

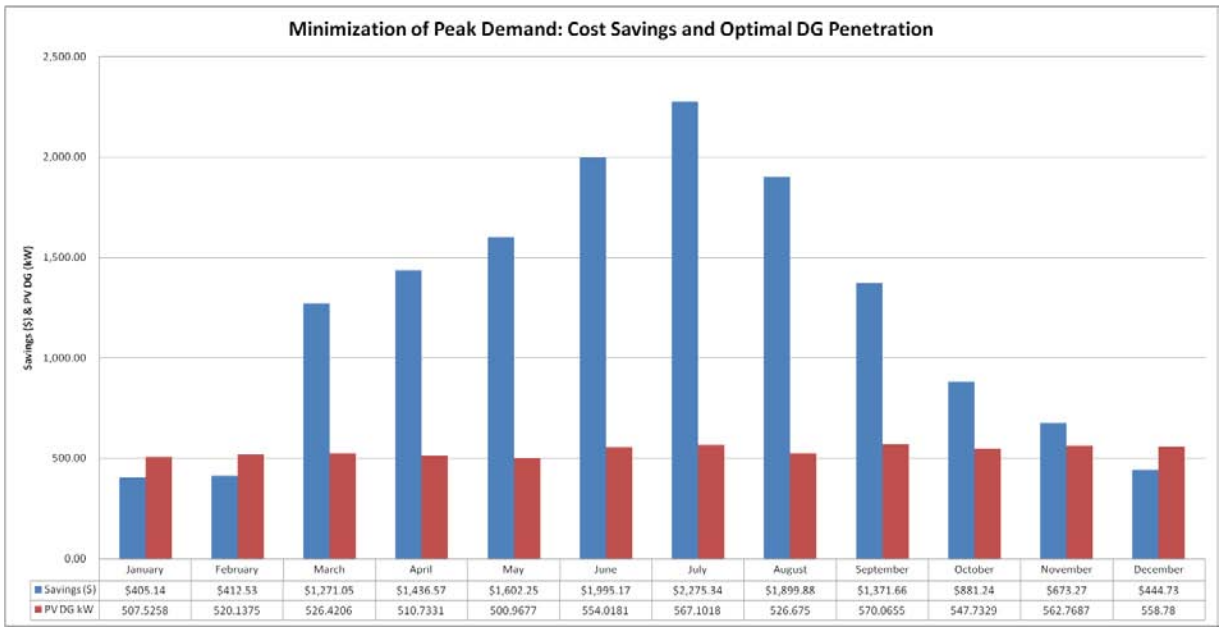

Figure 46 – Objective 3: Cost Savings and Optimal DG Penetration by Month

6.2.4 – Financial Evaluation of each Objective Function using a NPV Analysis

The NPV analysis is a standard accounting tool applied to cash flows – often used to determine present value savings and is therefore a suitable financial evaluation method for this work. Table 9 summarizes the results of the NPV analysis and the present value savings for each objective. Recall, the NPV analysis in this study uses an inflation rate of 2% and a monthly compounding period for Objectives 1 and 3 over a five year planning period. Therefore, for Feeder X alone, an optimal PV DG allocation could in a savings of $137, 278.51 over a five year planning period using monthly peak loading. Since the optimal allocation for each objective differs slightly, the actual savings would be slightly less than this number; nevertheless, these results prove that PV DG can result in significant savings for the utility over time due to loss reduction, asset investment deferral, and peak demand reduction.

Objective	Base Case Cost (no DG)	Test Case Cost (with DG)	Present Value Savings (Base Case - Test Case)
1*	$78,985.28	$52,410.66	$26,574.62
2**	$63,212.17	$22,200.75	$41,011.42
3*	$ 14, 777, 672.10	$14,707,839.36	$69, 832.74
Total →			**$137,418.78**

* NPV of Monthly Cash Flows Over a 5 Year or 60 Month Planning Horizon
**Objective 2 is not a Monthly Cash flow, but an Instantaneous Value therefore Average of 12 Months is taken for Year 1 of 5

Table 9 - Savings over 5 Year Planning Horizon Incurred by each Objective

6.3 – Discussion

The average total optimal output of PV DG for each objective was approximately 500 kW, approximately 25% of the peak load of the feeder (if the number of optimal and feasible locations was higher, the total output would likely have been greater). The percent reduction in costs for each objective is shown for clarity and to show the difference in variation patterns for each objective. For instance, the loss minimization objective clearly shows the largest reduction in the summer months due to high levels of PV DG power output. The asset investment deferral objective shows the highest reduction in the month of March, which corresponds to the highest load in 2010, and demonstrates the dependence of the objective function on the loading level. Finally, the transmission demand minimization charges shows greater savings in the months of July and August, which corresponds to high air conditioning demand during Kingston's tourist and student move-in season. April and June showed the next highest savings for the demand minimization objective perhaps due to increased activity in the industrial or commercial sectors. Note that the demand minimization objective yields the highest savings at $69, 832.74 versus $26,574.62 and $41,011.42 for the loss minimization and asset investment deferral objectives, respectively. It is important to realize that these savings are passed onto customer, by minor rate adjustments made during the year by accounting and regulatory staff and are not realized by LDC for future reinvestment.

Due to recent regulatory changes to the Distribution System Code, from 2010 onwards, conservation initiatives are also expected to have a similar impact to the FIT program's success in increased DG uptake in providing asset loading relief and demand minimization. Loss reduction would also be achieved due to lower load currents yielding in proportionally reduced losses; however, the benefit of DG is that local generation supports local load, minimizing the province's transmission and distribution line delivery losses.

Finally, if a test feeder, at the ideal PV DG penetration limit condition, could incur savings of approximately $137, 000 over five years, then extrapolating similar savings to the entire system's 110 feeders suggests that the system savings would be significant. The number of feeders can be better identified, perhaps with a socio-economic study, which would forecast DG uptake at specific feeders in the distribution territory based on, say, rooftop availability. Furthermore, the comprehensive three stage techno-economic method presented in this thesis can be applied to any feeder, and can be extended to entire regions and networks.

Chapter 7 – Conclusions and Recommendations for Future Work

7.1 – Conclusions

The three stage techno-economic method for quantifying the ideal technical penetration limit of PV DG on a feeder presents a valuable asset management tool for utility asset planning. In the generation sector, DG dispatchability is a concern; however, in distribution systems, an "averaged" approach using the monthly production of generation can be used to plan upgrades in areas of the network where generation does not offset load growth.

Three objective functions were selected based on their positive impacts to the LDC's financial "bottom line": minimization of real power loss (which represents lost revenue), minimization of present value of future asset reinforcements (due to equipment loading relief provided by PV DG allowing deferral of equipment upgrades), and minimization of peak demand (resulting in reduced charges paid to the transmission provider). Each objective was studied individually. The cost savings due to power loss minimization (Objective 1) and peak demand minimization (Objective 3) objectives were calculated on a monthly basis incorporating load and demand growth rates and forecasted over a five year planning horizon – a standard planning timeline for utilities. The minimization of the present value of future asset reinforcement costs (Objective 2) was calculated based on an average annual loading condition for Year 1 as a one-time cost since this is an instantaneous load-based value. The NPV financial evaluation method was applied to each objective function to identify savings incurred by each objective function over a five year planning horizon at monthly intervals. The monthly intervals were chosen to coincide with standard billing cycles and the five year horizon was chosen to coincide with the joint City-Utility infrastructure planning frequency.

A model of a heavily loaded feeder, located in the older downtown core of Kingston, was developed in CYMDIST and interfaced with MATLAB using the Component Object Model (COM) module – an additional software module purchased from CYME. Optimal siting was then performed

using the real power loss sensitivity factor method to determine the best locations at which to install PV DG. Next, a continuous domain GA was constructed for this thesis and then individually applied to each objective function to identify the real-valued optimal size of PV DG at 7 fixed nodes. The GA was tuned to achieve the best possible objective function value given the memory constraint of CYMDIST. At each iteration, the updated DG values were passed back and forth between MATLAB and CYMDIST to automate the update process of the optimal PV DG output. The metering group provided an experimentally-derived PV generation scaling factor, specific to Kingston, was applied to each objective to reflect the fact that solar insolation changes monthly and is especially weak during the winter months. The equipment ratings were obtained from utility equipment specifications and operating and loading restrictions provided by the system operators. Feeder loading data was obtained from the SCADA system and then allocated down the feeder using the "connected kVA" method available in CYMDIST. System characteristics such as load factor, load growth, load mix and operating loading limits were obtained through discussions with the system operators. The financial data such as the equipment discount (depreciation) rate, inflation rate and "sanity check" for reviewing how realistic the savings incurred due to the study was based on information provided by the accounting group. Modern replacement costs for the asset classes were obtained from estimates based on recent projects provided by engineering technologists. Therefore, significant effort was expended to obtain actual and verified data with which an accurate model could be built and to which reasonable study assumptions could be applied, and the results trusted.

7.2 – Recommendations for Future Work

This work has laid a solid foundation for future work in assessing DG penetration limits (either electronically coupled or machine based) from a utility perspective. The following opportunities for improvement, or secondary investigations, were identified through the sustained process of research, model development and data analysis.

- Model the secondary system, i.e. 120/240 V, 120/208 V and 347/600 V systems, and individual load and DG interaction to come up with a DG generation "diversity factor" similar to a load diversity factor. This varies based on load mix.
- Add reverse power flow feeder constraint to the main substation transformer e.g., 60% of rated capacity.
- Modify the assumption that replacement or upgrade of network asset occurs at 100% rated capacity to, say, 80% capacity.
- Perform a multi-objective analysis with weighted functions and compare results to those from individual objectives.
- Develop *daily* load and generation curves and use Time-of-Use rates from smart meter data to compute pricing at different times and load levels at daily, or even hourly, intervals. This would require several more simulations and may not yield that much more academic insight but would result in a more accurate cost savings calculation.
- Study the effects of various load models on optimal PV DG sizing and siting. Develop load curves for individual load classes, i.e. residential, commercial & industrial.
- Compare the performance, i.e. quality of solution and speed of simulation with other suitable heuristic algorithms such as DE, PSO, HSA etc.
- Add machine-based DGs to the study and apply the voltage stability index for optimal siting (which are relevant when a utility contains long feeders with machine based DG, e.g. wind plants). Optimizing reactive power production for voltage support could be considered.
- Design economic incentives for developers to install DG at favourable locations (from a LDC's view) rather than locations requiring system upgrades.
- Refine solar variation factor by incorporating future data as it becomes available and by adding PV technology and weather pattern data.

- Extend this research to other feeders or networks with different load growth rates, equipment replacement costs, or planning horizons and study the differences.
- Research and compare different financial mechanisms to evaluate savings.

References

[1] "Bi-Weekly FIT and microFIT Report," *http://fit.powerauthority.on.ca/Storage/103/11232_BiWeekly_FIT_and_microFIT_Report_April_1%2C_2011.pdf*, April 1, 2011.

[2] M. Mukerji & T. Brackenbury, "Kingston Hydro Distribution Availability Test (DAT) Standard Operating Procedure," Kingston Hydro Standard Operating Procedure GC-01-01, April 26 2010.

[3] Interview with Stephen Sottile, H.B. Comm, Queen's University Institute for Energy and Environmental Policy and Conservation Officer, Utilities Kingston, March 2011.

[4] Ontario Ministry of Energy: Nuclear Energy, Electricity Supply, *http://www.mei.gov.on.ca/en/energy/electricity/?page=nuclear-electricity-supply*, July 5, 2011.

[5] P. Chiradeja and R. Ramakumar, "An Approach to Quantify the Technical Benefits of Distributed Generation," *IEEE Trans. on Energy Conversion*, Vol. 19, No. 4, pp. 1686- 1693, December 2004.

[6] O. Gavasheli, "Optimal Placement of Reactive Power Supports for Loss Minimization: The Case of a Georgian Regional Power Grid", Master's Thesis, 2007, Chalmer's University of Technology, Division of Electric Power Engineering, Göteborg, Sweden.

[7] "CYME International - CYMDIST Software," *http://www.cyme.com/software/cymdist/*, July 2011.

[8] "Kingston Hydro Conditions of Service, Voltage Guidelines - Section 2.6.7," *http://www.kingstonhydro.com/Conditions_of_Service.aspx*, Jun. 2011.

[9] M. Gandomkar, M. Vakilian and M. Ehsan, "Optimal Distributed Generation Allocation in Distribution Network Using Hereford Ranch Algorithm," in *Proc. of the Eighth International Conference on Electrical Machines and Systems (ICEMS)*, pp. 916-918, Sept. 27-29, 2005.

[10] M.T. Ameli, V. Shokri and S. Shokri, "Using Fuzzy Logic & Full Search for Distributed generation allocation to reduce losses and improve voltage profile," in *Proc. Computer Information Systems and Industrial Systems*, pp. 626-630, Oct. 2010.

[11] M.R. Haghifam, H. Falaghi and O.P. Malik, "Risk-based distributed generation placement," *IET Generation, Transmission & Distribution*, Vol. 2, No. 2, pp. 252 – 260, 2008.

[12] S.G. Bharathi Dasan and R.P. Kumudinidevi, "Optimal Siting and Sizing of Hybrid Distributed Generation using EP", in *Proc. Third International Conf. on Power Systems*, pp. 1-6, Kharagpur, India, Dec. 2009.

[13] A. Parizad, A. Khazali and M. Kalantar, "Optimal Placement of Distributed Generation with Sensitivity Factors considering Voltage Stability and Losses Indices," in *Proc. 18th Annual Iranian Conference in Electrical Engineering (ICEE)*, pp. 848-855, Isfahan, Iran, May 11-13, 2010.

[14] D.Q. Hung, N. Mithulanathan and R.C. Bansal, "Multiple Distributed Generators Placement in Primary Distribution Networks for Loss Reduction," *IEEE Trans. on Industrial Electronics*, Vol. 57, Issue No. 4, 2011.

[15] "Kingston Hydro Corporate Website," *www.kingstonhydro.com*, June 2011.

[16] "Ontario Ministry of Agriculture, Food and Rural Affairs, Solar Photovoltaic Systems," *http://www.omafra.gov.on.ca/english/engineer/ge_bib/photo.htm*, Jun. 27, 2011.

[17] “Nanosolar Products cited in HowStuffWorks.com,” *http://science.howstuffworks.com/environmental/green-science/thin-film-solar-cell.htm*, Jun. 11, 2011

[18] *CYMDIST Equipment Manual, Chapter 6: Generators, Electronically Coupled Generators,* Rev. 5.0, CYME International, 2011.

[19] Aurora 5000 Canadian Inverter Datasheet, *http://www.power-one.com/sites/power-one.com/files/pvi5000outdus2_0.pdf*, Rev. 1.1 Jun. 10, 2009.

[20] *Ontario Utility Distribution Standards, Section 01 – Overhead Primary Framing, Standards 01-300, 01-312 & 01-313*, Utilities Standards Forum (USF), Cambridge, ON, 2006.

[21] C. Borges and D. Falcão, “Impact of Distributed Generation Allocation and Sizing on Reliability, Losses and Voltage Profile,” in *Proc. IEEE Power Tech Conference*, Bologna, Italy, June 23-26, 2003.

[22] G. Celli, S. Mocci, F. Pilo and G.G. Soma, “A Multiobjective Approach for the Optimal Distributed Generation Allocation with Environmental Constraints,” in *Proc. of 10th International Conf. on Probabilistic Methods Applied to Power Systems (PMAPS*), pp. 1 – 8, Rincon, Puerto Rico, USA, May 25-29, 2008.

[23] I. Ziari, G. Ledwich, A. Ghosh, D. Cornforth and M. Wishart, “Optimal Allocation and Sizing of DGs in Distribution Networks,” in *Proc. Power and Energy Society (PES) General Meeting*, pp. 1-8, Jul. 25-29, 2010.

[24] A. Parizad, A.H. Khazali and M. Kalantar, “Siting and sizing of distributed generation through Harmony Search Algorithm for improve voltage profile and reduction of THD and losses,” in *Proc. 23rd Canadian Conference on Electrical and Computer Engineering (CCECE)*, Calgary, Canada, pp. 1-6, May 2-5, 2010.

[25] D. Singh and K.S. Verma, “Multiobjective Optimization for DG Planning with Load Models,” *IEEE Trans. On Power Systems*, Vol. 24, No. 1, pp. 427-436, Feb. 2009.

[26] H.A. Hejazi, M.A. Hejazi, G.B. Gharehpetian and M. Abedi, “Distributed Generation Site and Size Allocation Through a Techno Economical Multi-Objective Differential Evolution Algorithm,” in *Proc. IEEE International Conference on Power and Energy (PECon)*, pp. 874 – 879, Kuala Lumpur, Malaysia, Nov. 29-Dec. 1, 2010.

[27] T.K.A. Rahman, S.R.A. Rahim and I. Musirin, “Optimal Allocation and Sizing of Embedded Generators,” in *Proc. National Power & Energy Conference (PECon)*, pp. 288-294, Kuala Lampur, Malaysia, Nov. 29-30, 2004.

[28] Y. Zhang, C. Gu and F. Li, “Evaluation of Investment Deferral Resulting from Microgeneration for EHV Distribution Networks,” in *Proc. Power and Energy Society (PES) General Meeting*, pp. 1-5, Jul. 25-29, 2010.

[29] D. Wang, L. Ochoa and G. Harrison, “DG Impact on Investment Deferral: Network Planning and Security of Supply,” *IEEE Trans. on Power Systems*, Vol. 25, No. 2, May 2010.

[30] A. Piccolo and P. Siano, “Evaluating the Impact of Network Investment Deferral on Distributed Generation Expansion,” *IEEE Trans. on Power Systems*, Vol. 24, No. 3, pp. 1559 - 1567 Aug. 2009.

[31] H.A. Gil and G. Joos, "Models for Quantifying the Economic Benefits of Distributed Generation," *IEEE Trans. on Power Systems*, Vol. 23, No. 2, May 2008.

[32] H.A. Gil and G. Joos, "On the Quantification of the Network Capacity Deferral Value of Distributed Generation," *IEEE Trans. On Power Systems*, Vol. 21, No. 4, Nov. 2006.

[33] M. Lafortune, "Phase Balancing for Distribution Systems Using Tabu Search," Master's Thesis, Royal Military College (RMC), Kingston, 2007.

[34] "Morgan Solar Refractive Lens PV," *http://www.morgansolar.com/*, Jun. 21, 2011.

[35] "Heuristic," *http://en.wikipedia.org/wiki/Heuristic*, July 4, 2011.

[36] D.C. Dracopoulos, *Course Notes for 2AIT608: Machine Learning – Genetic Algorithms*, University of Westminster, UK, Spring Semester 2010 available at: *http://users.wmin.ac.uk/~dracopd/DOCUM/courses/2ait608/genetic_algorithms_lecture_notes.pdf*

[37] R. Haupt and S.E. Haupt, *Practical Genetic Algorithms – 2nd Edition*, New Jersey, NY: John Wiley & Sons Inc., 2004.

[38] Interview with Sherry Gibson, M.B.A., Regulatory Analyst, Utilities Kingston, April 2011.

[39] Interview with Randy Murphy, C.A., Manager of Finance, Utilities Kingston, April 2011.

[40] "Net Present Value Analysis," *http://en.wikipedia.org/wiki/Net_present_value*, July 3, 2011.

[41] *IEEE Application Guide for IEEE Std 1547, IEEE Standard for Interconnecting Distributed Resources with Electric Power Systems (2008)*, http://ieeexplore.ieee.org/xpl/freeabs_all.jsp?arnumber=1225051.

[42] *Ontario Energy Board (OEB) Guideline G-2008-0001 Electricity Distribution Retail Transmission Rates, Section 2 – Ontario Uniform Transmission Rates*, Rev. 3.0, June 22, 2011 available at: *http://www.ontarioenergyboard.ca/OEB/_Documents/Regulatory/G-2008-0001_Guideline_EDRTSR_Rev3_20110622.pdf*

[43] H.L. Willis, *Electrical Transmission and Distribution Reference Book, Chapter 24, Characteristics of Distribution Loads*, ABB Power T&D, Raleigh, NC, 1997.

[44] "Kingston Hydro's Guide for Distributed Generators, Version 2.7," *http://www.kingstonhydro.com/pdf_downloads/100317%20%20-%20Guide%20for%20Distributed%20Generators-%20Micro%20Generator%20Connection%20Request%20Form.pdf*, May 19, 2011.